

1
1707



This is to certify that the
thesis entitled

THE ROLE OF MACROCYCLIC TRICHOTHECENE
MYCOTOXINS IN THE NASAL TOXICITY OF MICE
EXPOSED TO STACHYBOTRYS CHARTARUM

presented by

KARA NICHOLE CORPS

has been accepted towards fulfillment
of the requirements for the

Master of degree in Comparative Medicine and
Science Integrative Biology


Major Professor's Signature

6/23/09
Date

**THE ROLE OF MACROCYCLIC TRICHOTHECENE MYCOTOXINS IN THE
NASAL TOXICITY OF MICE EXPOSED TO *STACHYBOTRYS CHARTARUM***

By

KARA NICHOLE CORPS

A THESIS

**Submitted to
Michigan State University
In partial fulfillment of the requirements
for the degree of**

MASTER OF SCIENCE

Comparative Medicine and Integrative Biology

2009

ABSTRACT

THE ROLE OF MACROCYCLIC TRICHOHECENE MYCOTOXINS IN THE NASAL TOXICITY OF MICE EXPOSED TO *STACHYBOTRYS CHARTARUM*

By

KARA NICHOLE CORPS

The contribution of *Stachybotrys chartarum* to damp building-related illness (DBRI) has not been fully established. The purpose of this thesis research was to investigate the role of macrocyclic trichothecene mycotoxins in nasal and pulmonary toxicity in mice. Repeated exposures to Roridin A (RA) resulted in atrophy of olfactory epithelium (OE), loss of olfactory sensory neurons (OSNs), and neutrophilic rhinitis. Additional effects were observed in respiratory epithelium (RE), nasal transitional epithelium (NTE), and glands of the nose. Loss of OSNs persisted 3 wks after the last intranasal instillation of RA. In a second study, nasal pathology in response to repeated intranasal instillations of Satratoxin G (SG) was compared in weanling and adult mice. Weanling and adult mice were equally susceptible to the effects of SG with respect to atrophy of OE, loss of OSNs, and neutrophilic rhinitis. Repeated intranasal instillations of the spores of *S. chartarum*, SG, or a combination of both revealed that nasal pathology is dependent on macrocyclic trichothecenes and that spores do not play a role in atrophy of OE and loss of OSNs. In contrast, SG did not impact changes in the lungs that were induced by exposure to spores. Taken together, the results of these studies indicate that macrocyclic trichothecenes could contribute to reported nasal symptoms of DBRI.

For Monkey, Moother, Twinkles, and Fatmouse.

ACKNOWLEDGEMENTS

A journey such as the one I've completed is never accomplished without the help and input of others, and many thanks are certainly due.

I first need to acknowledge my mentor, Dr. Jack Harkema. His willingness to take on an overly ambitious student with big plans was greatly appreciated from that first summer we worked together. I am and will be a better scientist as a result of working with Jack, and have learned many of the things that I need to be successful in the future.

Lori Bramble, so much more than a lab manager or technician, is both a great friend and a fantastic teacher. I owe many of the skills I'm now proficient in to her, and this experience absolutely would not have been as rewarding without her. I consider myself lucky to be among those who have interacted with her.

Dr. Zahidul Islam taught me many of the techniques I have used repeatedly since beginning this journey. We spent many hours together huddled in a tiny animal room instilling mice. I am grateful for that time and for his help with everything, particularly his willingness to spend hours teaching techniques involving our ever-present subjects, the mold and the toxin.

To everyone in the lab – Drs. James Wagner, Daher Ibrahim-Aibo, Stephan Carey, Neil Birmingham, and Daven Jackson-Humbles – how lucky I was to be surrounded by so many wonderful people, and most of them already real doctors! (Sorry Jim, I just had to.) I learned so much from all of these people, and I'm grateful for our discussions and our friendship. Many thanks also

to Ryan Lewandowski, master of the molecular, for both his stories and explanations of molecular techniques.

Vilma Yuzbasiyan-Gurkan, to whom I owe so much, touches many lives in the best of ways. Thanks for all of her help and guidance through this process. My committee, Drs. James Pestka, Colleen Hegg, and Susan Ewart, are owed many thanks for all of their suggestions, guidance, and input on my work and documents. It has been a rewarding experience to work with each of them.

To the many wonderful friends who encouraged me through this process – there are so many of you – for all of your laughter and support.

To Patrick, for his patience, encouragement, cups of tea, and faith in me. To my sister Kit for her ability to make me laugh even when the computer has eaten the 10 pages I've just written, and for the constant exchange of mutual encouragement.

Finally to my parents, Michael and Belinda, for always allowing this overly ambitious child to be who she is. I hope my accomplishments are always a testament to the parents you are.

TABLE OF CONTENTS

LIST OF TABLES	viii
LIST OF FIGURES	ix
LIST OF ABBREVIATIONS	xi
CHAPTER 1 – INTRODUCTION	1
Bibliography.....	6
CHAPTER 2 – LITERATURE REVIEW	7
Damp Building-Related Illness.....	8
Damp Indoor Environments and Mold.....	10
<i>Stachybotrys chartarum</i>	12
Secondary Metabolites of <i>S. chartarum</i>	13
Mycotoxins of <i>S. chartarum</i>	15
Trichothecene Mycotoxins.....	16
Mechanisms of Trichothecene Mycotoxin Toxicity.....	20
Assessing <i>S. chartarum</i> Exposure: Detection.....	23
General Microbiological Methods.....	23
Specific Detection of <i>S. chartarum</i>	24
Detection of Trichothecene Mycotoxins.....	25
Assessing <i>S. chartarum</i> Exposure: Risk of Exposure.....	27
Pathogenicity of <i>S. chartarum</i>	30
Infectivity of <i>S. chartarum</i>	31
Allergenicity of <i>S. chartarum</i>	31
Pulmonary Toxicity.....	33
Pulmonary Studies in Infant Rats.....	34
Differential Pulmonary Effects of the Chemotypes of <i>S. chartarum</i>	35
Murine Strain Differences in Pathology Resulting from Exposure to <i>S. chartarum</i>	38
Intranasal Instillations of <i>S. chartarum</i>	38
Nasal Pathology and Intranasal Instillations of <i>S. chartarum</i>	39
Bibliography.....	44
CHAPTER 3 - Epithelial, Inflammatory, and Mucous Responses in the Nasal Airways Of Mice Repeatedly Exposed to the Macrocyclic Trichothecene Mycotoxin Roridin A: Dose-response and Persistence of Toxicant-Induced Injury	57
Introduction.....	60
Materials and Methods.....	62

Results.....	71
Discussion.....	105
Bibliography.....	115
CHAPTER 4 - Nasal Toxicity in Weanling and Adult Mice Repeatedly Exposed to the Macrocyclic Trichothecene Mycotoxin, Satratoxin G.....	
Introduction.....	121
Materials and Methods.....	123
Results.....	126
Discussion.....	132
Bibliography.....	141
CHAPTER 5 - Nasal Toxicity and Pulmonary Inflammation in Mice Exposed to the Spores and Macrocyclic Trichothecene Mycotoxin, Satratoxin G, of <i>Stachybotrys chartarum</i>.....	
Introduction.....	154
Materials and Methods.....	157
Results.....	160
Discussion.....	168
Bibliography.....	186
CHAPTER 6 – Conclusions and Future Directions.....	204

LIST OF TABLES

Table 1. Summary of dose response nasal lesions induced by RA at 24h following the final instillation.....	95
Table 2. Experimental Groups for spores and SG instillations.....	163
Table 3. Summary of the changes in the OE in all groups.....	177

LIST OF FIGURES

IMAGES IN THIS THESIS ARE PRESENTED IN COLOR

Figure 1. General structures of (A) simple trichothecenes and (B) macrocyclic trichothecenes (Tuomi et al., 1998).....	17
Figure 2. Structures of some of the macrocyclic trichothecene mycotoxins produced by <i>S. chartarum</i> (Nielsen, 2003; Pestka et al., 2008).....	19
Figure 3. Chemical structure of Roridin A.....	41
Figure 4. Location of nasal epithelial populations.....	65
Figure 5. Airway mucosubstances in nasal section T3 of mice instilled with 250 µg/kg RA.....	73
Figure 6. Marked edema and neutrophilic influx (rhinitis) of the MT and lateral wall in nasal section T1.....	76
Figure 7. Dose-dependent neutrophilic rhinitis in mice instilled with RA.....	77
Figure 8. RA-induced changes in the volume density (V_s) of mucus in the respiratory epithelium lining the NPM.....	79
Figure 9. RA-induced changes in the volume density (V_s) of mucus in the LNG.....	82
Figure 10. Loss of OSNs in the DM of T2. (A) Diagrammatic representation of nasal section T2.....	86
Figure 11. Dose-dependent atrophy of OE and loss of OSNs.....	87
Figure 12. Atrophy and inflammation of the OB.....	91
Figure 13. Loss of OSNs in the VO.....	94
Figure 14. Cytology of nasal lavage fluid from mice repeatedly instilled with saline alone or 250 µg/kg RA.....	96
Figure 15. Relative Expression (fold increase) of proinflammatory cytokine genes in the ET, MNT, and OB.....	99
Figure 16. Persistence of RA-induced mucus-related changes.....	101

Figure 17. Persistence of loss of OSNs in the DM.....	103
Figure 18. Persistence of loss of OSNs in OE lining ET2.....	104
Figure 19. Location of SG-induced OE injury and morphometric analyses.....	129
Figure 20. Light photomicrographs of the DM in nasal section T1 (OMP).....	135
Figure 21. Loss of OSNs in the DM in T1.....	136
Figure 22. Light photomicrographs of the DM in nasal section T1 (H & E).....	137
Figure 23. Atrophy of OE in the DM in T1.....	138
Figure 24. Light photomicrographs of the DM in nasal section T1 (Neutrophils).....	139
Figure 25. Neutrophilic inflammation in the DM in T1.....	140
Figure 26. Location of SG-induced OE injury and morphometric analyses.....	165
Figure 27. Photomicrographs of the DM from mice instilled with (A) saline, (B) 5×10^5 spores, (C) 25 $\mu\text{g}/\text{kg}$ SG, (D) 25 $\mu\text{g}/\text{kg}$ SG + 5×10^5 spores, (E) 100 $\mu\text{g}/\text{kg}$ SG, or (F) 100 $\mu\text{g}/\text{kg}$ SG + 5×10^5 spores.....	172
Figure 28. Loss of OSNs in the DM of T2.....	173
Figure 29. Photomicrographs of the DM from mice instilled with (A) saline, (B) 5×10^5 spores, (C) 25 $\mu\text{g}/\text{kg}$ SG, (D) 25 $\mu\text{g}/\text{kg}$ SG + 5×10^5 spores, (E) 100 $\mu\text{g}/\text{kg}$ SG, or (F) 100 $\mu\text{g}/\text{kg}$ SG + 5×10^5 spores.....	175
Figure 30. Atrophy of OE in the DM of T2.....	176
Figure 31. (A) Total cells, (B) neutrophils, and (C) eosinophils in BALF.....	179
Figure 32. Lymphocytes and (B) macrophages in BALF.....	182
Figure 33. (A) TNF- α , (B) MCP-1, and (C) IL-6 in BALF.....	183
Figure 34. (A) INF- γ and (B) IL-12 in BALF.....	187

LIST OF ABBREVIATIONS

Alcian Blue/Periodic Acid Schiff	AB/PAS
Analysis of Variance	ANOVA
Apoptosis-Inducing Factor	AIF
Bcl-2-associated X Protein	BAX
Body Weight	BW
Bronchoalveolar Lavage Fluid	BALF
C-Jun N-Terminal Kinase	JNK
Caspase-Activated DNase	CAD
Centers for Disease Control and Prevention	CDC
Damp Building-Related Illness	DBRI
Deoxynivalenol	DON
Dorsal Meatus	DM
Double-Stranded RNA-Activated Protein Kinase	PKR
Endotoxin / Lipopolysaccharide	LPS
Enzyme-Linked Immunosorbent Assay	ELISA
Ethmoid Turbinates	ET
Ethmoid Turbinate 2	ET2
Ethmoid Turbinate 3	ET3
Ethmoid Turbinate 4	ET4
Extracellular Signal-Related Kinases	ERK
Gas Chromatography	GC
High-Performance Liquid Chromatography	HPLC

Idiopathic Pulmonary Hemorrhage	IPH
Immunohistochemistry	IHC
Inducible Nitric Oxide Synthase	iNOS
Interferon Gamma	INF-γ
Institute of Medicine	IOM
Interleukin	IL
Intraperitoneal	IP
Intratracheal	IT
Lateral Nasal Glands	LNG
Liquid Chromatorgraphy	LC
Lowest Observed Adverse Effect Level	LOAEL
Macrophage Inflammatory Protein-2	MIP-2
Macrophage Chemotactic Protein-1	MCP-1
Mass Spectrometry	MS
Maxilloturbinate	MT
Maxilloturbinate and Nasoturbinate	MNT
Mitogen-Activated Protein Kinase	MAPK
Mucin 5B	MUC5b
Nanogram	NG
Nasal Transitional Epithelium	NTE
Nasopharyngeal Meatus	NPM
National Institute for Occupational Safety and Health	NIOSH
Neural Crest-Derived Pheochromocytoma Cell Line	PC-12

Nitric Oxide	NO
Nivalenol	NIV
No Observed Adverse Effect Level	NOAEL
Olfactory Bulb	OB
Olfactory Marker Protein	OMP
Ovalbumin	OVA
Phosphate Buffered Saline	PBS
Pulmonary Arterial Hypertension	PAH
Reactive Oxygen Species	ROS
Real-Time Polymerase Chain Reaction	rt-PCR
Respiratory Epithelium	RE
Roridin A	RA
Satratoxin G	SG
Surfactant protein-D	SP-D
Tumor Necrosis Factor	TNF
Verrucarin A	VA
Volatile Organic Compounds	VOC
Volume Density	Vs
Vomeronasal Organ	VO

CHAPTER 1
INTRODUCTION

Exposure to various mold species in damp indoor environments garnered sufficient public concern that the Centers for Disease Control requested that an Institute of Medicine (IOM) committee undertake a thorough review of the available literature discussing the link between damp indoor spaces and health effects [1]. Damp Building-Related Illness (DBRI) is poorly defined and includes a variety of ill health effects and vague symptoms. Reports indicate that DBRI is a worldwide issue [2]. The IOM committee identified several areas of research currently lacking in the literature, including potential exposure and risk assessment, further animal studies to characterize mechanisms of pathology, identification of target organs, quantification of mycotoxins in indoor environments, and evaluation of the mechanistic involvement of mycotoxins. Particularly, the committee cited the need for establishment of mycotoxin dose-response relationships and interactions with other potential environmental contaminants that may be present in a damp indoor environment [1]. The nose represents a potential target organ for inhaled mold spores and mycotoxins due to its ability to trap inhaled particulate matter [3]. *Stachybotrys chartarum* is a ubiquitous fungus that has been the center of much public attention due to its suggested involvement in DBRI, particularly with regard to the macrocyclic trichothecene mycotoxins it produces [1,4]. The purpose of the following studies was to characterize and quantify the nasal pathology resulting from intranasal exposure to a representative macrocyclic trichothecene, Roridin A (RA); to compare the effects of intranasal exposure to Satratoxin G (SG), a macrocyclic trichothecene produced by *S. chartarum*, in the noses of weanling and adult

mice; and to investigate the effects of intranasal exposure to *S. chartarum* spores, SG, and co-exposures of both spores and SG on the noses and lungs of mice. The hypothesis driving my thesis research is that *S. chartarum* - induced toxicity is dependent on macrocyclic trichothecene mycotoxins.

Chapter 2 contains a review of the current literature, including discussions of DBRI, *S. chartarum* and its secondary metabolites, suggested mechanisms of macrocyclic trichothecene toxicity, methods for environmental detection and quantification of indoor molds and mycotoxins, the pathogenicity of *S. chartarum*, and the results of various *in vivo* studies.

In Chapter 3, I will present the results of my investigation of the dose-response effects of a representative macrocyclic trichothecene mycotoxin, RA, that was repeatedly instilled into the nasal passages of mice. Histopathology, morphometric lesion analyses, flow cytometric inflammatory cytokine data, and inflammatory gene mRNA expression data are discussed. The persistence of lesions induced by repeated exposures to RA is also presented. Gene expression data presented in this chapter were contributed by Dr. Zahidul Islam, and histopathology reports were contributed by Dr. Jack Harkema.

In Chapter 4, I discuss my study comparing the effects of SG, a macrocyclic trichothecene produced by *S. chartarum*, in the noses of weanling and adult mice. Histopathology and morphometric analyses of pathological changes in the olfactory epithelium are presented. Histopathology reports were contributed by Dr. Jack Harkema.

Chapter 5 contains a co-exposure study investigating the effects of *S. chartarum* spores and SG on the nasal passages and lungs of mice. Bronchoalveolar lavage fluid (BALF) cytology and inflammatory cytokine data, nasal histopathology, and morphometric analyses of nasal lesions are discussed. Histopathology reports were contributed by Dr. Jack Harkema.

In Chapter 6, I present my overall conclusions resulting from the above mentioned studies, as well as suggestions for future directions for further studies investigating *S. chartarum* and macrocyclic trichothecene mycotoxins.

CHAPTER 1 BIBLIOGRAPHY

1. Institute of Medicine. (2004) *Damp Indoor Spaces and Health*. Washington DC: National Academies Press.
2. Hodgson M. (2002) Indoor Environmental Exposures and Symptoms. *Environmental Health Perspectives* 110 (Supplement 4):663-667.
3. Harkema JR, Carey SA, Wagner JG. (2006) The nose revisited: a brief review of the comparative structure, function, and toxicologic pathology of the nasal epithelium. *Toxicological Pathology* 34:252-269.
4. Cooley JD, Wong WC, Jumper CA, Straus DC. (1998) Correlation between the prevalence of certain fungi and sick building syndrome. *Occupational Environmental Medicine* 55:579-584.

CHAPTER 2
LITERATURE REVIEW

Damp Building-Related Illness

Indoor air quality has been the subject of much investigation in recent years due to increasing reports of Damp Building-Related Illness (DBRI). DBRI is a term commonly applied to the range of signs and symptoms associated with damp indoor environments. It is thought to be a product of modern, climate-controlled buildings with self-contained ventilation systems. Though associations have been made between ill health effects and specific buildings for 30 years, establishing causality has proven difficult. Complaints of illness due to specific buildings have been noted in most countries throughout the world that record such information [2]. Exposure to a damp environment can occur in the home or in an occupational setting, and these different exposures could potentially result in different clinical manifestations. People who report symptoms associated with specific indoor spaces often note a resolution of those symptoms when they leave the environment in which they are affected [4].

A variety of causes have been postulated to explain DBRI. Inhalation of volatile organic compounds (VOC), which originate from organisms such as bacteria and fungi, or construction materials, such as drywall and concrete, have been linked to headaches and nose irritation, and appear to contribute to fatigue in human studies [5]. Headaches have also been linked to discomfort due to the temperature of the indoor environment. Odors may also trigger otherwise unexplained symptoms [2]. Fungi have been found colonizing air filters, metal air ducts, and building insulation in an office environment, often in areas of water collection in air flow ducts. Samples from these surfaces also contained VOC,

thought to have originated from the *Penicillium spp.* and *Cladosporium spp.* that were isolated [6,7]. A variety of building conditions, such as humidity levels, have recently been investigated in relation to human discomfort [8]. One characteristic that appears in many reports of DBRI is the presence of excessive moisture or humid conditions [1]. Often damp conditions are discovered upon investigation of such buildings after complaints of illness by occupants.

Some authors have chosen to categorize building-related symptoms into five groups, which include sensory irritation (eye, nose, and throat), neurologic or general symptoms, nonspecific hypersensitivity reactions, skin irritation, and odor or taste symptoms [5]. An Institute of Medicine (IOM) report concluded that damp indoor environments are associated with upper respiratory tract symptoms (nasal congestion, runny or itchy nose, sneezing, and throat irritation) as well as some lower respiratory tract symptoms and syndromes (wheeze, cough, asthma exacerbation, and hypersensitivity pneumonitis in susceptible people). The report also concluded that sufficient evidence did not exist to link a variety of other symptoms and conditions, such as dyspnea (shortness of breath), sinusitis, airflow obstruction, and cognitive dysfunction, to damp indoor conditions [2].

Buildings can become damp in a variety of ways, some of which may not be noticed by occupants. Water device failure, plumbing problems, rainwater leakage, groundwater infiltration, and even occupant activity can create a moist environment. Building materials also play a role due to their porous nature. Materials consisting of larger pores or a higher number of pores, such as composites made from paper and wood, cellulose, and gypsum, are of particular

concern because moisture content or humidity need not be high to allow growth of fungal organisms. Conditions in which water continually or intermittently reaches these materials such that drying does not occur are most conducive to creating a damp environment [1]. Modern ventilation systems in many office buildings prove to be the source of moisture, or materials within ventilation systems previously became damp and are found to harbor fungal organisms [4].

Damp Indoor Environments and Mold

Mold growth was extremely common in the gulf coast in water-damaged buildings, including the majority of damaged dwellings, following the recent hurricanes Katrina and Rita. The indoor and outdoor concentrations of mold and mold products, as well as bacterial endotoxin (lipopolysaccharide, LPS), were found to be exceptionally high and led to warnings urging the use of respirators and protective equipment [9].

It has been suggested that 20-40% of North American and Northern European buildings have mold growth [10]. The presence of certain molds in indoor environments has been linked to hypersensitivity reactions in allergic individuals and infections in immunocompromised individuals [11,12]. Recently both mold spores and mold fragments, such as portions of hyphae and particles derived from extra- and intracellular structures, have been associated with allergenicity and asthma [13]. A survey study conducted by the National Institute for Occupational Safety and Health (NIOSH) found a link between a building with long-term, repeated water damage and respiratory symptoms such as adult

onset asthma, nasal and eye irritation, wheezing, hypersensitivity pneumonitis and exacerbation of existent asthma in employees who had worked there for one or more years. A strong association with the need to take sick days due to respiratory symptoms was also found among employees working in this particular building [14]. Studies have shown a link between damp, moldy conditions in schools and poor performance of the attending students, as well as symptoms fitting DBRI in both students and teachers [15]. Cooley et al. investigated the role of mold in DBRI in 48 schools in the United States. Several different mold species were isolated from each of the schools. Notably, two species were found to be strongly associated with DBRI – *Penicillium spp.* and *Stachybotrys chartarum* [4].

A number of mold species, including *Penicillium spp.*, *Rhizopus spp.*, *Alternaria spp.*, *Cladosporium spp.*, and *Aspergillus spp.*, are frequently isolated from damp buildings [4,7,16,17,18]. *S. chartarum* is isolated less commonly, and has been shown to occur in approximately 13% of homes, compared to 96% of homes for *Penicillium spp.*, or 89% of homes for *Cladosporium spp.* [16,18]. When isolated, it is typically found in lower quantities than other molds like *Aspergillus spp.*, and has not been found as the sole mold contaminant of water-damaged materials [16,19]. Similarly, *S. chartarum* was not isolated in a study of outdoor recreational exposure to mold species, whereas spores resembling *Cladosporium*, *Penicillium*, and *Aspergillus spp.* were commonly isolated [20]. *S. chartarum* has, however, resulted in great public health concern due to its association with a cluster of cases of idiopathic pulmonary hemorrhage (IPH) in

infants [21,22]. Other authors have also suggested that the presence of *S. chartarum* should be cause for concern for the occupants of affected buildings due to variety of reported ill health effects [16,23,24,25]. Given the increased public interest and potential implications for litigation resulting from exposure to moldy conditions [18,26], further investigation of *S. chartarum* is warranted.

Stachybotrys chartarum

S. chartarum is a ubiquitous, saprophytic fungus that grows on cellulose-containing materials [16,23]. It is commonly referred to as “black mold” or “toxic black mold” [26]. It was known in the past as both *S. alternans* and *S. atra*, though these names are now considered obsolete [16,18]. It may be found in a variety of outdoor materials, such as soil, hay, grains, and plant debris, but is not commonly isolated in the air. The spores form in clusters and are coated in a layer of polysaccharide “slime,” thus making dissemination into the air less likely without drying and disturbance of the spores [16,18]. *S. chartarum* is a member of the *fungi imperfecti*, having septate hyphae and lacking a known sexual stage of reproduction [18,27]. The spores, or asexual reproductive structures, of *S. chartarum* are approximately 7-12 X 4-6 μm [28,29]. While the hyphae are typically colorless, the spores are dark, oval in shape and either smooth or rough-walled [27]. Growth of *S. chartarum* requires a relatively high amount of humidity compared to other molds such as *Aspergillus spp.*, with optimal growth occurring at 93% humidity at 25°C (77°F) [18]. The necessary conditions for growth of *S. chartarum* can occur in small, local environments even when the

overall humidity in a given room is lower than the required level. In particular, wood and wood composites, commonly used in building construction, allow mold growth at low levels of water activity, or local relative humidity [10].

Secondary Metabolites of *S. chartarum*

Molds produce secondary metabolites, products that are unnecessary for the growth and reproduction of the fungi, in addition to compounds needed for survival of the organism. One structural component common to the cell walls of many fungi, bacteria, and plants is (1→3)-β-D-glucan. A recent review concluded that there may be an association between exposure to this cell wall component and airway inflammation and other airway symptoms. The author notes, however, that evidence is currently lacking for a definitive link to human health effects [30].

Andersen et al. recently reported that 2 major groups, or “chemotypes,” of *S. chartarum* exist, with the groups producing different types of mycotoxins. The mold produces a variety of active secondary metabolites with a number of biological effects [31]. VOC appear to contribute very little to symptoms attributed to exposure to *S. chartarum* [32]. Approximately 40 different spirocyclic drimanes are produced. These compounds are known to inhibit enzyme activity, inhibit Tumor Necrosis Factor (TNF)-α release, disrupt complement, and result in cytotoxicity and neurotoxicity. Additionally, spirocyclic drimanes are capable of stimulating plasminogen, fibrinolysis, and thrombolysis. They are produced in large quantities, and the exact role in the biology of the

fungus as well as the implications for human health are unknown [10,26,31,33]. A cyclosporine analogue that may lead to immune suppression is also produced, though its potential role in human health effects has not been investigated [10,16].

Proteinases produced by *S. chartarum* have been suggested as contributors to health effects. In a recent study investigating two strains representing the two chemotypes of *S. chartarum*, multiple proteinases were produced by both strains. Interestingly, it appeared that the chemotype considered less toxic with respect to the types of mycotoxins produced had higher proteinase activity than the more toxic chemotype. Growth conditions also impacted production of proteinases. The majority of these were identified as serine proteinases, though only one, stachyrase A, has been characterized [34]. Proteinases and a hemolytic compound, stachylysin, may be partly responsible for pulmonary pathology related to changes in collagen IV dynamics and thus may play a role in pulmonary hemorrhage in infants [26,34]. Stachylysin was isolated and characterized in 2001. It is a slow-acting hemolysin that completely lyses red blood cells in the same manner as a β -hemolysin of bacteria [35]. It was localized to the inner cell wall of the spore of *S. chartarum* [36]. Stachylysin was found to cause hemorrhage in an earthworm model and was therefore proposed as a potential mechanistic explanation for reported instances of hemorrhage [37]. Like the proteinases, it appears that the less toxic chemotype tends to produce more stachylysin than the more toxic chemotype. Also similar

to the proteinases, growth conditions affect the production of the hemolysin [34,35].

Mycotoxins of *S. chartarum*

Mycotoxins are perhaps the most studied products of fungi. Mycotoxins are low-molecular-weight secondary metabolites produced by a variety of fungal species and thus are widely varied in structure and toxic effects [38,39]. In some cases, mycotoxins are produced in situations of low nutrient availability or less than ideal growth conditions [16]. Health effects resulting from mycotoxin exposure are most commonly associated with ingestion of moldy grains and other food sources. The aflatoxins produced by *Aspergillus spp.* and ergot alkaloids produced by *Claviceps spp.*, for example, are known to produce toxicoses significant to human and animal health [16,39]. Mycotoxicoses, the toxic syndromes caused by exposure to various mycotoxins, are not explained by infection with the fungal organism or by allergic hypersensitivity to the fungus [16,40]. *S. chartarum* produces several different mycotoxins capable of producing different effects. The two chemotypes of *S. chartarum* are divided specifically by the types of mycotoxins produced, with one group producing atranones and the other producing macrocyclic trichothecenes [31,41].

Atranones A-G were structurally characterized in 2000. They possess various stereochemical variations based on a carbocyclic ring of eleven carbons, and are related to dolabellane diterpenes [41]. Two-thirds of *S. chartarum* isolates produce atranones [31]. These strains tend to be less cytotoxic than

those producing macrocyclic trichothecenes, though exposure to spores of the less cytotoxic chemotype results in production of inflammatory mediators such as Interleukin (IL)-6, TNF- α , and Nitric Oxide (NO) [33].

Trichothecene Mycotoxins

Both chemotypes of *S. chartarum* are capable of producing simple, trichothecene mycotoxins, such as trichodermol and trichodermin, in varying quantities [31,33]. Trichothecenes are sesquiterpenoid metabolites with the base formula C₁₅H₂₄. They are characterized by a 9,10-double bond and a 12,13-epoxytrichothene, a tetracyclic 12,13-epoxy ring present in all trichothecenes. A number of rearrangements and side chains differentiate the various types of trichothecenes, particularly with respect to oxygenation patterns (**Figure 1**) [38,42,43]. These mycotoxins are resistant to ultraviolet light, sunlight, heat (up to 120°C), and x-rays. They are acid stable but alkali labile [18].

Trichothecenes are divided into four groups, with Groups A, B, and C encompassing the simple, or non-macrocyclic, trichothecenes [42]. T-2 toxin, from Group A, and 4-deoxynivalenol (DON), from Group B, are of note due to their production by *Fusarium spp.*, which have a propensity for contaminating grain crops and animal feeds [16,38,42]. The Group C trichothecene baccharin is produced by *Baccharis megapotamica*, a plant species, and is not of concern with respect to human health [26,42]. The Group D, or macrocyclic, trichothecenes contain a 4,15-macrocyclic ester linkage [38]. They are produced by *Trichothecium*, *Myrothecium*, and *Stachybotrys spp.* and include the roridins,

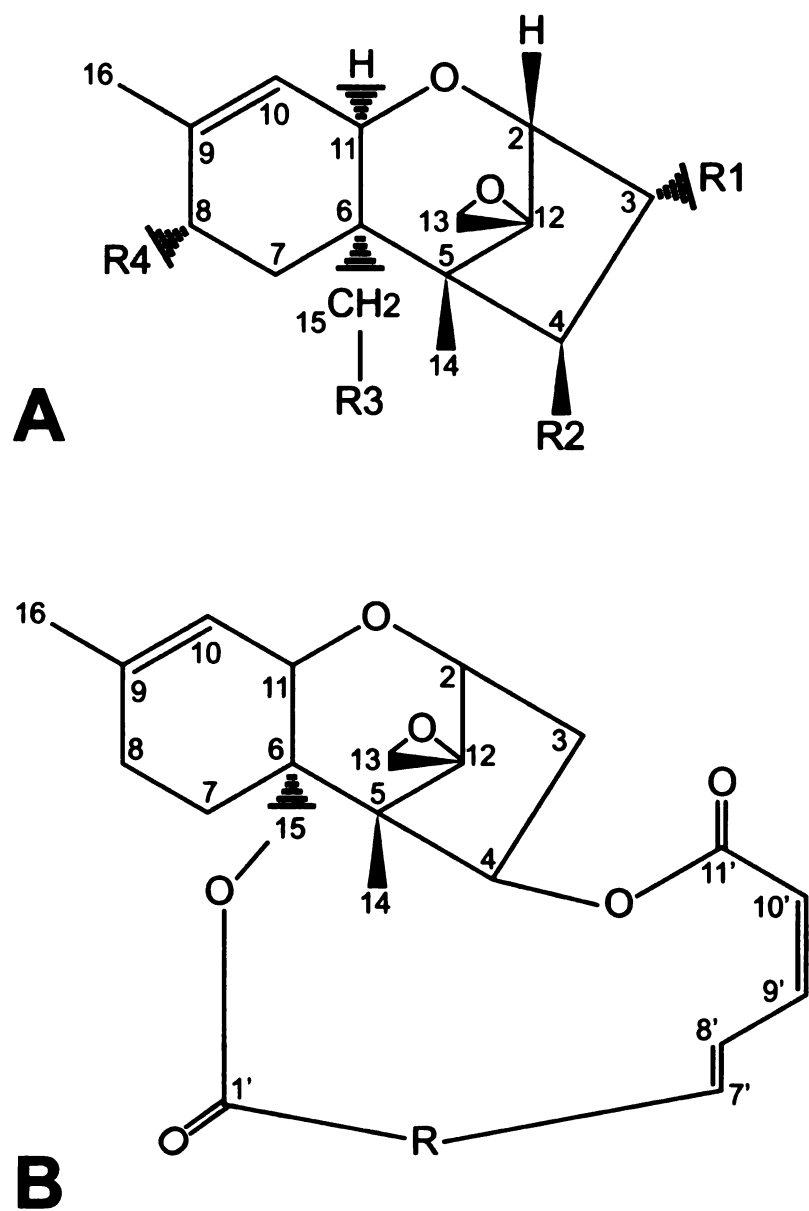


Figure 1. General structures of (A) simple trichothecenes and (B) macrocyclic trichothecenes (Adapted from Tuomi et al., 1998).

satratoxins, and verrucarins [38,42]. Macrocylic trichothecenes are produced via modification of a simple trichothecene, trichodermol, which may be processed further to one of two other simple trichothecenes, trichodermin or verrucarol. The immediate precursors of macrocylic trichothecenes, trichoverroids, are derived from verrucarol [33].

The macrocylic trichothecenes Satratoxin G (SG), Roridin A (RA), and Verrucarin A (VA) had greater cytotoxic effects than the simple trichothecenes T-2 toxin, DON, and nivalenol (NIV) [44]. SG was shown to induce expression of proinflammatory cytokines in the same macrophage cell line at lower doses than DON [45]. Engler et al. [46] showed that VA and RA had greater toxicity in a β -galactosidase inhibition toxicity assay than T-2 toxin, DON, and NIV. Based on the results of these studies, it is thought that macrocylic trichothecenes are more toxic than simple trichothecenes. Approximately one-third of *S. chartarum* isolates produce macrocylic trichothecenes [31]. Those produced include roridin E, roridin L-2, verrucarins B and J, isosatratoxins F and G, and satratoxins F, G, and H (**Figure 2**) [10,28,31]. Macrocylic trichothecenes have been primarily localized to the outer plasmalemma and inner cell wall, with a small amount in the outer cell wall of spores [47]. Trichothecenes including satratoxins have been identified in spores aerosolized from cultures of *S. chartarum* [48]. Yike et al. observed that the JS5817 strain of *S. chartarum* contained approximately 1 picogram of SG per spore [49]. Recently macrocylic trichothecenes have been identified on particulates smaller than spores, including house dust [50]. Some authors have indicated that macrocylic

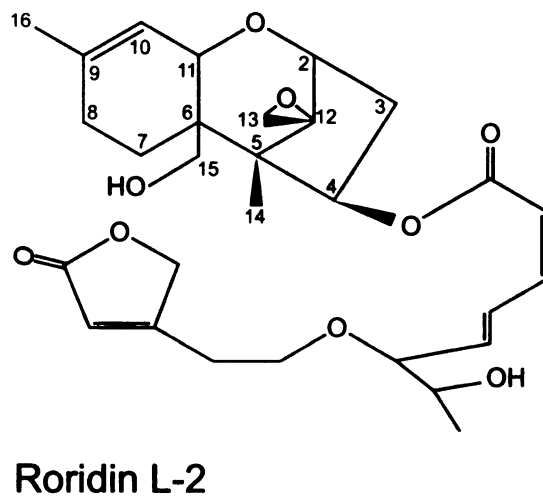
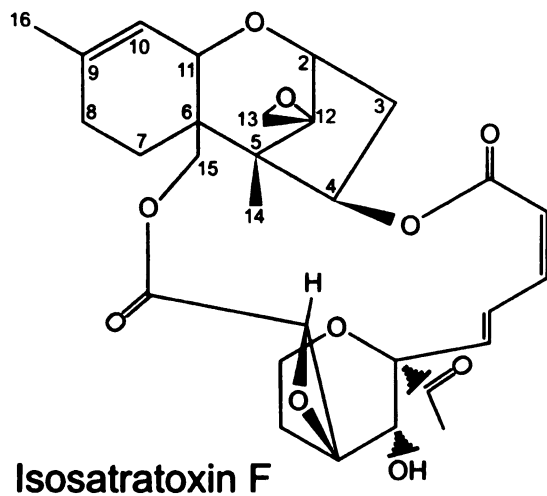
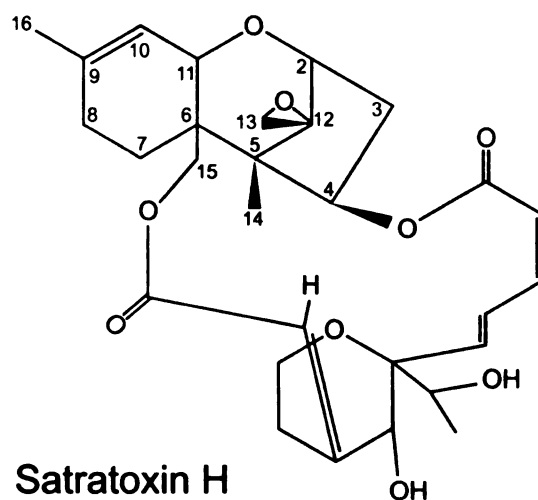
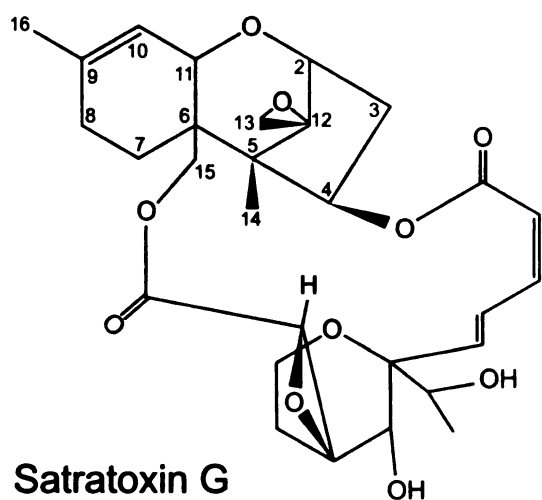


Figure 2. Structures of some of the macrocyclic trichothecene mycotoxins produced by *S. chartarum* (Adapted from Nielsen, 2003; Pestka et al., 2008).

trichothecenes may displace out of *S. chartarum* spores and into aqueous solutions [26,28,51]. Macrocyclic trichothecenes from *S. chartarum* have also been identified in indoor air samples [52,53]. It was observed that the macrocyclic trichothecenes in aqueous supernatant fluid from washed spores are capable of inhibiting protein synthesis [51], indicating that these mycotoxins may produce adverse effects in the absence of spores.

Mechanisms of Trichothecene Mycotoxin Toxicity

Trichothecenes are particularly known for their interference with ribosome function. They are potent inhibitors of protein synthesis, a function mediated by binding to the peptidyl transferase site of 60S eukaryotic ribosomes [38,54,55]. Trichothecenes inhibit polypeptide chain initiation or elongation depending on various side chain substitutions [56]. The 12,13-epoxytrichothene is responsible for protein synthesis inhibition, and removal of the epoxide group, or removal of the 9,10-double bond, has been shown to decrease toxicity [38,42].

Leukocyte cultures have been utilized to elucidate some of the cellular mechanisms by which trichothecenes induce toxicity. Trichothecenes, including satratoxins and roridins, have been shown to activate c-Jun N-terminal kinase (JNK), mitogen-activated protein kinases (MAPK) such as p38, p53, and extracellular signal-related kinase (ERK) [44,55,57,58,59]. Activation of JNK and p38 alone was found to be insufficient for induction of apoptosis [55]. Cytotoxicity induced in leukocytes by satratoxins was correlated with apoptosis and induction of MAPK [44]. Interestingly, it appears that trichothecenes may

induce both apoptotic and anti-apoptotic intracellular signaling simultaneously [59]. DON and SG have been shown to induce mRNA expression of macrophage inflammatory protein-2 (MIP-2) [45], and it was recently demonstrated that T-2 toxin and DON are capable of causing cleavage of rRNA and inducing RNases [60]. Trichothecenes may stimulate the immune system or cause immune suppression, depending on the dose of mycotoxin given. This is likely due in part to the sensitivity of leukocytes to the effects of trichothecenes both *in vitro* and *in vivo* [61]. Together, all of these pathways have been suggested to facilitate a “ribotoxic stress response” resulting in apoptosis of cells and upregulation of proinflammatory cytokines [44,45,55,57,59,60,61].

Production of reactive oxygen species (ROS) has also been postulated as a potential mechanism of toxicity [44]. Satratoxin H has been shown to induce lipid peroxidation, ROS generation, and apoptosis in cultured neural crest-derived pheochromocytoma cells (PC-12) [62]. In this study, the authors suggested that ROS may also contribute to the development of a “ribotoxic stress response.” In another recent study it was reported that macrocyclic trichothecenes induced DNA fragmentation in fetal lung fibroblasts [63]. Wang and Yadav [64] applied methanol-extracted toxins from *S. chartarum* spores to mouse alveolar macrophages. DNA damage was followed by apoptosis, confirmed by DNA comet formation and activation of caspases 3 and 7. The authors did not detect increases in inflammatory cytokines but noted a decrease in intracellular reduced glutathione accompanied by an increase in oxidized

glutathione, indicating oxidative stress. Expression of p53 and the MAPK p38 and JNK occurred in the macrophages [64].

Islam et al. [65] recently used cultured neural crest-derived pheochromocytoma (PC-12) cells to investigate the cellular apoptosis mechanisms of SG. Satratoxin H was recently shown to induce apoptosis in this cell line [66]. SG induced DNA fragmentation and expression of proapoptotic genes 2 days after exposure to SG. Double-stranded RNA-activated protein kinase (PKR), CAD, and p53 expression was significantly increased in SG-treated cells. Expression of BAX was upregulated at 18 hours and 2 days after treatment with SG. The authors of this study did not detect changes in caspase-3 expression at any point during the experiment. Application of inhibitors of caspase 3 failed to prevent apoptosis induced by SG, suggesting that the mechanism may be caspase 3-independent. Inhibition of PKR resulted in prevention of apoptosis and suppression of proapoptotic gene expression. The authors also observed that SG causes translocation of apoptosis-inducing factor (AIF) to the nucleus, and that this translocation is prevented by application of a PKR inhibitor. They therefore concluded that SG-induced apoptosis is caspase 3-independent and PKR-dependent in PC-12 cells [65]. However, PKR inhibitors did not prevent apoptosis and expression of pro-apoptotic genes in cultured OP-6 cells, a line of immortalized cells representing a late stage of olfactory sensory neuron development [Dr. James J. Pestka, personal communication]. These studies indicate that the toxic effects of trichothecene mycotoxins appear to

involve extensive intracellular signaling, immune modulation, induction of proinflammatory cytokines, and apoptotic mechanisms.

Assessing *S. chartarum* Exposure: Detection

Determining what constitutes a realistic exposure to *S. chartarum* for humans in water-damaged buildings is important to allow contextual evaluation of the results of animal studies. Several authors have suggested that studies investigating DBRI should assess whether exposure to both *S. chartarum* and its mycotoxins may have occurred in damp indoor environments [28,50,53,67]. A number of methods for sampling indoor fungi exist, many of which were recently reviewed [67] and will not be discussed here. Methods specifically applicable to detection and quantification of *S. chartarum* and its secondary metabolites are considered here.

General Microbiological Methods

Culturing is commonly used with vacuum or air sampling methods that allow impaction of fungal spores onto culture media, though sampling may be accomplished using sterile swabs on contaminated surfaces as well [10,67,68]. Andersen and Nissen [69] tested 22 different fungal culture media and found that only those containing plant-based materials resulted in good growth of *S. chartarum*. The primary benefit of this method is the ability to identify fungi to the species level, though several authors have noted that precise identification requires the skills of a trained mycologist and may be time consuming [67,68].

Additionally, culturing does not evaluate non-viable spores. High-Performance Liquid Chromatography (HPLC) analysis of toxin production revealed that *S. chartarum* spores remain toxigenic following storage on cellulose-containing materials for two years [70], indicating that methods assessing only viable spores may not reflect realistic exposures. Total fungal propagule counts utilize air sampling methods with filters that collect all spores, but this method does not allow identification to the species level [68], which is important when using indirect detection methods, such as mycotoxin measurement [67,71]. Culture methods are plagued by results that differ based on the nutrient media used, laboratory that processes samples, and competition between multiple species of mold [68]. This is of particular concern given that *S. chartarum* is typically found with many other mold species and has proven difficult to culture from indoor samples [16,19,23,53,68,72]. Air sampling has been considered problematic due to the short sampling periods typically used for individual rooms [68]. A recent advance that improves on traditional air sampling techniques involves a personal sampler that collects samples in disposable tubes, allowing assessment by a variety of different methods [73].

Specific Detection of *S. chartarum*

Xu et al. [74] recently described a protein found specifically in the spores and mycelia of *S. chartarum*. Polyclonal antibodies were raised against this protein and were demonstrated to lack cross-reaction with a variety of other mold species. The authors suggest that the antibody could be used as a sensitive

assessment method for environmental *S. chartarum*. A monoclonal antibody specific for a protein found in spores of *S. chartarum* was utilized to detect aerosolized spores in an experiment conducted by Green et al. [13]. A fairly specific competitive enzyme-linked immunosorbent assay (ELISA, immunochemical assay for a specific antigen in a sample) was used to detect stachylysin, though the authors note that all isolates of *S. chartarum* tested in this study produced stachylysin, and thus the assay is not useful for estimating exposure to mycotoxins [75]. An exceptionally specific real-time polymerase chain reaction (rt-PCR, technique used to amplify and quantify a targeted DNA molecule or sequence) assay for *S. chartarum* was applied to assess house dust and other samples taken from indoor environments, though this method does not differentiate the two chemotypes of *S. chartarum* or measure mycotoxins [26,76,77].

Detection of Trichothecene Mycotoxins

Samples for detection of trichothecenes can be taken from a variety of sources, such as carpet, house dust, and room air [10,67,71]. A sensitive bioassay for trichothecenes utilizing luciferase expression has been described [78]. Polyclonal antibodies to SG have been developed and used in a competitive ELISA to detect macrocyclic trichothecenes [52,79]. This ELISA was used in a study of 19 flooded houses for measurement of macrocyclic trichothecenes that illustrates the difficulty of detecting these mycotoxins in indoor air samples. A statistically significant level of macrocyclic trichothecenes

was found only in dust samples from floor surfaces [53]. Brasel et al. [52] recently used an ELISA assay to test air samples collected in buildings contaminated with *S. chartarum*. The concentrations of trichothecenes detected in these samples were found to increase with air disturbance or increased sampling time.

Bloom et al. [80] successfully applied HPLC-tandem Mass Spectrometry (MS, technique used to determine chemical structure and fragmentation patterns of chemicals) and Gas Chromatography (GC, chromatography method utilizing an inert gas to separate components of solutions)-tandem MS to the detection of macrocyclic trichothecenes produced by *S. chartarum*. In this study, cultured fungi did not necessarily correlate with detected mycotoxins. These results were similar to those observed by another group [81]. Bloom et al. [80] suggested that MS-based methods may be an effective way to determine potential macrocyclic trichothecene exposure when culture fails to confirm the presence of *S. chartarum*. This method was applied to house dust, dust cultures, and vacuumed samples in addition to air samples. Importantly, the authors sampled the air in an area defined as the breathing zone, which is suggested to more closely approximate a potential human exposure [80,82].

Recently liquid chromatography (LC, technique to separate the components of solutions)-tandem MS were used to quantify Satratoxins G and H from indoor air samples collected over a 15 hour period. Airborne concentrations of Satratoxins G and H were 0.25 and 0.43 ng/m³, respectively, indicating a potential dose that a person might be exposed to via inhalation [83]. While the

authors noted that the building from which the samples were collected had a known problem with *S. chartarum* contamination, they did not describe the building in detail and thus broad application of the results to a variety of circumstances is questionable.

SG-serum albumin adducts were identified in elegant *in vitro* and *in vivo* studies utilizing human and animal samples [84]. The authors suggest that these adducts represent a potential biomarker for detection of exposure to *S. chartarum*. Interestingly, SG adducts were found in 2 domestic cats that developed acute pulmonary hemorrhage during anesthesia. The cats came from an indoor environment found to have mold growth [85].

Assessing *S. chartarum* Exposure: Risk of Exposure

Assessing the risk of exposure to *S. chartarum* and its macrocyclic trichothecene mycotoxins has been addressed due to the potential health effects resulting from exposure [1,18,29,67,81]. Materials containing cellulose with long-term water damage, particularly from damaged or poorly constructed roofs, have been considered those most at risk for mold contamination [86]. Tuomi et al. determined that assessments of inhalation exposure risk should not be made solely from analysis of the fungal contaminants of construction material samples [81]. As has been noted [18], the presence of *S. chartarum* does not guarantee that a toxigenic strain is present, and the identification of macrocyclic trichothecenes does not mean that the mold is present, nor does it indicate exposure. Water activity (local relative humidity) has been indicated as the most

important factor determining *S. chartarum* growth on various materials [86].

Some sampling methods, such as vacuuming, are suggested to overestimate potential exposure levels, and it has therefore been suggested that sampling be performed only under normal room conditions and activity levels [16].

Questions have been raised regarding the feasibility of inhalation exposure to *S. chartarum* and macrocyclic trichothecenes [11,12,18,32,87]. The number of spores in indoor air is affected by physical activity in a building, outdoor airflow that may impact airflow within a building, and changes in ventilation and other factors that are caused by the act of sampling areas of mold growth [10]. The spores of *S. chartarum* were found to be highly resistant to dispersion in the air, likely due to the polysaccharide coat in which the spores grow. When exposed to airflow at low velocity, they are initially released in a large cloud, followed by sporadic release of individual or small numbers of spores [29,88]. Low humidity appears to enhance the release of mold spores from growth surfaces [10]. Due to the size of *S. chartarum* spores, they are likely to settle and thus may not be detected in air samples [16,29].

It has been postulated that even if spores were inhaled, they would not reach the lungs due to their size [32]. However, particles less than 10 μm may reach the lungs, particularly those less than 2.5 μm in diameter. Lung deposition is greater for small particulates than for larger particulates, and smaller particles tend to remain in the lung for longer periods [89]. This highlights the significance of the studies by Brasel et al. [50,52] in that particulates smaller than spores in indoor air, such as house dust, could reach the lungs. Fungal fragments of *S.*

chartarum, which vary in size between 0.03 and 0.79 μm , have 230-250-fold higher deposition in the respiratory tract than spores [88]. Dry spores of *S. chartarum* have been shown to aerosolize and have a mean respirable diameter of 5 μm [28,90]. Spores might lodge in the nose rather than reaching the lungs [32]. As noted above, macrocyclic trichothecene-containing spores have been found in indoor air [49]. Additionally, Tucker et al. indicate that 19 billion spores could be present in 1 square meter of *S. chartarum* growth on a surface. The results of their study indicate that approximately 0.2% of that growth may be released into the air if an airflow disturbance occurs. They note that if each spore contained 0.1 picogram of macrocyclic trichothecenes, this release would result in a toxin load in the air of approximately 4 μg [29].

It is possible that in some cases, both chemotypes of *S. chartarum* might be found and thus their combined effects should be considered [28], as should the potential combined effects of exposure to *S. chartarum* and other environmental compounds such as endotoxin [26]. Vesper et al. have proposed an "Environmental Relative Moldiness Index" based on 36 species of mold commonly isolated from homes and suggest it may be useful in assessing mold burdens [77]. Attempts to assess the potential results of exposure have often disregarded the difference between acute and chronic exposures and have involved very high doses of spores, effectively overestimating the risk of adverse effects [11]. Potential exposure levels for humans have thus not been established, though recommendations have been made for the remediation of

mold-contaminated buildings [1,11]. A variety of *in vitro* and *in vivo* studies have however attempted to characterize the effects of exposure to *S. chartarum*.

Pathogenicity of *S. chartarum*

S. chartarum was recognized as a problematic contaminant in the early 1930's when a group of horses developed a unique syndrome characterized by stomatitis, oral necrosis, rhinitis, and conjunctivitis, which typically progressed to include hemorrhage, thrombocytopenia, leukopenia, coagulopathy, and neurological alterations such as irritability, blindness, and gait disturbances. Death frequently followed these symptoms, though an "atypical" form was more highly fatal and involved loss of sensorimotor reflexes, hypersensitivity to pain, blindness, and extreme irritability. The syndrome was termed Stachybotryotoxicosis to reflect the theory that these signs were caused by a metabolite of the fungus [91]. An outbreak of stachybotryotoxicosis was also described in sheep. High mortality rates accompanied signs of anorexia, anemia, pulmonary edema and congestion, and hemorrhage in the lungs, trachea, bronchi, intestines, and nose [92]. Cases of stachybotryotoxicosis in people were reported in areas affected by the equine disease. Most developed a localized dermatitis, though some developed symptoms such as bloody rhinitis and cough and reported pain in the nose and throat, as well chest tightness that were attributed to inhalation exposure to mold-contaminated sources. Interestingly, these and other people exposed in occupational settings recovered

rapidly when exposure temporarily ceased, though symptoms returned upon re-exposure [91].

Infectivity of *S. chartarum*

Molds are known to cause deleterious effects on human health by three mechanisms – hypersensitivity or other adverse immune response, irritant and toxic effects due to secondary metabolites produced by the mold, or direct infection [18]. Studies have not shown infection to be a mechanism of injury involved in pathology attributed to *S. chartarum* [12,18]. Viable spores of *S. chartarum* were recovered in BALF from a young patient whose home was found to be contaminated with the mold [93]. *S. chartarum* has been observed to germinate in the lungs of 4 day-old, infant rats. Viable spores were recovered from 14 day-old rats but germination was not observed. In addition to germination, intratracheal (IT) instillation of spores resulted in neutrophilic inflammation and poorly formed granulomas associated with spores. Infant rats had decreased growth and increased mortality compared to control animals. The growth and mortality rate of 14 day-old rats was not significantly different from control animals. *S. chartarum* did not establish an infection in spite of germination [94].

Allergenicity of *S. chartarum*

Allergic and hypersensitivity reactions to molds are known to be either IgG or IgE mediated, with the most common form of reaction being acute

hypersensitivity mediated by IgE antibodies (Type I hypersensitivity). Generally, outdoor mold exposure is considered more relevant than indoor exposure to mold allergies [11,12]. Approximately 10% of the population in the United States is estimated to have antibodies to mold antigens, and 5% are expected to manifest some form of clinical disease as a result of exposure [11]. Occupational studies in which indoor mold exposure was confirmed have failed to detect specific antibodies to *S. chartarum* [95,96]. A study of intranasal exposure in mice also noted a lack of antibodies against *S. chartarum* in serum samples [97]. The protein recently isolated by Xu et al. was shown to be antigenic in people [74], and this would seem to support the production of anti-*S. chartarum* antibodies in humans. Hyphal fragments have been shown to release allergens and are found in higher quantities in indoor air than intact spores and may be capable of contributing to allergic responses [12,88]. The IOM report concluded that exposure to molds in indoor environments is likely to contribute to asthma symptoms [1]. *S. chartarum* has been found in the homes of asthmatic children in higher quantities than those found in the homes of nonasthmatic children, though an association could only be suggested because this increase was not statistically significant [98]. Two studies report differing results regarding the effects of *S. chartarum* spores in a model of ovalbumin (OVA) – induced sensitization. Rosenblum et al. [99] observed that allergic airway inflammation caused by OVA decreased the inflammatory response to spores, rather than increasing airway susceptibility to the effects of the spores. Leino et al. [100] showed that inflammatory cytokine and chemokine expression was increased in

OVA-sensitized mice exposed to spores, and that a severe pulmonary inflammation resulted. However, like several other studies, serum samples contained no antibodies specific to *S. chartarum*. Many researchers have noted a lack of overall evidence to support an exact link between allergic responses and *S. chartarum*, and thus further investigation of this aspect is warranted [12,16,18,26].

Pulmonary Toxicity

Several studies have investigated the pulmonary effects of exposure to spores of *S. chartarum*. A single IT instillation of 1×10^4 spores resulted in neutrophilic alveolitis and identification of spores in lung histopathology. At 3 days after the instillation, the inflammatory infiltrate consisted mainly of histiocytes, and by 7 days after the instillation inflammation had cleared and spores were no longer observed. The same group conducted repeated IT exposures of 1×10^5 spores and observed neutrophils, macrophages, multinucleated giant cells, and eosinophils in the alveoli 4 days after the last exposure [101]. IT instillations of approximately 7×10^4 *S. chartarum* spores in mice resulted in granulomatous pulmonary inflammation, occasional lymphocytes, and cellular debris in alveolar airspaces. Capillaries appeared dilated and engorged between 24 and 48 hours after the instillation. Macrophages were observed to contain hemosiderin between 24 and 72 hours after instillation. Immunohistochemistry revealed decreased collagen IV labeling

in spore-treated mice. The authors quantified alveolar airspace and found significant decreases in spore-treated mice while there were no changes in saline control animals. The authors also instilled a group of animals with isosatratoxin F and found no evidence of inflammation, decreased collagen IV staining, hemosiderin-laden macrophages, or decreased alveolar airspace [102].

Pulmonary Studies in Infant Rats

Studies in Cleveland, Ohio and Kansas City, Missouri found a link between damp indoor environments, *S. chartarum*, and IPH in infant humans. Subsequent reviews by the CDC and IOM concluded that a sufficient causative link between *S. chartarum* and IPH had not been established. The search for further evidence of a connection between IPH and exposure to *S. chartarum* led to several studies in infant rats [21,22,103,104,105]. Infant rats were exposed to various doses of spores via single IT instillation. 2.7×10^5 spores per gram body weight (bw), which corresponds to 270 nanograms (ng) of SG per gram bw, was the determined LD₅₀ dose. Rat pups that died were found to have significant pulmonary hemorrhage. 1.1×10^5 spores per gram bw was found to produce the lowest mortality while still inducing pathology. BALF from rat pups exposed to this dose contained primarily alveolar macrophages at 3 days after instillation, though lymphocytes and neutrophils were also present. IL-1 β and TNF- α levels were also increased in BALF. Inflammation appeared to resolve by 8 days after instillation, with no evidence of inflammatory cells or proinflammatory cytokines

detectable in the BALF. Decreased respiratory rate, increased tidal volume, and increased pulmonary resistance were observed in spore-exposed rat pups seven days after instillation. Evaluation of lung histopathology was conducted in infant rats exposed to 4-8 X10⁵ spores per gram bw. Focal hemorrhage, hemosiderin-laden macrophages, and granulomas were found, with more severe hemorrhage in animals instilled with higher numbers of spores [49]. A recent study produced interesting results, though the authors did not extrapolate beyond their findings. IT instillation of 1X10⁴ spores of *S. chartarum* over 4 to 12 weeks resulted in pulmonary arterial hypertension (PAH) in mice, which the authors suggested may be an applicable model for human PAH [106]. Intact, ethanol-extracted, and autoclaved spores were compared to determine if other proteins produced by *S. chartarum* were involved in pulmonary inflammation. IT instillations of 1X10⁵ spores in infant rats were used to evaluate effects on alveolar space and inflammatory cells and cytokines in BALF. Alveolar space was most significantly reduced by intact spores, followed by ethanol-extracted and autoclaved spores. Neutrophils, lymphocytes, macrophages, IL-1 β , TNF- α , and total protein were increased in BALF. The most significant changes in inflammatory cells, cytokines, and protein levels were seen in intact spores, followed by autoclaved and ethanol-extracted spores, indicating that fungal proteins may be contributing to the inflammatory response [107].

Differential Pulmonary Effects of the Chemotypes of *S. chartarum*

Rand et al. [108] observed significant changes in alveolar macrophages and type II alveolar cells in response to IT exposure to either *S. chartarum* spores or isosatratoxin F. These cells were found to be highly sensitive, and alterations such as swelling and irregularly aligned cristae were observed in the mitochondria of type II alveolar cells. In another study, a single IT instillation of *S. chartarum* spores or isosatratoxin F resulted in impaired incorporation of surfactant components [109]. Stachylysin and SG have been immunochemically identified in alveolar macrophages and type II alveolar cells [36,47]. IT exposure to the spores of a macrocyclic trichothecene producing-strain induced increased mRNA expression of macrophage inflammatory protein 2 (MIP-2) and surfactant protein-D (SP-D) compared to a non-toxin producing strain. The authors also noted an increase TNF- α expression in all groups receiving spores compared to control animals receiving IT saline [110]. In contrast, Leino et al. [97] did not detect differences in IL-1 β , IL-6, and TNF- α in BALF collected from mice receiving toxin-producing and non-toxin producing strains of *S. chartarum*. These cytokines were significantly increased compared to saline controls, as were several chemokines including MIP-2 and monocyte-chemoattractant protein (MCP-1). Inflammatory infiltrates in BALF were also similar between the two chemotypes, with an IT instillation of 1×10^5 spores inducing increases in macrophages, neutrophils, and lymphocytes.

Other groups have also addressed the differences in toxicity between the two chemotypes of *S. chartarum*. Ochiai et al. [101] noted a more severe inflammatory infiltrate in the alveoli of animals exposed to a toxin-producing

strain. In another study, IT exposure to the same macrocyclic trichothecene-producing strain resulted in dose-dependent increases in total protein, albumin, and IL-6 in BALF compared to an atranone-producing strain, though total protein, albumin, and IL-6 were also increased in animals receiving the atranone-producing strain compared to control animals. The macrocyclic trichothecene-producing chemotype was also found to be more cytotoxic at a high exposure level (3000 spores per gram bw), but no difference in cytotoxicity was noted at the low exposure dose (30 spores per gram bw). Interestingly, TNF- α levels were similar in the BALF of animals exposed to both chemotypes of *S. chartarum*, and IL-1 β , while initially increased equally in both strains, remained significantly increased for a longer period in animals receiving the atranone-producing strain. These authors found a no adverse effect level (NOAEL) of 30 spores per gram bw for both chemotypes of *S. chartarum* [111]. They noted that some of the differences in the known effects of exposure could likely be attributed to differences in the two strains, as has been suggested by previous studies [36,109].

When Yike et al. [49] exposed infant rats to ethanol-extracted, trichothecene-free spores, they found little adverse effect after IT instillation, and therefore concluded that pulmonary toxicity was at least in part due to toxins produced by *S. chartarum*. Rao et al. [112] found that methanol-extracted spores exhibited little toxicity compared to intact spores, and most parameters measured in BALF, such as inflammatory cell infiltration, hemoglobin concentrations, and

albumin content, were not significantly difference between rats receiving methanol-extracted spores and saline.

Murine Strain Differences in Pathology Resulting from Exposure to *S. chartarum*

Some important considerations were recently described by Rosenblum et al. [113] in a study comparing the pulmonary responses of BALB/c and C57BL/6 mice to IT instillation of *S. chartarum* spores. Comparable numbers of spores were found in the lungs of BALB/c and C57BL/6 mice immediately after instillation. BALB/c mice had significantly higher levels of TNF- α , KC, and MIP-2, MCP-1, IL-1 β , IL-6, and other cytokines and chemokines in BALF compared to C57BL/6 mice, though both strains had increases of these inflammatory cytokines compared to control animals. BALB/c mice also had a higher number of neutrophils and higher levels of a marker of neutrophil degranulation than the other strains. The authors concluded that BALB/c mice were the most sensitive to the pulmonary effects of *S. chartarum* exposure, and C57BL/6 mice were the most resistant. The authors note that alveolar macrophages from C57BL/6 mice have higher phagocytic capacity than those from BALB/c mice and suggest that this may partially explain the strain difference. They also point out that, while typically model-dependent, BALB/c mice tend to be Th2 immune response dominant, and C57BL/6 mice are Th1 dominant. Such differences in people may contribute to individual sensitivity to inhalation exposures of *S. chartarum*.

Intranasal Instillations of *S. chartarum*

Nikulin et al. [114] instilled SG-containing spores into the noses of mice and evaluated the resultant changes in the lung. A single instillation of 10^6 spores resulted in infiltration of neutrophils, lymphocytes, and macrophages into the alveolar spaces, bronchioles, and interstitium on histopathology. Hemorrhagic exudates were also noted in the alveolar spaces. In the same study, another group of mice was instilled with a *S. chartarum* strain that did not produce macrocyclic trichothecenes. The result of this study was similar to those reported by others [101,110] in that significantly milder pulmonary inflammation was noted in mice instilled with the strain that did not produce macrocyclic trichothecenes. In a subsequent study, mice instilled with 10^3 or 10^5 spores twice a week for 3 weeks had similar, dose-dependent inflammatory infiltration. The authors again compared the two chemotypes of *S. chartarum* and found a similar trend. Mice instilled with 10^5 spores that did not contain macrocyclic trichothecenes had only mild inflammation, and no inflammation was observed in the mice instilled with 10^3 spores [115].

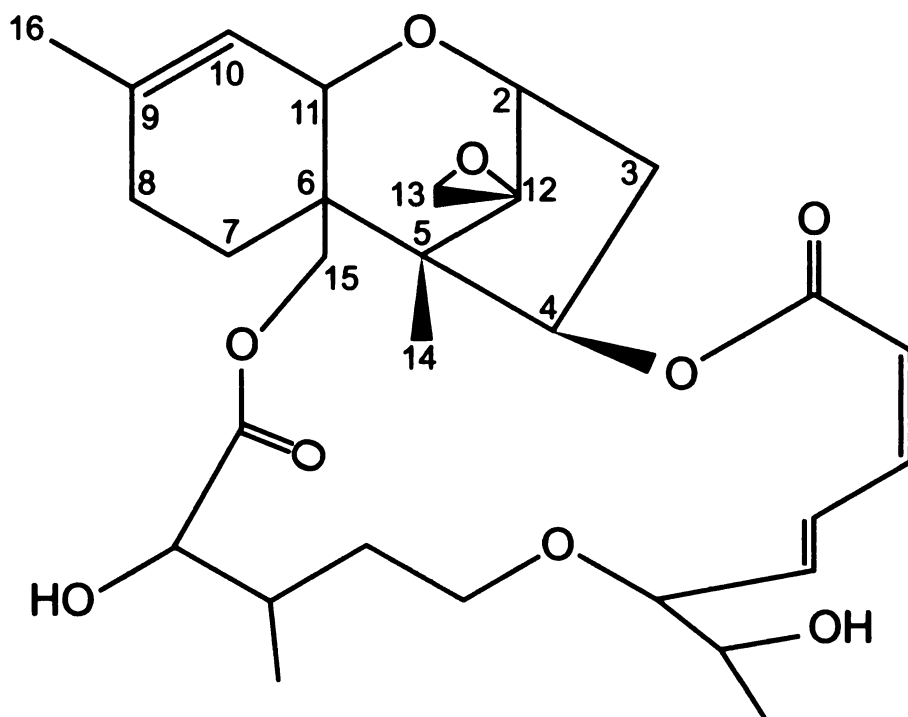
Nasal Pathology and Intranasal Instillations of *S. chartarum*

As previously mentioned, the nose represents a potential target of *S. chartarum* and macrocyclic trichothecene-induced toxicity due to the potential for spores to lodge in the nasal passages [32,88]. The nose has many functions, including conditioning of incoming air, absorption of water-soluble gases, trapping of particulates, and metabolism of inhaled xenobiotics [3]. Few studies

have investigated the effects of intranasal instillations of *S. chartarum* or macrocyclic trichothecenes in the nose [97,100]. A single intranasal instillation of SG was found to induce dose-dependent apoptosis of olfactory sensory neurons (OSNs) and atrophy of olfactory epithelium (OE) in C57BL/6 mice. Interestingly, the OE of the dorsal medial meatus was unaffected. A neutrophilic rhinitis was also observed at 24 hours post-instillation. NOAEL and lowest observed adverse effect level (LOAEL) were found to be 5 and 25 µg/kg bw, respectively.

Maximum atrophy of OE was observed at 3 days after instillation with a dose of 500 µg/kg bw. Ethmoid turbinates (ET) were microdissected and rt-PCR was used to evaluate pro-apoptotic gene expression. Fas, FasL, p75NGFR, p53, Bax, caspase 3, and caspase-activated DNase (CAD) were elevated in mice instilled with SG. Increased expression of the inflammatory cytokines TNF-α, IL-1α, IL-1β; and IL-6, and the chemokine MIP-2, was also observed. The olfactory nerve and glomerular layers of the olfactory bulb (OB) of the brain were also found to be atrophied. TNF-α, IL-6, and MIP-2 expression were also increased in the OB of SG-instilled animals. Mice exposed to 100 µg/kg bw for 5 consecutive days showed similar atrophy and apoptosis of OE [116].

A study investigating the effects of single intranasal instillations of another representative macrocyclic trichothecene mycotoxin, Roridin A (RA, **Figure 3**), recapitulated the observations of the SG study. RA is commercially available and was used as a surrogate for SG. Mice dosed with 250 or 500 µg/kg bw had apoptosis of OSNs and atrophy of OE and the olfactory sensory nerve layer of the OB at 1 and 3 days after the instillation but not at 6 and 12 hours following



Roridin A

Figure 3. Chemical structure of Roridin A. (Adapted from http://www.cbwinfo.com/Biological/Toxins/trichothecene_mycotoxins.htm)

instillation. Neutrophilic rhinitis was observed at 3 days after instillation of RA. Rt-PCR was again utilized to assess proapoptotic gene expression as well as proinflammatory cytokine and chemokine expression. Expression of Fas, PKR, p53, Bax, and CAD were observed. Expression of Fas was noted to increase at 6 hours following instillation, preceding apoptotic death of OSNs.

Proinflammatory cytokines and chemokines were assessed in microdissected ET and OB. TNF- α , IL-1 β , IL-6, and MIP-2 expression was increased at 6 hours and remained elevated at 1 day in ET. IL-6 and MIP-2 expression was elevated in OB between 6 and 12 hours [117].

The results of these studies indicate that the nose is indeed a potential target of macrocyclic trichothecene toxicity, though they provide information only on acute intranasal exposures in adult mice. The purposes of the following studies were to i) investigate the effects of repeated intranasal exposures to a representative macrocyclic trichothecene, RA, ii) compare the effects of SG in the nasal passages of weanling and adult mice, and iii) investigate the nasal and pulmonary effects of intranasal co-exposures to *S. chartarum* spores and SG.

CHAPTER 2 BIBLIOGRAPHY

- 1 Institute of Medicine. (2004) *Damp Indoor Spaces and Health*. Washington DC: National Academies Press.
- 2 Hodgson M. (2002) Indoor Environmental Exposures and Symptoms. *Environmental Health Perspectives* 110 (Supplement 4):663-667.
- 3 Harkema JR, Carey SA, Wagner JG. (2006) The nose revisited: a brief review of the comparative structure, function, and toxicologic pathology of the nasal epithelium. *Toxicological Pathology* 34:252-269.
- 4 Cooley JD, Wong WC, Jumper CA, Straus DC. (1998) Correlation between the prevalence of certain fungi and sick building syndrome. *Occupational Environmental Medicine* 55:579-584.
- 5 Molhave, L. (1992) Controlled experiments for studies of the sick building syndrome. *Annals of the New York Academy of Sciences* 641:46-55.
- 6 Ahearn DG, Crow SA, Simmons RB, Price DL, Noble JA, Mishra SK, Pierson DL. (1996) Fungal colonization of fiberglass insulation in the air distribution system of a multi-story office building: VOC production and possible relationship to a sick building syndrome. *Journal of Industrial Microbiology* 16:280-285.
- 7 Ahearn DG, Crow SA, Simmons RB, Price DL, Mishra SK, Pierson DL. (1997) Fungal colonization of air filters and insulation in a multi-story office building: production of volatile organics. *Current Microbiology* 35:305-308.
- 8 Reinikainen LM, Aunela-Tapola L, Jaakkola JJ. (1997) Humidification and perceived indoor air quality in the office environment. *Occupational and Environmental Medicine* 54:322-327.
- 9 Solomon GM, Hjelmroos-Koski M, Rotkin-Ellman M, Hammond SK. (2006) Airborne Mold and Endotoxin Concentrations in New Orleans, Louisiana, after Flooding, October through November 2005. *Environmental Health Perspectives* 114(9):1381-1386.
- 10 Nielsen KF. (2003) Mycotoxin production by indoor molds. *Fungal Genetics and Biology* 39:103-117.
- 11 Hardin BD, Kelman BJ, Saxon A. (2003) Adverse human health effects associated with molds in the indoor environment. *Journal of Occupational Environmental Medicine* 45(5):470-478.

- 12 Bush RK, Portnoy JM, Saxon A, Terr AI, Wood RA. (2006) The medical effects of mold exposure. *Journal of Allergy and Clinical Immunology* 117(2):326-333.
- 13 Green BJ, Tovey ER, Sercombe JK, Blachere FM, Beezhold DH, Schmechel D. (2006) Airborne fungal fragments and allergenicity. *Medical Mycology* 44 (Supplement):S245-S255.
- 14 Cox-Ganser JM, White SK, Jones R, Hilsbos K, Storey E, Enright PL, Rao CY, Kreiss K. (2005) Respiratory morbidity in office workers in a water-damaged building. *Environmental Health Perspectives* 113(4):485-490.
- 15 Wakefield J. (2002) Learning the Hard Way: The Poor Environment of America's Schools. *Environmental Health Perspectives* 110(6):A298-A305.
- 16 Kuhn DM and Ghannoum, MA. (2003) Indoor mold, toxigenic fungi, and *Stachybotrys chartarum*: infectious disease perspective. *Clinical Microbiology Reviews* 16(1):144-172.
- 17 Park J, Cox-Ganser JM, Kreiss K, White SK, Rao CY. (2008) Hydrophilic fungi and ergosterol associated with respiratory illness in a water-damaged building. *Environmental Health Perspectives* 116(1):45-50.
- 18 Hossain MA, Ahmed MS, Ghannoum MA. (2004) Attributes of *Stachybotrys chartarum* and its association with human disease. *Journal of Allergy and Clinical Immunology* 113(2):200-208.
- 19 Kuhn RC, Trimble MW, Hofer V, Lee M, and Nassof RS. (2005) Prevalence and airborne spore levels of *Stachybotrys spp.* in 200 houses with water incursions in Houston, Texas. *Canadian Journal of Microbiology* 51:25-28.
- 20 Sudakin D and Fallah P. (2008) Toxigenic fungi and mycotoxins in outdoor, recreational environments. *Clinical Toxicology* 46(8):738-744.
- 21 Dearborn DG, Yike I, Sorenson WG, Miller MJ, Etzel RA. (1999) Overview of Investigations into Pulmonary Hemorrhage among Infants in Cleveland, Ohio. *Environmental Health Perspectives* 107(Supplement 3):495-499.
- 22 Flappan SM, Portnoy J, Jones P, Barnes C. (1999) Infant Pulmonary Hemorrhage in a Suburban Home with Water Damage and Mold (*Stachybotrys atra*). *Environmental Health Perspectives* 107(11):927-930.

- 23 Andersson MA, Nikulin M, Koljalg U, Andersson MC, Rainey F, Reijula K, Hintikka EL, Salkinoja-Salonen M. (1997) Bacteria, molds, and toxins in water-damaged building materials. *Applied Environmental Microbiology* 63(2):387-393.
- 24 Johanning E, Biagini R, Hull D, Morey P, Jarvis B, and Landsbergis P. (1996) Health and immunology study following exposure to toxigenic fungi (*Stachybotrys chartarum*) in a water-damaged office environment. *International Archives of Occupational Environmental Health* 68:207-218.
- 25 Johanning E, Landsbergis P, Gareis M, Yang CS, Olmsted E. (1999) Clinical Experience and Results of a Sentinel Health Investigation Related to Indoor Fungal Exposure. *Environmental Health Perspectives* 107(Supplement 3):489-494.
- 26 Pestka JJ, Yike I, Dearborn DG, Ward MDW, and Harkema JR. (2008) *Stachybotrys chartarum*, trichothecene mycotoxins, and damp building-related illness: new insights into a public health enigma. *Toxicological Sciences* 104(1):4-26.
- 27 Larone DH. (2002) *Stachybotrys chartarum*, p.214, in *Medically Important Fungi, A Guide to Identification*. 4th Ed. ASM Press, Washington D.C.
- 28 Jarvis BB, Sorenson WG, Hintikka E, Nikulin M, Zhou Y, Jiang J, Wang S, Hinkley S, Etzel RA, Dearborn D. (1998) Study of toxin production by isolates of *Stachybotrys chartarum* and *Memnoniella echinata* isolated during a study of pulmonary hemosiderosis in infants. *Applied and Environmental Microbiology* 64(10):3620-3625.
- 29 Tucker K, Stolze JL, Kennedy AH, Money NP. (2007) Biomechanics of conidial dispersion in the toxic mold *Stachybotrys chartarum*. *Fungal Genetics and Biology* 44:641-647.
- 30 Douwes J. (2005) (1→3)-β-D-glucans and respiratory health: a review of the scientific evidence. *Indoor Air* 15:160-169.
- 31 Andersen B, Nielsen KF, Jarvis BB. (2002) Characterization of *Stachybotrys* from water-damaged buildings based on morphology, growth, and metabolite production. *Mycologia* 94(3):392-403.
- 32 Wilkins CK, Larsen ST, Hammer M, Poulsen OM, Wolkoff P, Nielsen GD. (1998) Respiratory effects in mice exposed to airborne emissions

from *Stachybotrys chartarum* and implications for risk assessment. *Pharmacology and Toxicology* 83:112-119.

- 33 Nielsen KF, Huttunen K, Hyvärinen A, Andersen B, Jarvis BB, Hirvonen M. (2002) Metabolite profiles of *Stachybotrys* isolates from water-damaged buildings and their induction of inflammatory mediators and cytotoxicity in macrophages. *Mycopathologia* 154:201-205.
- 34 Yike I, Rand T, Dearborn DG. (2007) The role of fungal proteinases in pathophysiology of *Stachybotrys chartarum*. *Mycopathologia* 164:171-181.
- 35 Vesper SJ, Magnuson ML, Dearborn DG, Yike I, Haugland RA. (2001) Initial characterization of the hemolysin stachylysin from *Stachybotrys chartarum*. *Infection and Immunity* 69(2):912-916.
- 36 Gregory L, Rand TG, Dearborn D, Yike I, Vesper S. (2003) Immunocytochemical localization of stachylysin in *Stachybotrys chartarum* spores and spore-impacted mouse and rat lung tissue. *Mycopathologia* 156:109-117.
- 37 Vesper SJ and Vesper MJ. (2002) Stachylysin may be a cause of hemorrhaging in humans exposed to *Stachybotrys chartarum*. *Infection and Immunity* 70(4):2065-2069.
- 38 Bennett JW and Klich M. (2003) Mycotoxins. *Clinical Microbiology Reviews* 16(3):497-516.
- 39 Jarvis BB and Miller JD. (2005) Mycotoxins as harmful indoor air contaminants. *Applied Microbiology and Biotechnology* 66:367-372.
- 40 Hendry KM and Cole EC. (1993) A review of mycotoxins in indoor air. *Journal of Toxicology and Environmental Health* 38:183-198.
- 41 Hinkley SF, Mazzola EP, Fettinger JC, Lam, Y, Jarvis BB. (2000) Atranones A-G, from the toxigenic mold *Stachybotrys chartarum*. *Phytochemistry* 55:663-673.
- 42 Fung F and Clark RF. (2004) Health effects of mycotoxins: a toxicological overview. *Journal of Toxicology Clinical Toxicology* 42(2):217-234.
- 43 Steinmetz WE, Robustelli P, Edens E, Heineman D. (2008) Structure and conformational dynamics of trichothecene mycotoxins. *Journal of Natural Products* 71(4):589-594.

- 44 Yang G, Jarvis BB, Chung Y, Pestka JJ. (2000) Apoptosis induction by the Satratoxins and other trichothecene mycotoxins: relationship to ERK, p38 MAPK, and SAPK/JNK activation. *Toxicology and Applied Pharmacology* 164:149-160.
- 45 Chung Y, Yang G, Islam Z, Pestka JJ. (2003) Up-regulation of macrophage inflammatory protein-2 and complement 3A receptor by the trichothecenes deoxynivalenol and satratoxin G. *Toxicology* 186:51-65.
- 46 Engler KH, Coker RD, Evans IH. (1999) A colorimetric technique for detecting trichothecenes and assessing relative potencies. *Applied Environmental Microbiology* 65(5):1854-1857.
- 47 Gregory L, Pestka JJ, Dearborn DG, Rand TG. (2004) Localization of Satratoxin-G in *Stachybotrys chartarum* spores and spore-impacted mouse lung using immunocytochemistry. *Toxicologic Pathology* 32:26-34.
- 48 Sorenson WG, Frazer DG, Jarvis BB, Simpson J, Robinson VA. (1987) Trichothecene mycotoxins in aerosolized conidia of *Stachybotrys atra*. *Applied and Environmental Microbiology* 53(6):1370-1375.
- 49 Yike I, Miller MJ, Sorenson WG, Walenga R, Tomaszefski Jr. JF, Dearborn DG. (2002) Infant animal model of pulmonary mycotoxicosis induced by *Stachybotrys chartarum*. *Mycopathologia* 154:139-152.
- 50 Brasel TL, Douglas DR, Wilson SC, Straus DC. (2005) Detection of airborne *Stachybotrys chartarum* macrocyclic trichothecene mycotoxins on particulates smaller than conidia. *Applied and Environmental Microbiology* 71(1):114-122.
- 51 Karunasena E, Cooley JD, Douglas DR, Straus DC. (2004) Protein translation inhibition by *Stachybotrys chartarum* conidia with and without the mycotoxin containing polysaccharide matrix. *Mycopathologia* 158:87-97.
- 52 Brasel TL, Martin JM, Carriker CG, Wilson SC, Straus DC. (2005) Detection of airborne *Stachybotrys chartarum* macrocyclic trichothecene mycotoxins in the indoor environment. *Applied and Environmental Microbiology* 71(11):7376-7388.
- 53 Charpin-Kadouch C, Maurel G, Felipo R, Quertalt J, Ramadour M, Dumon H, Garans M, Botta A, Charpin D. (2006) Mycotoxin identification in moldy dwellings. *Journal of Applied Toxicology* 26:475-479.

- 54 Ueno Y. (1984) General toxicology, p.135-145, in *Trichothecenes: Chemical, Biological, and Toxicological Aspects*. Ueno Y (ed.) Elsevier, New York.
- 55 Shifrin VI and Anderson P. (1999) Trichothecene mycotoxins trigger a ribotoxic stress response that activates c-Jun N-terminal kinase and p38 mitogen-activated protein kinase and induces apoptosis. *Journal of Biological Chemistry* 274(20):13985-13992.
- 56 Ehrlich KC and Daigle KW. (1987) Protein synthesis inhibition by 8-oxo-12,13-epoxytrichothecenes. *Biochimica et biophysica acta* 923(2):206-213.
- 57 Chung Y, Zhou H, Pestka JJ. (2003) Transcriptional and posttranscriptional roles for p38 mitogen-activated protein kinase in upregulation of TNF- α expression by deoxynivalenol (vomitoxin). *Toxicology and Applied Pharmacology* 193:188-201.
- 58 Moon Y and Pestka JJ. (2003) Deoxynivalenol-induced mitogen-activated protein kinase phosphorylation and IL-6 expression in mice suppressed by fish oil. *Journal of Nutritional Biochemistry* 14:717-726.
- 59 Zhou H, Islam Z, Pestka JJ. (2005) Induction of competing apoptotic and survival signaling pathways in the macrophage by the ribotoxic trichothecene deoxynivalenol. *Toxicological Sciences* 87(1):113-122.
- 60 Li M and Pestka JJ. (2008) Comparative induction of 28S ribosomal RNA cleavage by ricin and the trichothecenes deoxynivalenol and T-2 toxin in the macrophage. *Toxicological Sciences* 105(1):67-78.
- 61 Pestka JJ, Zhou H, Chung Y. (2004) Cellular and molecular mechanisms for immune modulation by deoxynivalenol and other trichothecenes: unraveling a paradox. *Toxicology Letters* 153:61-73.
- 62 Nusuetrong P, Pengsuparp T, Meksuriyen D, Tanitsu M, Kikuchi H, Mizugaki M, Shimazu K, Oshima Y, Nakahata N, Yoshida M. (2008) Satratoxin H generates reactive oxygen species and lipid peroxides in PC12 cells. *Biological and Pharmaceutical Bulletin* 31(6):1115-1120.
- 63 McCrae KC, Rand TG, Shaw RA, Mantsch HH, Sowa MG, Thliveris JA, Scott JE. (2007) DNA fragmentation in developing lung fibroblasts exposed to *Stachybotrys chartarum* (atra) toxins. *Pediatric Pulmonology* 42(7):592-599.
- 64 Wang H and Yadav JS. (2006) DNA damage, redox changes, and associated stress-inducible signaling events underlying the apoptosis

and cytotoxicity in murine alveolar macrophage cell line MH-S by methanol-extracted *Stachybotrys chartarum* toxins. *Toxicology and Applied Pharmacology* 214:297-308.

- 65 Islam Z, Hegg CC, Bae HK, Pestka JJ. (2008) Satratoxin G-induced apoptosis in PC-12 neuronal cells is mediated by PKR and caspase independent. *Toxicological Sciences* 105(1):142-152.
- 66 Nusuetrong P, Yoshida M, Tanitsu M, Kikuchi H, Mizugaki M, Shimazu K, Pengsuparp T, Meksuriyen D, Oshima Y, Nakahata, N. (2005) Involvement of reactive oxygen species and stress-activated MAPKs in Satratoxin H-induced apoptosis. *European Journal of Pharmacology* 507(1-3):239-246.
- 67 Portnoy JM, Barnes CS, Kennedy K. (2004) Sampling for indoor fungi. *Journal of Allergy and Clinical Immunology* 113(2):189-198.
- 68 Dillon HK, Miller, JD, Sorenson WG, Douwes J, Jacobs RR. (1999) Review of methods applicable to the assessment of mold exposure to children. *Environmental Health Perspectives* 107(S3):473-480.
- 69 Andersen B and Nissen AT. (2000) Evaluation of media for detection of *Stachybotrys* and *Chaetomium* species associated with water-damaged buildings. *International Biodeterioration & Biodegradation* 46: 111-116.
- 70 Wilson SC, Carriker CG, Brasel TL, Karunasena E, Douglas DG, Wu C, Andriychuk LA, Fogle MR, Martin JM, Straus DC. (2004) Culturability and toxicity of sick building syndrome-related fungi over time. *Journal of Occupational and Environmental Hygiene* 1:500-504.
- 71 Jarvis BB. (2003) Analysis of mycotoxins: the chemist's perspective. *Archives of Environmental Health* 58(8):479-483.
- 72 Sudakin DL. (1998) Toxicogenic fungi in a water-damaged building: an intervention study. *American Journal of Industrial Medicine* 34:183-190.
- 73 Lindsley WG, Schmechel D, Chen BT. (2006) A two-stage cyclone using microcentrifuge tubes for personal bioaerosol sampling. *Journal of Environmental Monitoring* 8(11):1136-1142.
- 74 Xu Z, Liang Y, Belisle D, Miller JD. (2008) Characterization of monoclonal antibodies to an antigenic protein from *Stachybotrys chartarum* and its measurement in house dust. *Journal of Immunological Methods* 332:121-128.

- 75 Vesper SJ, Dearborn DG, Yike I, Sorenson WG, Haugland RA. (1999) Hemolysis, toxicity, and randomly amplified polymorphic DNA analysis of *Stachybotrys chartarum* strains. *Applied and Environmental Microbiology* 65(7):3175-3181.
- 76 Vesper SJ, Varma M, Wymer LJ, Dearborn DG, Sobolewski J, Haugland RA. (2004) Quantitative polymerase chain reaction analysis of fungi in dust from homes of infants who developed pulmonary hemorrhaging. *Journal of Occupational and Environmental Medicine* 46(6):596-601.
- 77 Vesper SJ, McKinstry C, Haugland R, Wymer L, Bradham K, Ashley P, Cox D, Dewalt G, Friedman W. (2007) Development of an environmental relative moldiness index for US homes. *Journal of Occupational Environmental Medicine* 49(8):829-833.
- 78 Yike I, Allan T, Sorenson WG, Dearborn DG. (1999) Highly sensitive protein translation assay for trichothecene toxicity in airborne particulates: comparison with cytotoxicity assays. *Applied Environmental Microbiology* 65(1):88-94.
- 79 Chung YJ, Jarvis BB, Tak H, Pestka JJ. (2003) Immunochemical assay for satratoxin G and other macrocyclic trichothecenes associated with indoor air contamination by *Stachybotrys chartarum*. *Toxicology Mechanisms and Methods* 13:247-252.
- 80 Bloom E, Bal K, Nyman E, Must A, Larsson L. (2007) Mass spectrometry-based strategy for direct detection and quantification of some mycotoxins produced by *Stachybotrys* and *Aspergillus spp.* in indoor environments. *Applied and Environmental Microbiology* 73(13):4211-4217.
- 81 Tuomi T, Reijula K, Johnsson T, Hemminki K, Hintikka E, Lindroos O, Kalso S, Koukila-Kähkölä P, Mussalo-Rauhamaa H, Haahtela T. (2000) Mycotoxins in crude building materials from water-damaged buildings. *Applied and Environmental Microbiology* 66(5):1899-1904.
- 82 Bloom E, Bal K, Nyman E, Larsson L. (2007) Optimizing a GC-MS method for screening of *Stachybotrys* mycotoxins in indoor environments. *Journal of Environmental Monitoring* 9:151-156.
- 83 Gottschalk C, Bauer J, Meyer K. (2008) Detection of Satratoxin G and Satratoxin H in indoor air from a water-damaged building. *Mycopathologia* 166:103-107.

- 84 Yike I, Distler AM, Ziady AG, Dearborn DG. (2006) Mycotoxin adducts on human serum albumin: biomarkers of exposure to *Stachybotrys chartarum*. *Environmental Health Perspectives* 114(8):1221-1226.
- 85 Mader DR, Yike I, Distler AM, Dearborn DG. (2007) Acute pulmonary hemorrhage during isoflurane anesthesia in two cats exposed to toxic black mold (*Stachybotrys chartarum*). *Journal of the American Veterinary Medical Association* 231(5):731-735.
- 86 Gravesen S, Nielsen PA, Iversen R, Nielsen KF. (1999) Microfungal contamination of damp buildings – examples of risk constructions and risk materials. *Environmental Health Perspectives* 107(S3):505-508.
- 87 Fung F and Hughson WG. (2003) Health effects of indoor fungal bioaerosol exposure. *Applied Occupational and Environmental Hygiene* 18:535-544.
- 88 Cho S, Seo S, Schmechel D, Grinshpun SA, Reponen T. (2005) Aerodynamic characteristics and respiratory deposition of fungal fragments. *Atmospheric Environment* 39(30):5454-5465.
- 89 Salvi S. and Holgate ST. (1999) Mechanisms of particulate matter toxicity. *Clinical and Experimental Allergy* 29:1187-1194.
- 90 Yike I and Dearborn DG. (2004) Pulmonary effects of *Stachybotrys chartarum* in animal studies. *Advanced Applied Microbiology* 55:241-273.
- 91 Forgacs J. (1972) Stachybotryotoxicosis, p. 95-128, in *Microbial Toxins*, vol.8. Kadis S, Ciegler A, Aji SJ (ed.) Academic Press, Inc., New York, NY.
- 92 Schneider DJ, Marasas WFO, Kuys JCD, Kriek NPJ, Van Schalkwyk GC. (1979) A field outbreak of stachybotryotoxicosis in sheep. *Journal of the South African Veterinary Association* 50(2):73-81.
- 93 Elidemir O, Colasurdo GN, Rossmann SN, Fan LL. (1999) Isolation of *Stachybotrys* from the lung of a child with pulmonary hemosiderosis. *Pediatrics* 104:964-966.
- 94 Yike I, Vesper S, Tomashefski Jr. JF, Dearborn DG. (2003) Germination, viability and clearance of *Stachybotrys chartarum* in the lungs of infant rats. *Mycopathologia* 156:67-75.
- 95 Johanning E, Biagini R, Hull D, Morey P, Jarvis B, Lansbergis P. (1996) Health and immunology following exposure to toxigenic fungi

(*Stachybotrys chartarum*) in a water-damaged office environment. *International Archives of Occupational and Environmental Health* 68(4):207-218.

- 96 Trout D, Bernstein J, Martinez K, Biagini R, Wallingford K. (2001) Bioaerosol lung damage in a worker with repeated exposure to fungi in a water-damaged building.
- 97 Leino M, Mäkelä M, Reijula K, Haahtela T, Mussalo-Rauhamaa H, Tuomi T, Hintikka E, Alenius H. (2003) Intranasal exposure to a damp building mould, *Stachybotrys chartarum*, induces lung inflammation in mice by Satratoxin-independent mechanisms. *Clinical and Experimental Allergy* 33:1603-1610.
- 98 Vesper SJ, McKinstry C, Haugland RA, Kercksmar CM, Yike I, Schluchter MD, Kirchner HL, Sobolewski J, Allan TM, Dearborn DG. (2006) Specific molds associated with asthma in water-damaged homes. *Journal of Occupational and Environmental Medicine* 48(8):852-858.
- 99 Rosenblum JH, Molina RM, Donaghey TC, Brain JD. (2002) Murine pulmonary responses to *Stachybotrys chartarum* have genetic determinants. *American Journal of Respiratory and Critical Care Medicine* 165:A537.
- 100 Leino MS, Alenius HT, Fyhrquist-Vanni N, Wolff HJ, Reijula KE, Hintikka E, Salkinoja-Salonen MS, Haahtela T, Mäkelä MJ. (2006) Intranasal exposure to *Stachybotrys chartarum* enhances airway inflammation in allergic mice. *American Journal of Respiratory and Critical Care Medicine* 173:512-518.
- 101 Ochiai E, Kamei K, Hiroshima K, Watanabe A, Hashimoto Y, Sato A, Ando A. (2005) The Pathogenicity of *Stachybotrys chartarum*. *Japanese Journal of Medical Mycology* 46:109-117.
- 102 Rand TG, White K, Logan A, Gregory L. (2002) Histological, immunohistochemical and morphometric changes in lung tissue in juvenile mice experimentally exposed to *Stachybotrys chartarum* spores. *Mycopathologia* 156:119-131.
- 103 CDC: Update: pulmonary hemorrhage/hemosiderosis among infants – Cleveland, Ohio, 1993-1996. (2000) *MMWR* 49(9):180-184.
- 104 CDC: Errata: Vol. 49, No. 9 (2000) *MMWR* 49(10)
<http://cdc.gov/mmwr/preview/mmwrhtml/mm4910a7.htm>

- 105 CDC: Reports of Members of the CDC External Expert Panel on Acute Idiopathic Pulmonary Hemorrhage in Infants: A Synthesis (1999)
http://www.cdc.gov/mold/pdfs/aiphi_report.pdf
- 106 Ochiai E, Kamei K, Watanabe A, Nagayoshi M, Tada Y, Nagaoka T, Sato K, Sato A, Shibuya K. (2008) Inhalation of *Stachybotrys chartarum* causes pulmonary arterial hypertension in mice. *International Journal of Experimental Pathology* 89:201-208.
- 107 Yike I, Rand TG, Dearborn DG. (2005) Acute inflammatory responses to *Stachybotrys chartarum* in the lungs of infant rats: time course and possible mechanisms. *Toxicological Sciences* 84(2):408-417.
- 108 Rand TG, Mahoney M, White K, Oulton M. (2002) Microanatomical changes in alveolar type II cells in juvenile mice intratracheally exposed to *Stachybotrys chartarum* spores and toxin. *Toxicological Sciences* 65:239-245.
- 109 Mason CD, Rand TG, Oulton M, MacDonald JM, Scott JE. (1998) Effects of *Stachybotrys chartarum* (*atra*) conidia and isolated toxin on lung surfactant production and homeostasis. *Natural Toxins* 6:27-33.
- 110 Hudson B, Flemming J, Sun G, Rand TG. (2005) Comparison of immunomodulator mRNA and protein expression in the lungs of *Stachybotrys chartarum* spore-exposed mice. *Journal of Toxicology and Environmental Health Part A* 68:1321-1335.
- 111 Flemming J, Hudson B, Rand TG. (2004) Comparison of inflammatory and cytotoxic lung responses in mice after intratracheal exposure to spores of two different *Stachybotrys chartarum* strains. *Toxicological Sciences* 78(2):267-275.
- 112 Rao CY, Brain JD, Burge HA. (2000) Reduction of pulmonary toxicity of *Stachybotrys chartarum* spores by methanol extraction of mycotoxins. *Applied and Environmental Microbiology* 66(7):2817-2821.
- 113 Rosenblum Lichtenstein JH, Molina RM, Donaghey TC, Brain JD. (2006) Strain differences influence murine pulmonary responses to *Stachybotrys chartarum*. *American Journal of Respiratory Cell and Molecular Biology* 35(4):415-423.
- 114 Nikulin M, Reijula K, Jarvis BB, Hintikka E. (1996) Experimental lung mycotoxicosis in mice induced by *Stachybotrys atra*. *International Journal of Experimental Pathology* 77:2213-218.

- 115 Nikulin M, Reijula K, Jarvis BB, Veijalainen P, Hintikka E. (1997) Effects of intranasal exposure to spores of *Stachybotrys atra* in mice. *Fundamental Applied Toxicology* 35:182-188.
- 116 Islam Z, Harkema JR, Pestka JJ. (2006) Satratoxin G from the black mold *Stachybotrys chartarum* evokes olfactory sensory neuron loss and inflammation in the murine nose and brain. *Environmental Health Perspectives* 114(7):1099-1107.
- 117 Islam Z, Amuzie CJ, Harkema JR, Pestka JJ. (2007) Neurotoxicity and inflammation in the nasal airways of mice exposed to the macrocyclic trichothecene mycotoxin Roridin A: kinetics and potentiation by bacterial lipopolysaccharide coexposure. *Toxicological Sciences* 98(2):526-541.

CHAPTER 2 FIGURE BIBLIOGRAPHY

Figure 1:

Tuomi T, Saarinen L, Reijula K. (1998) Detection of polar and macrocyclic trichothecene mycotoxins from indoor environments. *Analyst* 123:1835-1841.

Figure 2:

Nielsen KF. (2003) Mycotoxin production by indoor molds. *Fungal Genetics and Biology* 39:103-117.

Pestka JJ, Yike I, Dearborn DG, Ward, MDW, Harkema JR. (2008) *Stachybotrys chartarum*, trichothecene mycotoxins, and damp building-related illness: new insights into a public health enigma. *Toxicological Sciences* 104(1):4-26.

Figure 3:

http://www.cbwinfo.com/Biological/Toxins/trichothecene_mycotoxins.htm

CHAPTER 3

**Epithelial, Inflammatory, and Mucous Responses in the Nasal Airways
Of Mice Repeatedly Exposed to the Macrocyclic Trichothecene Mycotoxin
Roridin A: Dose-response and Persistence of Toxicant-Induced Injury**

ABSTRACT

Macrocyclic trichothecene mycotoxins are produced by molds, like *Stachybotrys chartarum*, that contaminate water-damaged buildings and are associated with several illnesses including those of the upper respiratory tract. The purpose of the present study was to determine the adverse effects of repeated exposures to a representative macrocyclic trichothecene, Roridin A (RA), on the nasal airways of laboratory mice. Female C57BL/6 mice were exposed to a single daily, intranasal, instillation of RA (0.4, 2, 10, or 50 $\mu\text{g}/\text{kg}$ bw) in saline (50 μl) or saline alone (controls), five days per week for two consecutive weeks, followed by four days in a third consecutive week. Other mice were intranasally instilled with 250 $\mu\text{g}/\text{kg}$ RA, once a day, four or five days per week, for two weeks (nine days total). All mice were sacrificed 24 hours after the last instillation and nasal airways were processed for histopathologic, immunohistochemical and morphometric analyses. Dose-response analyses revealed that the no-effect and lowest-effect levels were 2 and 10 $\mu\text{g}/\text{kg}$ bw, respectively. RA exposure induced a dose-dependent neutrophilic rhinitis with mucus hypersecretion, atrophy and exfoliation of nasal transitional and respiratory epithelium, olfactory epithelial atrophy, and loss of olfactory sensory neurons (OSNs). Mice exposed to 10, 50 and 250 $\mu\text{g}/\text{kg}$ bw had approximately 20%, 70% and 90% less OSNs, respectively, in their markedly atrophic OE compared to that in control mice. Though nasal inflammation and excess luminal mucus was resolved by three weeks after the last intranasal instillation, loss of OSN was still present in OE. These results suggest that nasal inflammation, mucus hypersecretion, and olfactory

neurotoxicity may be important adverse health effects associated with repeated airborne exposures to RA or similar mycotoxins found in the indoor air of severely water-damaged buildings.

INTRODUCTION

Damp building-related illness (DBRI) includes a number of respiratory, immunological, and neurological conditions that have been associated with airborne exposure to toxic black mold, *Stachybotrys chartarum* (Andersson et al., 1997; Nielsen, 2003). An Institute of Medicine expert committee recently concluded that there is sufficient scientific evidence to suggest an association between exposure to moldy, damp indoor environments and upper respiratory tract symptoms (nasal congestion, runny or itchy nose, sneezing, throat irritation) as well as some lower respiratory tract symptoms and syndromes (wheeze, cough, asthma exacerbation, and hypersensitivity pneumonitis in susceptible people) (Institute of Medicine, 2004). This committee, however, also concluded that there was insufficient evidence to link damp conditions to other health conditions, including pulmonary hemorrhage and neurological effects (e.g., memory loss).

S. chartarum is a saprophytic fungus that grows on damp cellulosic building materials such as wallboards, ceiling tiles, and cardboard (Andersson et al., 1997; Boutin-Forzano et al., 2004; Tuomi et al., 1998; Tuomi et al., 2000). It has been suggested that *S. chartarum* or its trichothecene mycotoxins could be possible etiologic contributors to building-associated respiratory illness (Fung et al., 1998; Hossain et al., 2004; Jarvis et al., 1986; Jarvis et al., 1998; Kilburn, 2004). Pestka et al. (2008) have recently reviewed the state of research on *S. chartarum*, trichothecene mycotoxins, and DBRI. It is clear from this review and the recent Institute of Medicine report (2004), that DBRI still remains a public

health enigma and much more research is needed in the areas of mechanisms, dose-response and exposure assessments.

Satratoxins are macrocyclic trichothecene mycotoxins that are found in spores and mycelial fragments of *S. chartarum* (Gregory et al., 2004). Both fungal spores and mycelial fragments may become airborne and inhaled under the right conditions. In a recent study, we demonstrated that mice intranasally instilled once with a relatively low amount (250 ng) of Satratoxin G (SG) develop rapid and dramatic loss of olfactory sensory neurons (OSNs) through apoptosis in both the nose and brain (Islam et al., 2006). In a subsequent study, we found that Roridin A (RA), another macrocyclic trichothecene of similar chemical structure, also induced rapid apoptosis and marked loss of OSNs in the nasal airways and the olfactory bulb (OB) of mice after a single intranasal instillation (Islam et al. 2007).

The purpose of the present study was to extend our research on the nasal toxicity of macrocyclic trichothecenes by determining the long-lasting effects of repeated intranasal exposures of RA on the nasal epithelium of mice. RA was again chosen as a representative macrocyclic trichothecene due to the lack of commercially available SG and the difficulty in purifying large amounts of this mycotoxin for *in vivo* research. RA is commercially available and is produced in large quantities by the *Myrothecium* genus of fungus. As previously mentioned, we have shown that the acute nasal toxicity of RA mimics that of SG in the murine nose and brain after a similar, single, intranasal dose (Islam et al., 2007).

MATERIALS AND METHODS

Experimental Design

Studies were carried out in accordance with National Institutes of Health guidelines and overseen by the All University Committee on Animal Use and Care at Michigan State University. Pathogen-free female C57BL/6 mice (7-8 weeks, Charles River, Portage, MI) were randomly assigned to experimental groups (n = 6). Mice were housed in polycarbonate cages containing *Cell-Sorb Plus* bedding (A & W products, Cincinnati, OH) and covered with filter bonnets. Room lights were set on a 12-hour light/dark cycle. Temperature and relative humidity were maintained between 21-24°C and 40-55% humidity, respectively. RA was purchased from Sigma Chemical Co. (St. Louis, MO). The toxin was evaluated by HPLC and a single peak was detected at 260 nm, indicating purity > 99% (Hinkley and Jarvis 2001).

We initially conducted a study to determine the dose-response relationships of RA and nasal injury in mice receiving repeated daily intranasal instillations. For these instillations, mice were lightly anesthetized using a mixture of 3.5% isoflurane (Abbott Laboratories, IL) and 96.5% oxygen. Mice received an intranasal instillation of 0, 0.4, 2, 10, or 50 µg/kg body weight (approximately 0, 7, 36, 180, or 900 ng, respectively) of RA in 50 µL of pyrogen-free saline (Abbott Laboratories, IL; 25 µL per nostril) once a day, five days a week for two consecutive weeks, followed by four consecutive days in the third week. Therefore at the end of the last instillation, mice had received a total intranasal dose of 0, 0.1, 0.5, 2.5 or 12.6 µg of RA. An additional group of mice similar in

strain, gender, and age (n = 6), were intranasally instilled once daily with a high RA dose of 4,500 ng (250 µg/kg body weight) for nine days (five consecutive days the first week and four consecutive days the second week, total intranasal dose of 40.5 µg).

A subsequent study was conducted to determine the persistence of toxin-induced nasal lesions at three weeks after the end of the last instillation. We chose only the highest daily dose (250 µg/kg body weight) for this study. Mice (n=6/group) received single daily intranasal instillations for nine days (five consecutive days the first week and four consecutive days the second week). Mice were sacrificed at one day or three weeks after the last instillation.

Animal Necropsies and Tissue Processing

At the designated time of sacrifice, mice were deeply anesthetized with an intraperitoneal (ip) injection of 0.1 ml of 12% sodium pentobarbital and euthanized by exsanguination via the abdominal aorta. After death, the head from each mouse was immediately removed from the carcass and the lower jaw, skin, muscles, eyes, and dorsal cranium were removed. The nasal cavities were flushed with 500 µL of 10% neutral buffered formalin (Fischer Scientific, Fair Lawn, NJ) using a 1 mL syringe and 20-gauge cannula, retrograde through the nasopharyngeal meatus. Nasal cavities were then immersed in a large volume of the same fixative and stored for 24 hours prior to further processing. Following fixation, the heads were decalcified in 13% formic acid for 7 days and then rinsed in tap water for at least four hours.

Transverse tissue blocks at four specific anatomic locations from the heads of the mice were selected for light microscopy as previously described (Young, 1981; Harkema et al., 2006; Islam et al., 2006). Briefly, the proximal section (T1) was taken immediately caudal to the upper incisor teeth; the middle section (T2) was taken at the level of the incisive papilla of the hard palate; the third nasal section (T3) was taken at the level of the second palatal ridge; and the most caudal nasal section (T4) was taken at the level of the intersection of the hard and soft palates, through the proximal portion of the olfactory bulb (OB) of the brain (**Figure 4**).

Nasal tissue blocks were processed for histopathologic, immunohistochemical and morphometric analyses. All of these blocks were embedded in paraffin, and the anterior face of each block was sectioned at a thickness of five microns and stained with hematoxylin and eosin for routine light microscopic examination. Additional slides were stained with Alcian Blue (pH 2.5)/Periodic Acid Schiff (AB/PAS) to identify acidic and neutral mucosubstances stored in mucus-secreting cells of airway surface epithelium and underlying nasal glands (septal and lateral nasal glands and Bowman's glands).

Immunohistochemistry

Additional tissue sections were immunohistochemically stained to identify neutrophils in the nasal mucosa and mature OSNs in olfactory epithelium (OE). Tissue sections intended for olfactory marker protein (OMP; present only in mature OSNs) immunohistochemistry, T1-T4, were first incubated with a

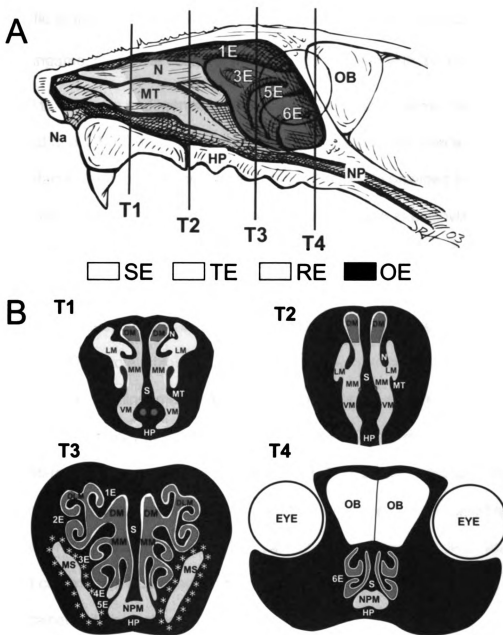


Figure 4. Location of nasal epithelial populations (A) Right nasal passage of the murine nose with septum removed, exposing nasoturbinates (N), maxilloturbinates (MT), and ethmoid turbinates (E1-6); vertical lines indicate anterior surfaces of transverse tissue blocks (T1-T4) that were selected for microscopic examination. SE, squamous epithelium; TE, transitional epithelium; RE, respiratory epithelium; OE, olfactory epithelium. (B) Cross-sectional views of T1-4. Na, nasus; NP, nasopharynx; NPM, nasopharyngeal meatus; OB, olfactory bulb; HP, hard palate; DM, dorsal medial meatus; DLM, dorsal lateral meatus; LM, lateral meatus; MM, middle medial meatus; VM, ventral meatus; NPM, nasopharyngeal meatus; MS, maxillary sinus; S, septum. Asterisk = location of the lateral nasal glands.

nonspecific protein blocking solution containing normal sera (Vector Laboratories Inc., Burlingame, CA). The sections were then pre-treated with 3% H₂O₂ in methanol to eliminate endogenous peroxidase. The sections were then transferred to a 1:4000 dilution of primary polyclonal antibodies directed against OMP-containing sensory neurons (goat anti-OMP antibody provided by Dr. Frank Margolis, University of Maryland). Sections were incubated in biotinylated anti-species IgG. Immunoreactivity of OMP was visualized using Vector R.T.U. Elite ABC-Peroxidase Reagent followed by Nova Red Chromagen.

T1-T4 sections designated for anti-neutrophil staining were first incubated with a nonspecific protein blocking solution containing normal sera (Vector Laboratories Inc., Burlingame, CA). The sections were then transferred to a 1:200 dilution of primary monoclonal antibodies directed against neutrophils (rabbit anti-rat neutrophil antibody provided by Dr. Robert Roth, Michigan State University). Anti-neutrophil antibody treatment was followed by anti-rabbit IgG, Streptavidin-Phosphatase complex (KPL Laboratories, Gaithersburg, MD), and Fast Red chromagen. Following immunohistochemistry, slides were lightly counterstained with hematoxylin.

Light Microscopy and Morphometric Analysis

Standard morphometric techniques were used to estimate the numeric cell density of OSNs in the OE lining the medial surface of second ethmoid turbinates (ET2; T3), the dorsal meatus (DM; T2), and the septal vomeronasal organ (VO; T1) (**Figure 4**). All cell counts were determined using light microscopy at a final

magnification of 790X. Numeric cell density was quantitatively estimated by counting the number of nuclear profiles of OMP-positive cells and dividing by the length of the underlying basal lamina. The length of basal lamina was determined by measuring the contour of the basal lamina on a digital image using Scion Image (Scion Corporation, Fredrick, MD).

To morphometrically estimate the severity of the nasal inflammatory response, nuclear profiles of immunohistochemically stained neutrophils were counted in the nasal mucosa lining the maxilloturbinates (MT) in T1. Numeric cell densities for these inflammatory cells were calculated like OSNs and expressed as the number of neutrophils per length of basal lamina.

Thickness of OE lining the 1) dorsal medial meatus (T2) and 2) the medial surface of ethmoid turbinate (ET2) was morphometrically estimated using a standard cycloid grid overlay and computer software specifically designed for point and intercept counting (Stereology Toolbox, Davis, CA) as previously described in detail (Hyde et al., 1990; Hyde et al., 1991; Islam et al., 2006). Briefly, microscopic measurements were made at a final magnification of 1920X using a light microscope coupled to a 3.3 megapixel digital camera (Q-color 3 Camera, Quantitative Imaging Corp., Burnaby, BC, Canada) and a Dell Dimension 8200 (Dell, Austin, TX). The thickness (τ) of OE, as measured by volume (μm^3) of OE per unit area (μm^2) of basal lamina, was estimated from point and intercept counts with a 136-point, 35-curve cycloid grid by the equation: $\tau = (3.2 \times Pp)/(2 \times Io)$, where Pp is the number of points counted for the OE and Io is the number of intercepts of the basal lamina. OE thickness at the two

intranasal sites was calculated for each mouse from point and intercept counts covering the entire dorsal medial meatus (T2) and the entire medial surface of ET2 in both the right and left nasal airways.

The volume density (V_s) of AB/PAS-stained mucosubstances in the respiratory epithelium lining the nasopharyngeal meatus (NPM) in the T4 nasal section was quantified using computerized image analysis and standard morphometric techniques. The area of AB/PAS-stained mucosubstance was calculated from the automatically circumscribed perimeter of stained material using a Dell XPS 400 computer and Scion Image (Scion Corporation, Frederick, MD). Basal lamina length was calculated from the contour length on the digitized image. The volume of mucosubstances per unit of surface area of basal lamina was estimated using a previously described method (Harkema et al., 1987). The V_s of the intraepithelial mucosubstances was expressed as nanoliters of mucosubstance per mm^2 of basal lamina.

The V_s of AB/PAS-stained mucosubstances in subepithelial Bowman's Glands in the lamina propria of ET2 in the T3 nasal section was quantified using a technique similar to that described above. The V_s of mucosubstances in Bowman's Glands was also expressed as nanoliters of mucosubstance per mm^2 of basal lamina.

The V_s of AB/PAS-stained mucosubstances in the Lateral Nasal Glands (LNG, Stenos Glands) surrounding the maxillary sinus in T3 was quantified using image analysis and standard morphometric techniques. The area of AB/PAS-stained mucosubstance was calculated from the automatically circumscribed

perimeter of stained material using a Dell XPS 400 computer and Scion Image (Scion Corporation, Fredrick, MD). The length of the basal lamina underlying the modified respiratory epithelium lining the maxillary sinus was calculated from the contour length on the digitized image. The dorsal, ventral, and medial areas of the glands, which contain PAS-staining mucosubstances, were selected for measurement purposes. The volume of mucosubstances per unit of surface area of basal lamina was estimated using a previously described method (Harkema et al., 1987). The Vs of the mucosubstances was expressed as nanoliters of mucosubstance per mm^2 of basal lamina.

Nasal Lavage, Cytology and Flow Cytometry

The nasal passages of mice receiving 0 and 250 $\mu\text{g}/\text{kg}$ RA and sacrificed at one day after the last instillation were lavaged immediately after death and prior to tissue fixation with 500 μL of saline retrograde through the nasopharyngeal meatus using a 20 gauge cannula and a 1 mL syringe. Approximately 98% of the lavage fluid was recovered. 85 μL of the collected nasal lavage fluid was taken for cytopsin and 10 μL was taken for hemocytometry. After cytopsin was complete, the slides were prepared and stained using a standard Diff Quick staining protocol (Dade Behring, Newark, DE). Differential cell counts were used to quantify cells on stained slides.

The concentrations of IL-6, IL-10, MCP-1, TNF- α , INF- γ , and IL-12 in nasal lavage fluid were determined using Cytometric Bead Array Mouse Inflammation Kit (BD Biosciences, San Diego, CA). Concentrations of IL-2, IL-4, and IL-5 were

also determined using a Cytometric Bead Array mouse Th1/Th2 Cytokine CBA (BD Biosciences, San Diego, CA). Measurements were carried out according to manufacturer's instructions using a FACSCalibur and BD CBA Analysis software (BD Biosciences, San Jose, CA). Cytokine concentrations are expressed as pg/ml.

Real-time PCR analyses for inflammatory cytokines and chemokines

Animals designated for Real-Time PCR (rt-PCR) analysis of nasal and brain tissues (only mice exposed to 0 or 250 µg/kg RA) were sacrificed 24 hours after the final intranasal instillation of RA. The head of each mouse was removed and the skin, muscles, eyes, and lower jaw were removed from the head. The nose was split in a sagittal plane adjacent to the midline of the head. The nasal septum was removed to expose the nasal turbinates, found on the lateral wall of each nasal passage. A dissection microscope and ophthalmic surgical instruments were used to remove the ethmoid turbinates (ET), maxillo- and nasoturbinates (MNT), and OB. Collected tissues were then submerged in an appropriate volume of RNeasyTM (Ambion Inc., Austin, TX). RNA was isolated using RNeasy[®] Protect Mini kit (Qiagen Inc. Valencia, CA) within 7 days of tissue collection. Rt-PCR for cytokine genes IL-1, IL-6, TNF-α, iNOS, MCP-1, MUC5b, and MIP-2 were performed on an ABI PRISM[®] 7900HT Sequence Detection System using Taqman One-Step RT-PCR Master Mix and Assays-on-DemandTM primer/probe gene expression products according to the manufacturer's

protocols (Applied Biosystems, Foster City, NY). Relative quantification of gene expression was carried out using an 18S RNA control and an arithmetic formula method as previously described (Islam et al., 2006; Audige et al., 2003).

Statistics

All data was analyzed using SigmaStat v. 3.1 (Jandel Scientific, San Rafael, CA). Criterion for significance was set at $p \leq 0.05$. Morphometric data were analyzed using a one-way or two-way analysis of variance (ANOVA) with Student-Newman-Keuls post hoc test. The dose-response effects of RA were evaluated by comparing groups receiving RA to a control group receiving only the saline vehicle. The persistence of nasal lesions quantified using morphometric techniques were evaluated by comparing groups receiving RA to their respective saline vehicle controls, as well as comparing between groups sacrificed at one day and three weeks after the last instillation of RA.

RESULTS

Animal responses to RA instillations

In the initial dose-response study, no significant clinical signs were observed in mice repeatedly instilled with doses of 50 $\mu\text{g}/\text{kg}$ bw RA or less. In contrast, mice instilled with the highest dose of RA, 250 $\mu\text{g}/\text{kg}$ bw, became markedly lethargic with signs of respiratory distress (dyspnea) after the ninth day of RA instillation. It was therefore decided not to continue with the high-dose intranasal instillations and to sacrifice these mice the following day.

Repeated intranasal RA exposure induced dose-dependent rhinitis and mucus hypersecretion at one day post-exposure

As an illustrative guide to complement the nasal histopathology described below, **Figure 4** provides a diagrammatic representation of the key intranasal landmarks and surface epithelial cell populations lining the nasal airways (meatus) throughout the murine nose.

Repeated RA instillations induced nasal epithelial and inflammatory lesions predominantly in mice that received the two highest doses (50 and 250 $\mu\text{g}/\text{kg}$ bw). Only minimal epithelial changes were found in mice instilled with 10 $\mu\text{g}/\text{kg}$ RA, and no nasal lesions were present in any of the mice receiving lower doses of RA or the saline vehicle alone. Mice instilled with the highest dose of RA and sacrificed 24h after the ninth daily instillation had a severe, bilateral rhinitis characterized by a marked, mixed, inflammatory cell infiltrate composed mainly of neutrophils and lesser numbers of mononuclear cells (lymphocytes and monocytes). This exposure-induced neutrophilic rhinitis was also associated with marked mucosal edema and atrophy of airway surface epithelium. Inflammatory changes in the mucosal tissues were present throughout the nasal airways (T1-T4), but slightly more severe in the proximal airways (T1-2 compared to T3-4).

Concurrent with RA-induced rhinitis, there were also copious amounts of secreted AB/PAS-stained mucus, containing inflammatory cells (mainly neutrophils) and epithelial cellular debris, in the proximal and distal nasal airway lumens of high-dose RA-instilled mice (**Figure 5**). Mucopurulent material

T3

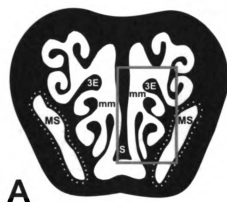


Figure 5. Airway mucosubstances in nasal section T3 of mice instilled with 250 $\mu\text{g}/\text{kg}$ RA. (A) Cross-section representation of nasal section T3. Blue box indicates area represented in panels B-E. Yellow outline indicates location of lateral nasal glands surrounding the maxillary sinus (MS). 3E, ethmoid turbinate 3; mm, medial meatus. Panels B-E, following page.

Figure 5 continued.

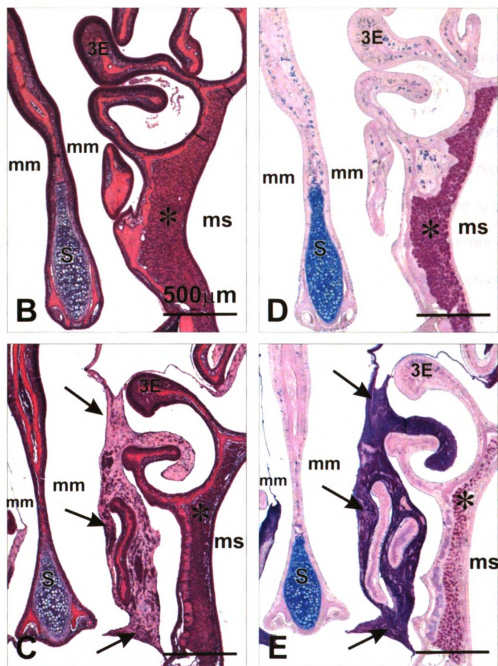


Figure 5 cont'd. (B-E) Photomicrographs of H&E (B,C) or AB/PAS (D,E) stained nasal section T3 in animals intranasally instilled with saline (B,D) or RA (C,E). Arrows indicate significant accumulation of mucus in the airways of animals instilled with RA. Asterisk indicates the lateral nasal glands surrounding the maxillary sinus (MS), with loss of PAS-staining mucosubstances in mice instilled with RA (C,E). 3E, ethmoid turbinate 3; mm, medial meatus; S, septum.

partially occluded some of the smaller meatuses between the ETs in the more distal nasal sections (T3, T4). Considerably less luminal mucus was present in the nasal airways of mice that received 50 µg/kg RA. Though these mice had conspicuous RA-associated nasal inflammatory and epithelial lesions of the same morphologic character as the high dose RA mice, these changes were less severe, as reflected in the morphometric analyses described later in this report.

In the most proximal nasal sections (T1, T2) of RA mice exposed to the two highest doses of RA, there was marked interstitial edema and neutrophil infiltration in the mucosal tissues lining the MNT (**Figure 6**), and to a slightly lesser degree in the mucosa lining the lateral walls and nasal septum. Mice repeatedly instilled with 50 and 250 µg/kg RA had 784% and 1,685% more neutrophils in the mucosa lining the maxilloturbinates (T1) as compared to saline-instilled control mice (**Figure 7**). The numeric densities of neutrophils in the maxilloturbinates of mice exposed to 10 µg/kg RA, or lower doses, did not differ significantly from those of control mice.

In mice exposed to 50 or 250 µg/kg RA, nasal transitional epithelium (NTE) lining the lateral meatus in T1 was mildly to markedly atrophic due to toxin-induced epithelial degeneration, necrosis and exfoliation (**Figure 6**). In a few areas, the normally low cuboidal, nonciliated NTE was replaced by a thin squamoid regenerative epithelium. In addition, there was histologic evidence of necrosis of turbinate bone (mild loss of trabecular bone with numerous lacunae without osteocytes), that was most prominent in the proximal aspects of maxilloturbinates of mice instilled with the highest dose of RA. Interestingly, RA

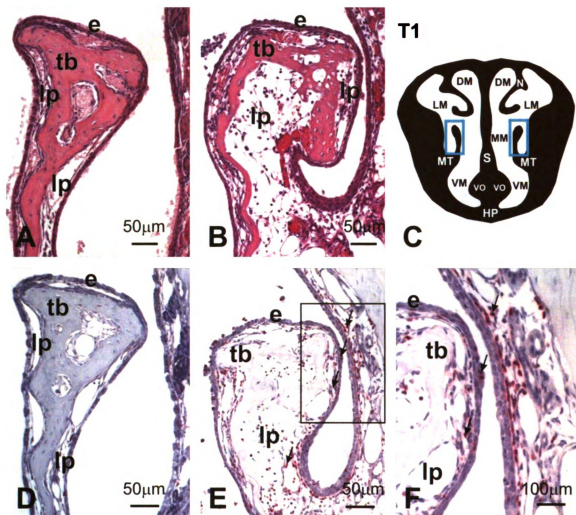


Figure 6. Marked edema and neutrophilic influx (rhinitis) of the MT and lateral wall in nasal section T1. Light photomicrographs of the MT and lateral wall from mice instilled with saline alone (A,C) or 250 µg/kg RA (B,E,F). Blue rectangle in C indicates the location of photomicrographs in nasal section T1. Tissues A and B were stained with H & E. Tissues D, E, and F were immunohistochemically stained with a monoclonal antibody directed against murine neutrophils (red-stained cells indicated by arrows). Rectangle in E indicates the location of the tissue in F. e, nasal transitional epithelium; lp, lamina propria; tb, turbinate bone; DM, dorsal meatus; LM, lateral meatus; MM, medial meatus; S, septum; VM, ventral meatus; VO, vomeronasal organ; HP, hard palate.

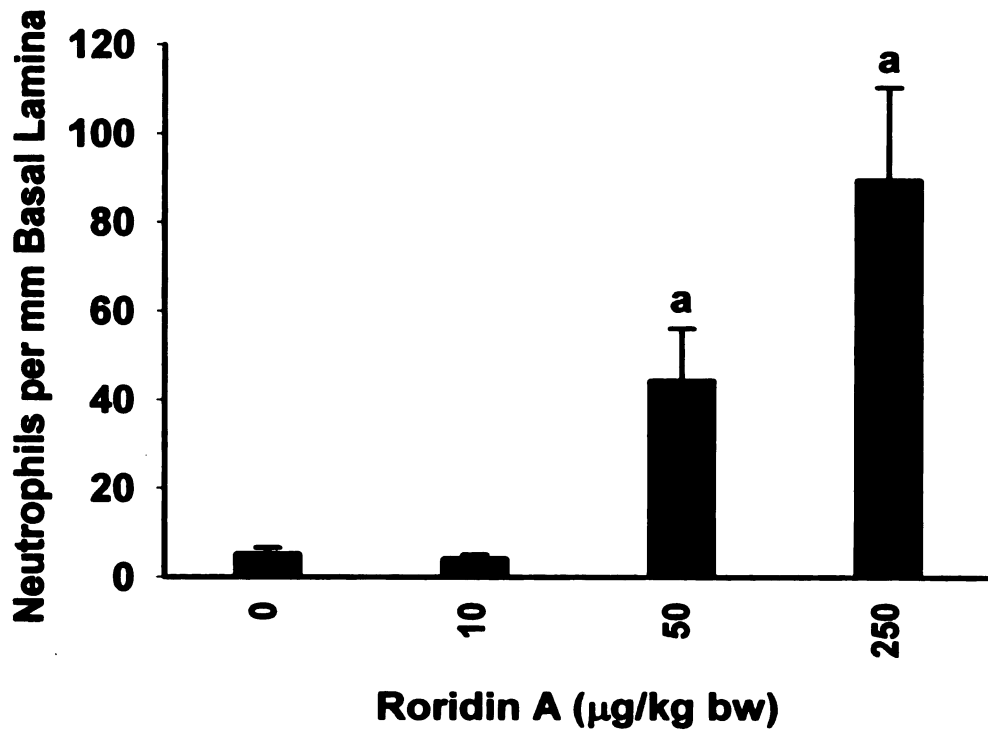


Figure 7. Dose-dependent neutrophilic rhinitis in mice instilled with RA. Significant neutrophilic influx in the epithelium and lamina propria (mucosa) of mice instilled with 50 or 250 µg/kg RA. Bars represent group means ± standard error of the mean (SEM). a indicates significantly different from respective saline control group ($p \leq 0.05$).

induced only minimal to mild changes to respiratory epithelium (RE) lining the mid and dorsal nasal septum (T1, T2), the dorsal meatus (T1), lateral wall (T2), and distal aspects of the MNT (T2). In some focal sites, there was attenuation or loss of surface cilia with replacement of the RE with a thin nonciliated, low cuboidal or squamoid regenerative epithelium. These changes in RE were more severe and consistent in mice instilled with 250 $\mu\text{g}/\text{kg}$, compared to those instilled with 50 $\mu\text{g}/\text{kg}$ RA.

Concomitant with the marked accumulation of luminal mucus in the nasal airways of high-dose RA mice, there was conspicuous loss of AB/PAS-stained mucosubstances in the mucous goblet cells of RE lining the mid and ventral aspects of the proximal septum (T1) and the more distal NPM (T4; **Figure 8**). Compared to saline-instilled control mice, animals exposed to 50 and 250 $\mu\text{g}/\text{kg}$ RA, had 42% and 86% less AB/PAS-stained mucosubstances in RE of the NPM, respectively. In contrast, mice exposed to 10 $\mu\text{g}/\text{kg}$ RA had a 48% increase in stored mucosubstances in the RE lining the NPM, as compared to controls (**Figure 8**).

In addition to the decreases in stored mucosubstances in the RE lining the nasal airways of mice instilled with the two highest doses of RA, these same mice also had marked loss of AB/PAS-stained mucosubstances in nasal glands located in the subepithelial lamina propria of the proximal septum (septal glands; T1, T2) and in the lateral wall surrounding the maxillary sinus (T3; lateral nasal gland; **Figure 9**). Mice instilled with 50 and 250 $\mu\text{g}/\text{kg}$ RA had 55% and 95% less AB/PAS-stained mucosubstances in the LNG, respectively, as compared to

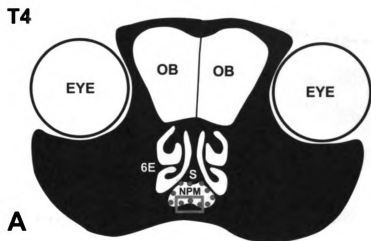


Figure 8. RA-induced changes in the volume density (V_s) of mucus in the respiratory epithelium lining the NPM. (A) Diagrammatic representation of nasal section T4. Red dots indicate location of morphometric measurement of mucus V_s . Blue rectangle indicates the location of photomicrographs. OB, olfactory bulb; 6E, ethmoid turbinate 6; S, septum. Panels B-E, following page.

Figure 8 continued.

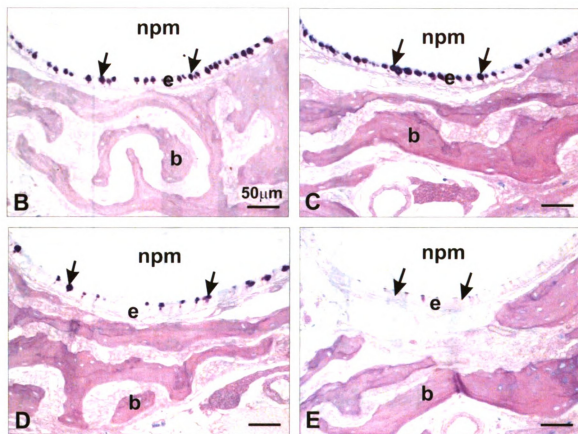


Figure 8 cont'd. (B-E) Light photomicrographs of mucus (arrows) in respiratory epithelium (e) in animals instilled with saline alone (B), 10 µg/kg (C), 50 µg/kg (D), or 250 µg/kg RA (E). b, bone. Panel F, following page.

Figure 8 continued.

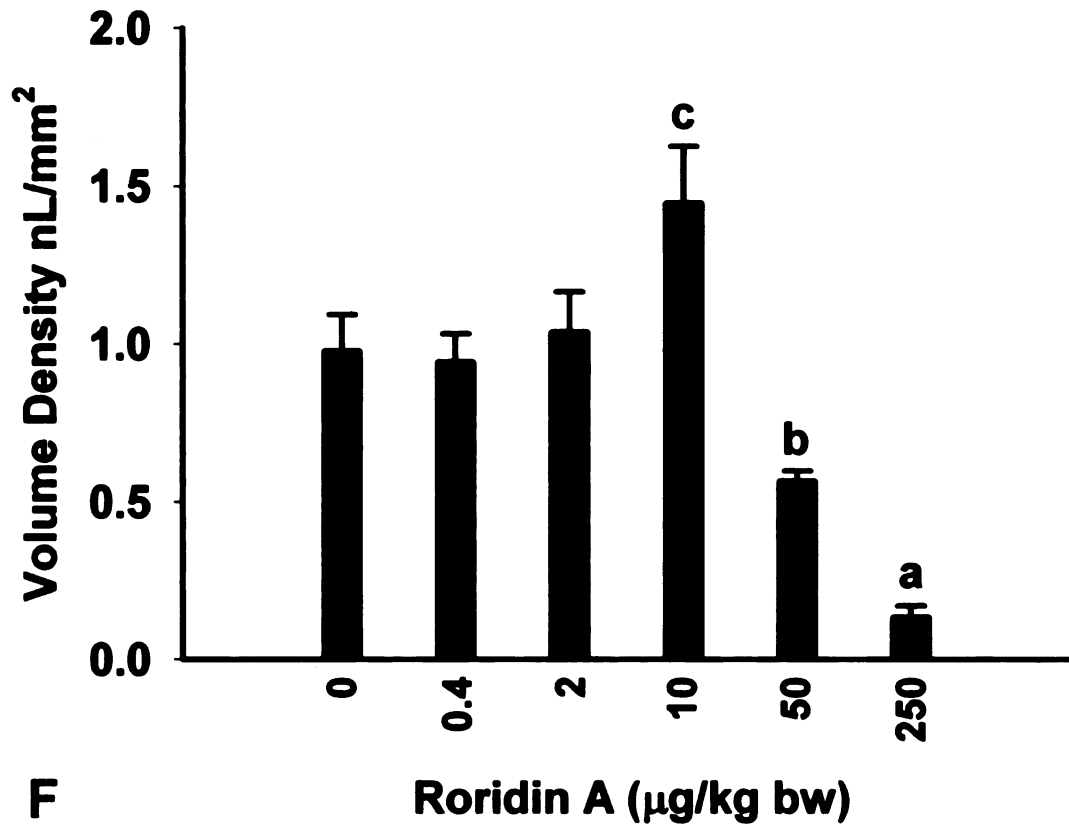


Figure 8 cont'd. (F) Dose-dependent changes in the Vs of mucus in the epithelium lining the NPM. Bars represent group means \pm standard error of the mean (SEM). a indicates significantly different from respective saline control group, b indicates significantly different from saline and 250 µg/kg groups, and c indicates significantly different from saline, 50 µg/kg, and 250 µg/kg groups, ($p \leq 0.05$).

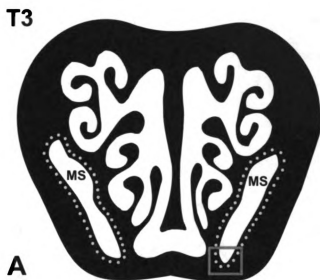


Figure 9. RA-induced changes in the volume density (V_s) of mucus in the LNG. (A) Diagrammatic representation of nasal section T3. Yellow dots indicate the location of the LNG surrounding the maxillary sinus (MS). Blue rectangle indicates the location of photomicrographs. Panels B-E, following page.

Figure 9 continued.

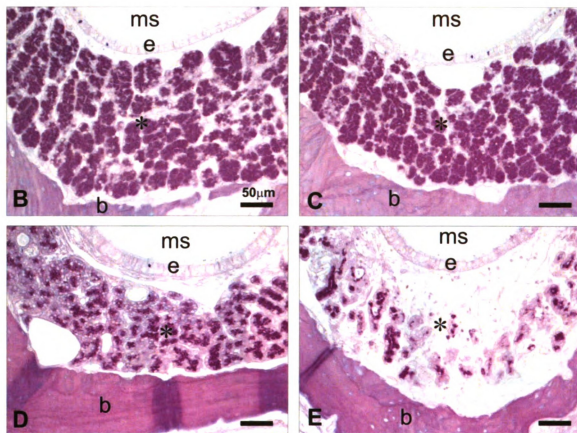


Figure 9 cont'd. (B-E) Light photomicrographs of the LNG (asterisk) of mice instilled with saline alone (B), 10 μg/kg (C), 50 μg/kg (D), or 250 μg/kg RA (E). e, respiratory epithelium lining the MS; b, bone. Panel F, following page.

Figure 9 continued.

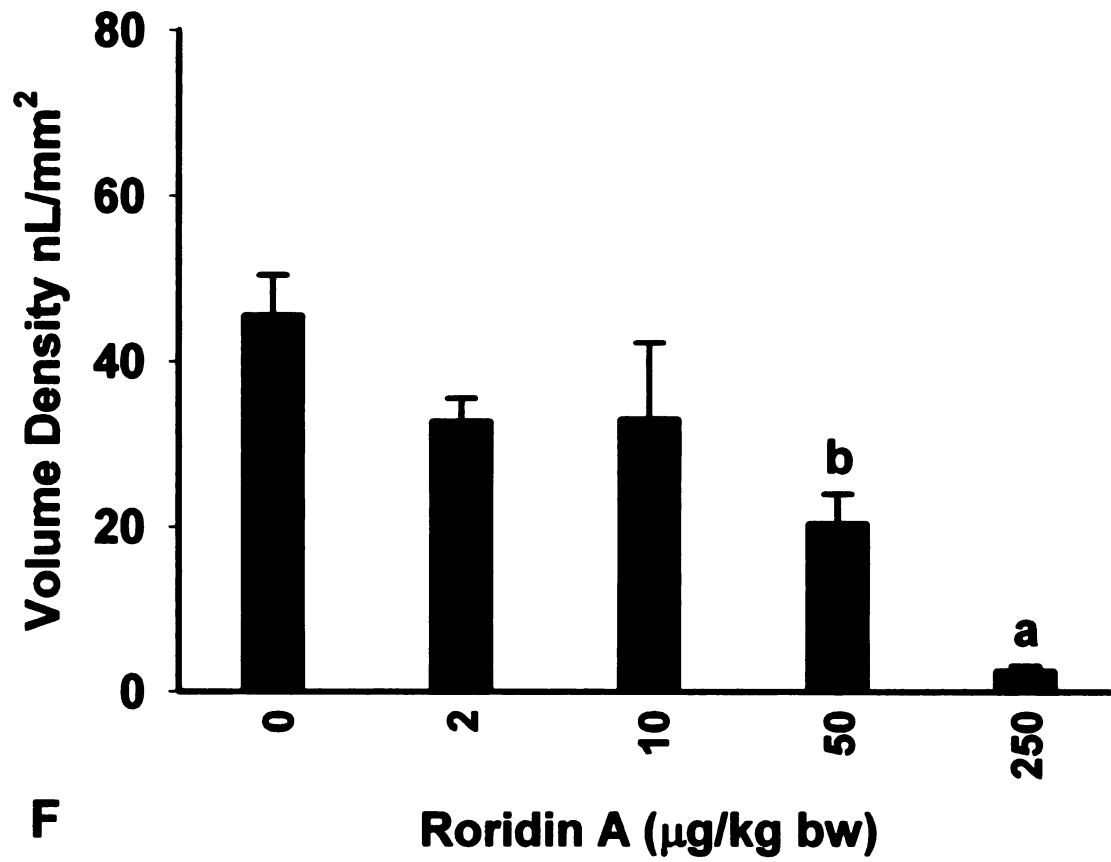


Figure 9 cont'd. (F) Dose-dependent decreases in the Vs of mucus in the LNG of mice instilled with 50 or 250 µg/kg RA. Bars represent group means ± standard error of the mean (SEM). a indicates significantly different from respective saline control and 50 µg/kg groups; b indicates significantly different from respective saline control group, (p≤0.05).

saline-instilled control mice (**Figure 9**). Interstitial edema and neutrophil infiltration were also present in the interstitial tissue surrounding these affected glands. With this marked loss of intracellular mucosubstances, there was also bilateral atrophy of the glandular tissue, but without histologic evidence of epithelial cell necrosis or apoptosis. No significant exposure-related histologic changes were present in the nasal glands of mice that were repeatedly instilled with lower RA doses of 0.4, 2, or 10 µg/kg bw.

In contrast to RA-induced changes in the amount of intraepithelial mucosubstances in the RE lining the airway surfaces and the subepithelial nasal glands, there was no histologic evidence of any change in the amount or character of mucosubstances in Bowman's glands underlying the OE at one day after RA exposure. Morphometric determinations of the Vs of mucosubstances in these olfactory glands in ET2 (T3) did not statistically differ among the experimental groups (saline-controls similar to RA-exposed mice; data not shown).

Repeated RA exposure induces OE atrophy and loss of OSNs

Another prominent nasal epithelial lesion that was present in both the 50 and 250 µg/kg RA-instilled mice was widespread atrophy of the OE that normally lines the dorsocaudal regions of the nasal airways (T1-T4; **Figures 10, 11**). This marked atrophy of OE was due to selective loss of OMP-stained OSNs, rather than a loss of adjacent sustentacular or basal cells in this neuroepithelial tissue. There was also concomitant atrophy of nerve bundles in the lamina propria

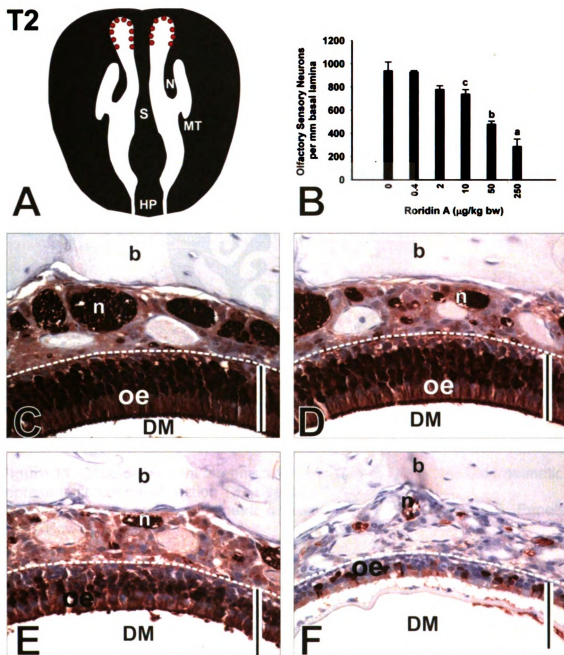


Figure 10. Loss of OSNs in the DM of T2. (A) Diagrammatic representation of nasal section T2. Red dots indicate location of morphometric analysis and photomicrographs. (B) Dose-dependent loss of OSNs in the DM. Bars represent group means \pm standard error of the mean (SEM). a indicates significantly different from respective saline control, 50 $\mu\text{g/kg}$, and 10 $\mu\text{g/kg}$ groups; b indicates significantly different from respective saline control and 50 $\mu\text{g/kg}$ groups; c indicates significantly different from respective saline control group, ($p \leq 0.05$). (C-F) Photomicrographs of OMP-stained tissue sections from mice instilled with saline (C), 10 $\mu\text{g/kg}$ (D), 50 $\mu\text{g/kg}$ (E), and 250 $\mu\text{g/kg}$ RA (F). Bar = 50 μm . DM, dorsal meatus; oe, olfactory epithelium; n, nerve bundle; b, bone.

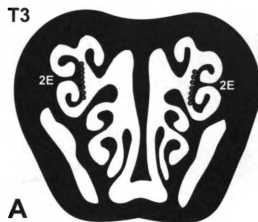


Figure 11. Dose-dependent atrophy of OE and loss of OSNs. (A) Diagrammatic representation of nasal section T3. Red dots indicate location of photomicrographs and morphometric analyses. 2E, ethmoid turbinate 2. Panels B-E, following page.

Figure 11 continued.

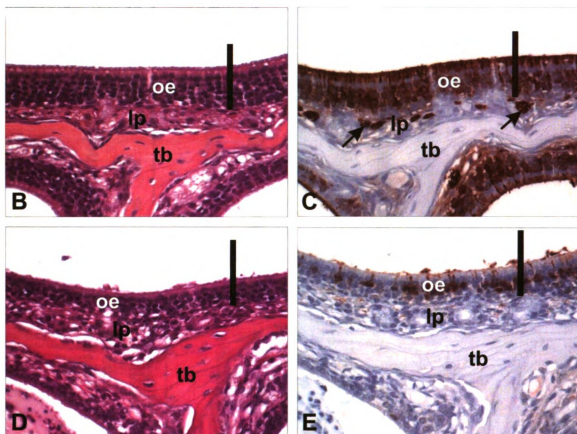


Figure 11 cont'd. (B-E) Light photomicrographs of mice instilled with saline alone (B,C) and 250 $\mu\text{g}/\text{kg}$ RA (D,E). Sections were stained with H & E (B,D) or an antibody directed against OMP (C,E). oe, olfactory epithelium; lp, lamina propria; tb, turbinate bone; arrows indicate OMP-stained nerve bundles. Bar = 50 μm . Panels F-G, following page.

Figure 11 continued.

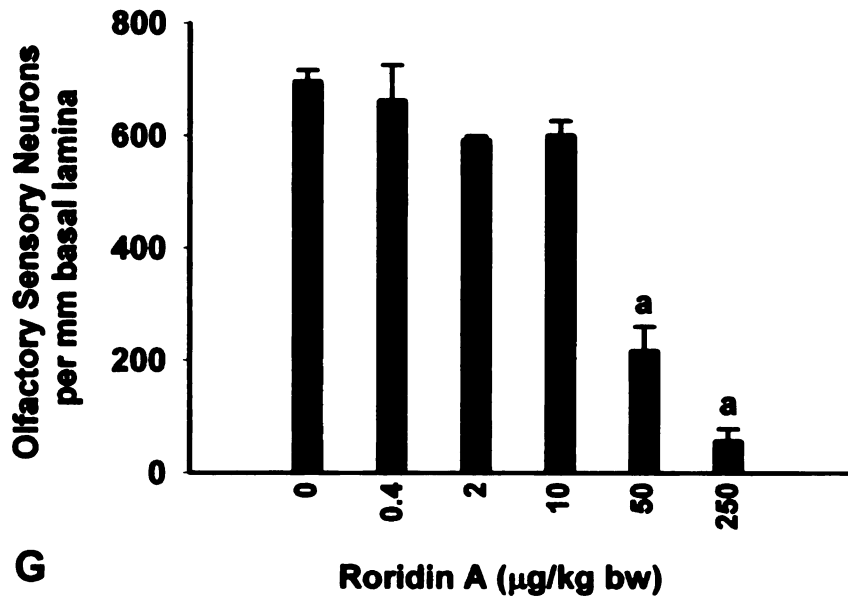
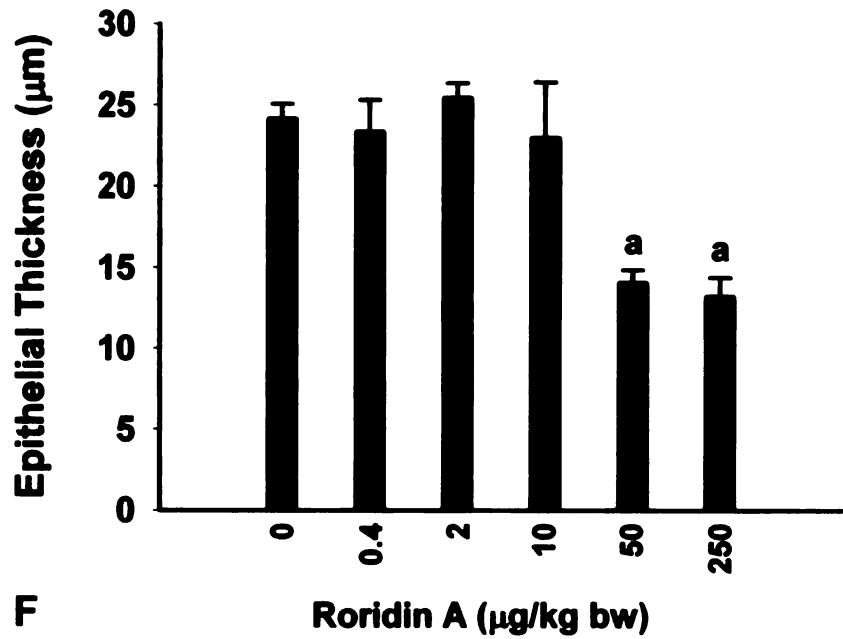


Figure 11 cont'd. (F,G) Morphometric analyses of the thickness of olfactory epithelium (OE) lining 2E (F) and the number of olfactory sensory neurons (OSNs) per mm basal lamina (G). Bars represent group means \pm standard error of the mean (SEM). a indicates significantly different from respective saline control group ($p \leq 0.05$).

underlying the affected OE. Associated with these neuroepithelial changes was a mild to moderate inflammatory cell influx (mainly neutrophils) in the lamina propria, and to a lesser extent in the OE. As compared to saline-instilled controls, mice exposed to 250 µg/kg RA had a 51% reduction in OE thickness (atrophy) and 70% less OMP-stained OSNs in the OE lining the DM (T2) at one day post-exposure. Though mice exposed to 10 and 50 µg/kg RA had no morphometrically detected reductions in OE thickness, these mice had significant losses of OMP-stained OSNs in the DM, 21% and 50%, respectively (**Figure 10**).

In a more distal intranasal site lined by OE, the medial aspect of ET2, mice exposed to 50 and 250 µg/kg RA had 41% and 45% reductions in OE thickness (atrophy) with 69% and 92% less OMP-stained OSNs, respectively, compared to saline-instilled control mice (**Figure 11**). Mice exposed to 10 µg/kg RA or less had no morphometrically detectable alterations in either OE thickness or OSN numeric density.

Concurrent with the dramatic loss of OMP-positive OSNs in the OE and lamina propria in the nasal mucosa of mice exposed to the highest dose of RA, there was also marked bilateral atrophy and vacuolation of the outer tissue layer (olfactory nerve layer) of the olfactory bulbs (OB; T4; **Figure 12**). Loss of OMP-staining was also evident in the adjacent glomerular layer of the OB where axons of OSNs first synapse with other neurons of the brain. A conspicuous influx of neutrophils was also present in these affected areas of the brain (i.e., mild toxic

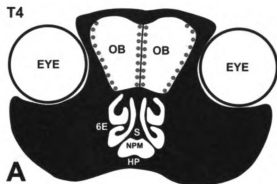


Figure 12. Atrophy and inflammation of the OB. (A) Diagrammatic representation of nasal section T4. Red dots indicate area of atrophy. OB, olfactory bulb; 6E, ethmoid turbinate 6; S, septum; NPM, nasopharyngeal meatus; HP, hard palate. Panels B-G, following page.

Figure 12 continued.

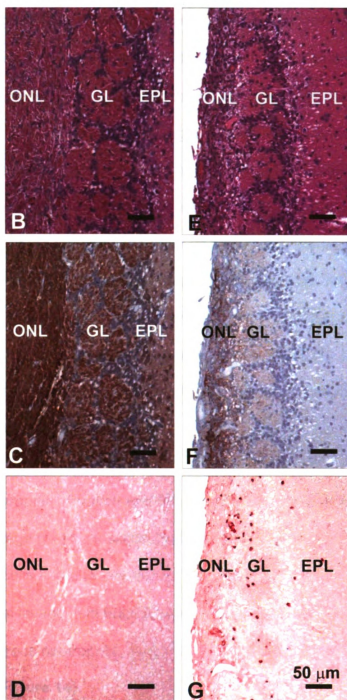


Figure 12 cont'd. (B-G) Light photomicrographs of outer layers of the OB in T4 of mice instilled with saline alone (B,C,D) or 250 µg/kg RA (E,F,G). Tissues B,E stained with H & E. Tissues C, F immunohistochemically stained to detect OMP in OSNs located in the olfactory neuronal layer (ONL) and glomerular layer (GL). Tissues D,G immunohistochemically stained with an antibody directed against murine neutrophils. EPL, external plexiform layer. Bar = 50 µm.

encephalitis; **Figure 12**). These histopathologic changes were also evident, but to a lesser degree, in mice exposed to 50 µg/kg, but not to lower doses of RA.

Interestingly, only mice exposed to 250 µg/kg RA also had marked atrophy of the OE in the bilateral vomeronasal organ located within the ventral septum in T1 (**Figure 13**) and the OE of the organ of Massera (septal organ) bilaterally lining small focal areas in the proximal ventral septum (T2). Like in the RA-induced atrophy of the OE lining the main nasal airways, the OE atrophy in these intranasal chemosensory organs was due to a selective loss of OSNs (**Figure 13**). Mice exposed to this high dose of RA had 83% less OSNs in the VO, compared to saline-controls, at one day post-exposure (**Figure 13**). A summary of all dose-related nasal lesions induced by repeated RA instillations one day post-exposure are provided in **Table 1**.

RA induces neutrophil infiltration and inflammatory cytokines in nasal lavage fluid

Nasal lavage fluid from saline-instilled control mice contained only a few nasal epithelial cells and only occasional neutrophils or other inflammatory cells. In contrast, nasal lavage fluid from mice repeated instilled with 250 µg/kg RA contained numerous neutrophils, some mononuclear inflammatory cells, and few epithelial cells (**Figure 14**).

Nasal lavage fluids from saline controls and 250 µg/kg RA mice were analyzed for INF-γ, TNF-α, MCP-1, IL-6, IL-10, IL-12, IL-2, IL-4, and IL-5. IL-2, IL-4, and IL-5 were not detected in any samples. Levels of INF-γ, IL-10, and IL-12

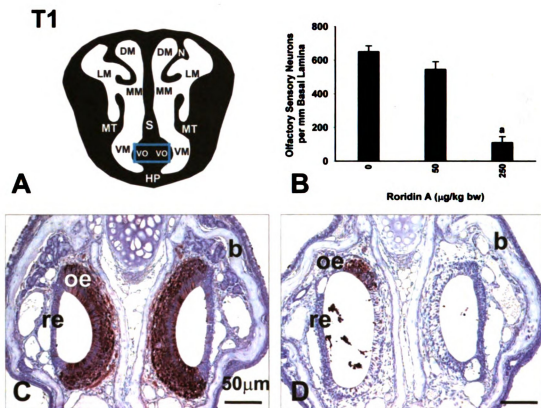


Figure 13. Loss of OSNs in the VO. (A) Diagrammatic representation of nasal section T1. Blue rectangle indicates location of photomicrographs and morphometric analysis. DM, dorsal meatus; LM, lateral meatus; MM, medial meatus; MT, maxilloturbinate; S, septum; VM, ventral meatus; VO, vomeronasal organ; HP, hard palate. (B) Loss of OSNs in the vomeronasal organ (VO). Mice instilled with 250 µg/kg had significantly fewer OSNs per mm basal lamina than saline control mice. Bars represent group means \pm standard error of the mean (SEM). a indicates significantly different from respective saline control group ($p \leq 0.05$). (C,D) Light photomicrographs of the VO in mice instilled with saline alone (C) or 250 µg/kg RA (D). Tissues were stained with an antibody directed against OMP. Mice instilled with RA had significant loss of OSNs. oe, olfactory epithelium; re, respiratory epithelium; b, bone.

Table 1. Summary of dose response nasal lesions induced by RA at 24h following the final instillation. Note that intraepithelial mucus in the NPM was increased at 10 µg/kg RA (upward arrow).

Nasal Lesions Induced by RA: Dose-Response				
	Saline	10 µg/kg	50 µg/kg	250 µg/kg
Airway Mucus				X
Neutrophil Infiltration, MT (T1)			X	X
Loss of Mucus, NPM (T4)		↑	X	X
Loss of Mucus, LNG (T3)			X	X
Atrophy; Necrosis, NTE &RE			X	X
OE Atrophy, DM (T2)				X
Loss of OSNs, DM (T2)		X	X	X
OE Atrophy, ET2 (T3)			X	X
Loss of OSNs, ET2 (T3)			X	X
Atrophy; Loss of OMP, OB (T4)			X	X
Loss of OSNs, VO (T1)				X

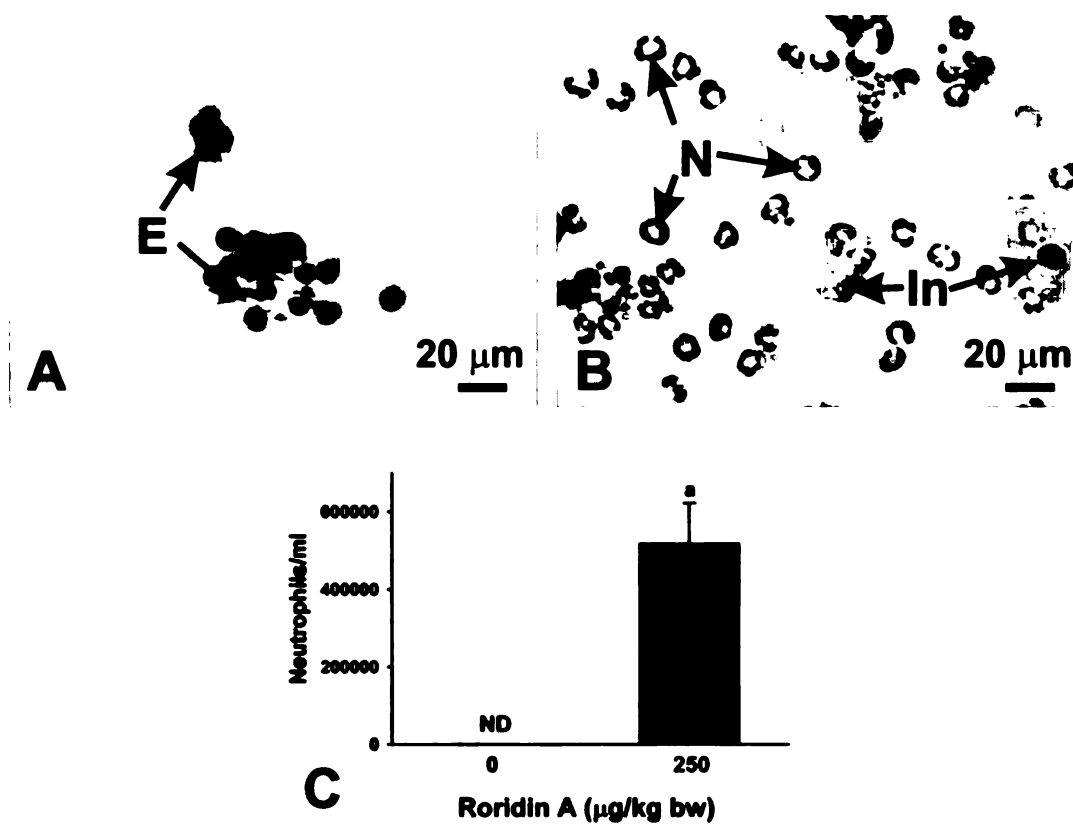
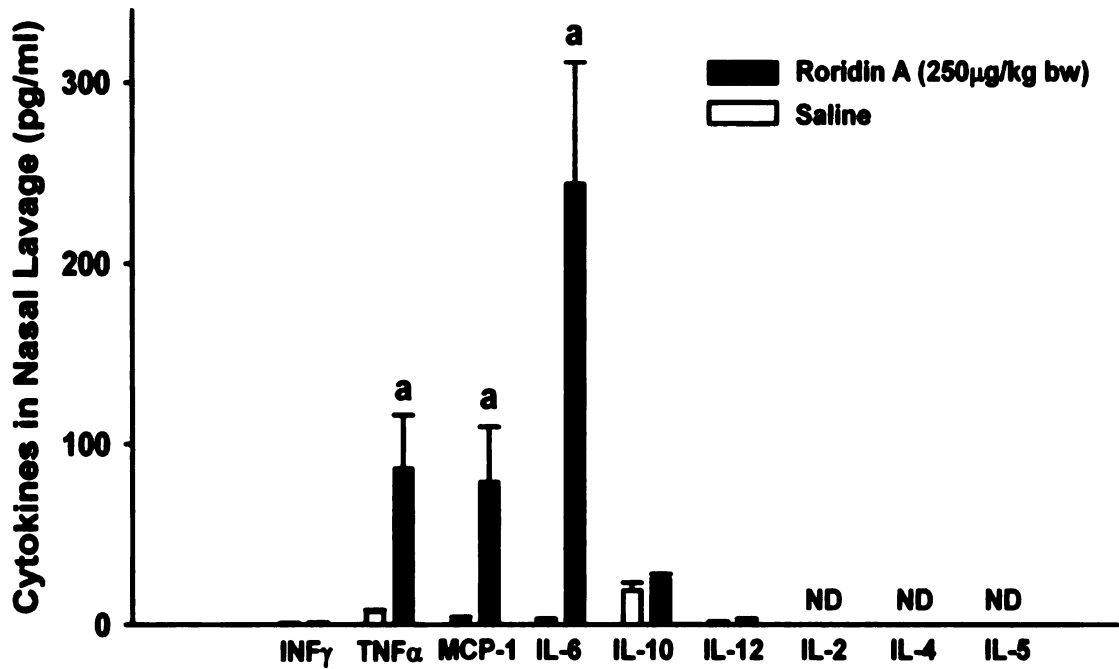


Figure 14. Cytology of nasal lavage fluid from mice repeatedly instilled with saline alone or 250 µg/kg RA. (A) Photomicrograph of nasal lavage from a saline-instilled control mouse. Control animals had only a few epithelial cells (E) in nasal lavage. (B) Photomicrograph of nasal lavage from a RA-instilled mouse. RA-treated mice had numerous neutrophils (N) and other inflammatory cells (In), such as macrophages and lymphocytes, in their nasal lavage. Samples were stained with standard Diff Quick protocol. (C) Number of neutrophils in the lavage fluid from mice exposed to 250 µg/kg RA compared to controls. Bars represent group means ± standard error of the mean (SEM). a indicates significantly different from respective saline control group ($p \leq 0.05$). ND = not detected. Panel D, following page.

Figure 14 continued.



D

Figure 14 cont'd. (D) Flow cytometric determination of selected inflammatory cytokines in nasal lavage fluid from mice repeatedly exposed to saline alone or 250 μ g/kg RA. TNF- α , MCP-1, and IL-6 were detected at levels significantly higher than those in lavage fluid from control animals. Bars represent group means \pm SEM. a indicates significantly different from respective saline control group (p \leq 0.05). ND = not detected.

were similar in controls and RA-exposed mice. Statistically significant increases in TNF- α , MCP-1, and IL-6 were detected in the lavage fluid of RA-instilled mice 12-fold, 28-fold, and 109-fold greater than the nasal lavage from controls, respectively (**Figure 14**).

RA induces inflammatory gene expression in nasal tissues at 24 hours.

Microdissected ET, MNT, and OB from mice instilled with either saline or 250 μ g/kg RA were analyzed by real-time PCR for inflammatory gene expression. Analysis revealed upregulation of inflammatory genes IL-1 α , IL-1 β , TNF- α , IL-6, iNOS, MCP-1, MIP-2, and MUC5b at 24 hours after the final intranasal instillation. IL-1 α expression was significantly increased in RA treated mice compared to controls only in MNT tissue, though ET and OB tissues showed increased expression that was not significantly different from the controls. IL-1 β expression was significantly increased in all tested tissues, with MNT tissue showing an increase of 250-fold increase over controls. IL-6 expression was markedly increased in ET and MNT, and was increased but not significantly different from controls in OB. iNOS showed 14-fold and 8-fold increases in ET and MNT, respectively. MCP-1 was significantly increased in all tissues, with 100-fold, 140-fold, and 25-fold increases in ET, MNT, and OB, respectively. MIP-2 showed the highest expression of all genes tested with a 256-fold increase in ET and a 363-fold increase in MNT when compared to control tissues. MUC5b also showed significant increases in ET and MNT, with 9-fold and 7-fold increases, respectively (**Figure 15**).

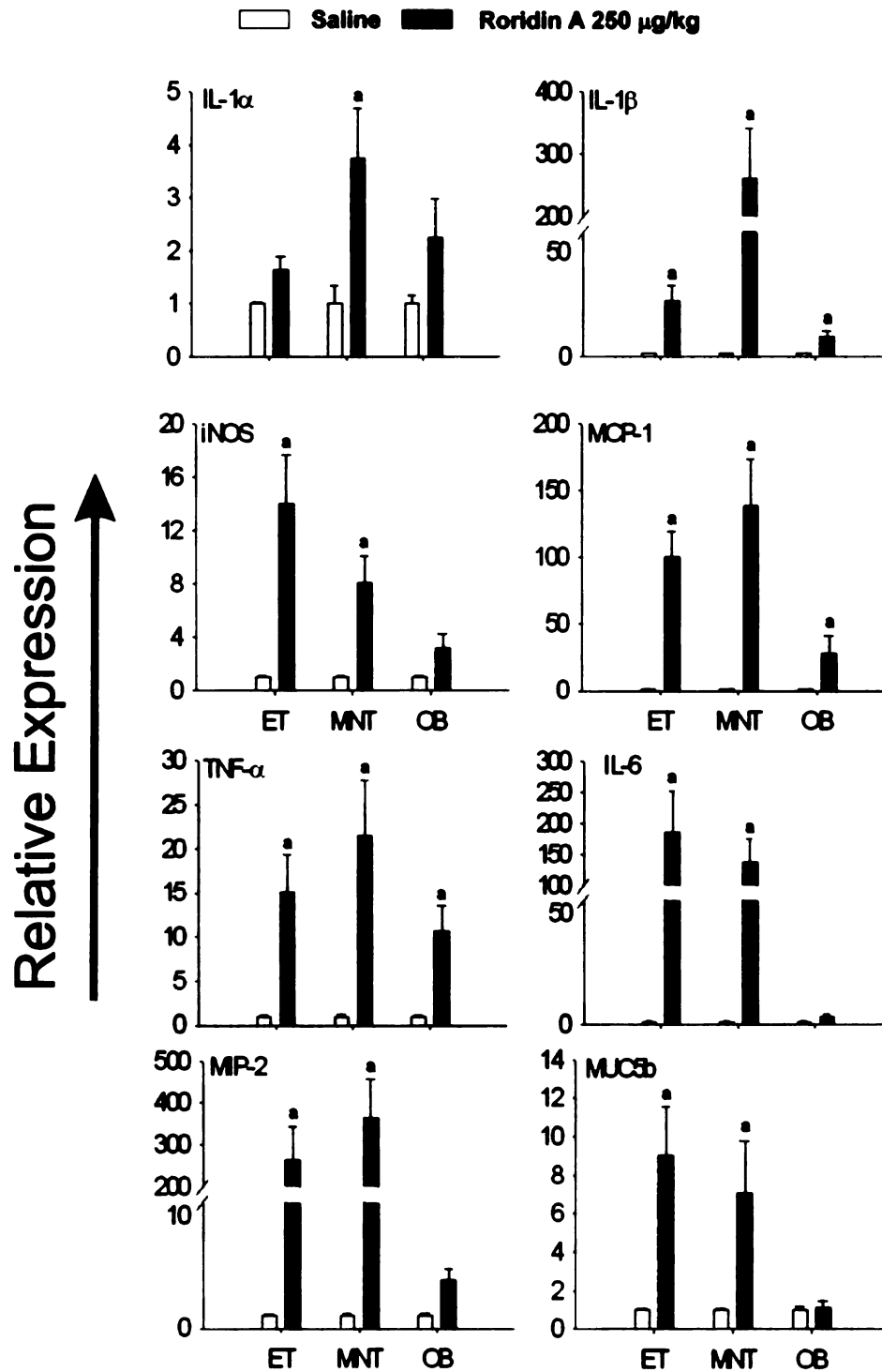


Figure 15. Relative Expression (fold increase) of proinflammatory cytokine genes in mice repeatedly exposed to 250 $\mu\text{g}/\text{kg}$. IL-1 β , iNOS, MCP-1, TNF- α , IL-6, MIP-2, and MUC5B were significantly increased in the ET and MNT. IL-1 α was increased only in the MNT. IL-1 β , MCP-1, and TNF- α were also significantly increased in the OB. Bars represent group means \pm SEM. a indicates significantly different from respective saline control group ($p \leq 0.05$).

Transient and long-lasting effects of RA on nasal airway epithelium

RA-induced rhinitis with airway mucus accumulation and atrophy of nasal surface epithelium and glands were no longer present three weeks post-exposure in mice repeatedly instilled with 250 µg/kg RA. In addition, toxicant-induced necrosis of bone with loss of lacunal osteocytes was not present in the MT of mice instilled with this high dose of RA and sacrificed three weeks after the end of the last instillation. There was complete restoration of the turbinate bone at three weeks post-exposure to this high dose of RA.

In contrast, some RA-induced epithelial lesions were still evident in the nasal airways of RA-instilled mice three weeks post-exposure. There was a conspicuous increase in amount of AB/PAS-stained mucosubstances in mucous goblet cells within the RE lining the nasopharyngeal meatus and in Bowman's glands underlying OE (**Figure 16**). Though there was minimal or no OE atrophy in mice sacrificed three weeks after intranasal instillations of 250 µg/kg, there was still some loss of OMP-stained OSNs in the OE of these mice. This was especially apparent in the OE lining the dorsal medial meatus in T2 (70% less than controls, **Figure 17**) and in the dorsal medial meatus, dorsal lateral meatus, and ET2 in T3 (75% less than controls, **Figure 18**). In some of these areas hyalinosis was present in sustentacular cells of the affected OE that had noticeable loss of OSNs. Though there was some remaining loss of OSNs in OE, there was no histologic evidence of atrophy of OMP-stained axons of OSNs in the OB (no detectable atrophy of the olfactory nerve or glomerular layer). In

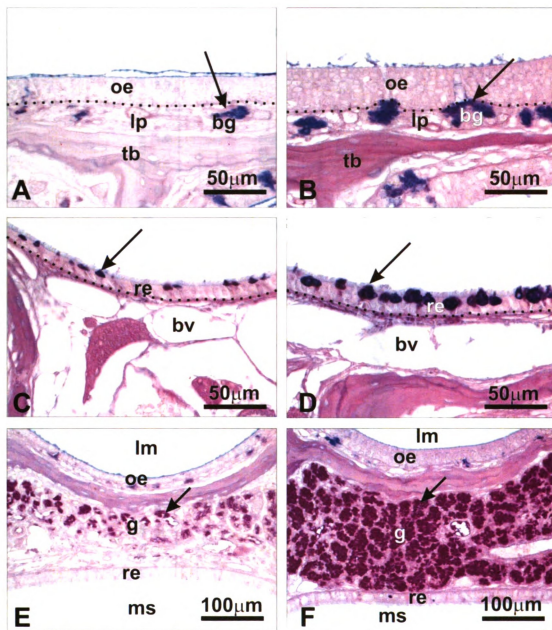


Figure 16. Persistence of RA-induced mucus-related changes. (A,B) Light photomicrographs of Bowman's Glands (bg) in the lamina propria (lp) of ET2, (C,D) mucus in the RE lining the NPM, and (E,F) LNG. Mice were instilled with 250 mg/kg RA and sacrificed at 24h (A,C,E) or 3 wks (B,D,F) post-instillation. oe, olfactory epithelium; tb, turbinate bone. (A,B) Arrow indicates AB/PAS-stained mucus. (C,D) re, respiratory epithelium; bv, blood vessel. Arrow indicates mucus in the respiratory epithelium. (E,F) lm, airway lumen; oe, olfactory epithelium; g, glands; re, respiratory epithelium; ms, maxillary sinus. Arrows indicate mucus in the LNG. All tissues were stained with AB/PAS. Panels G-I, following page.

Figure 16 continued.

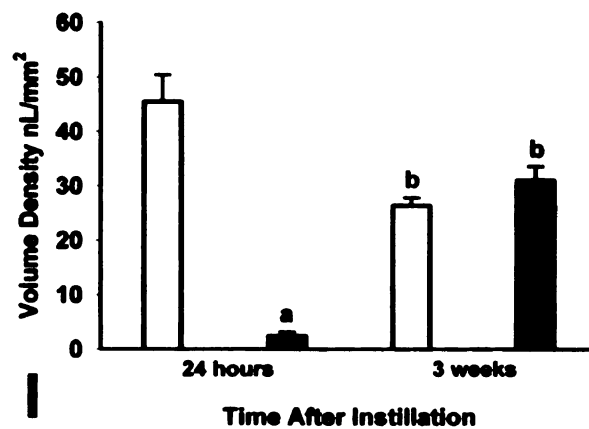
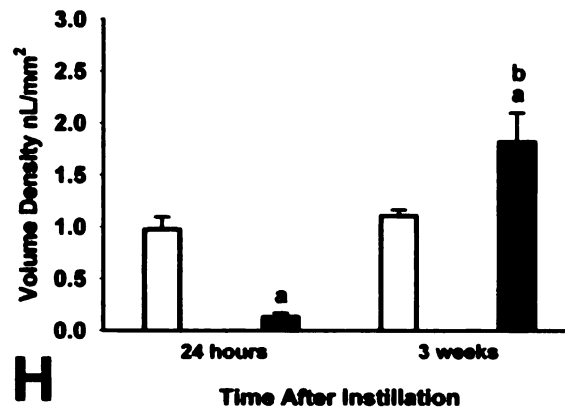
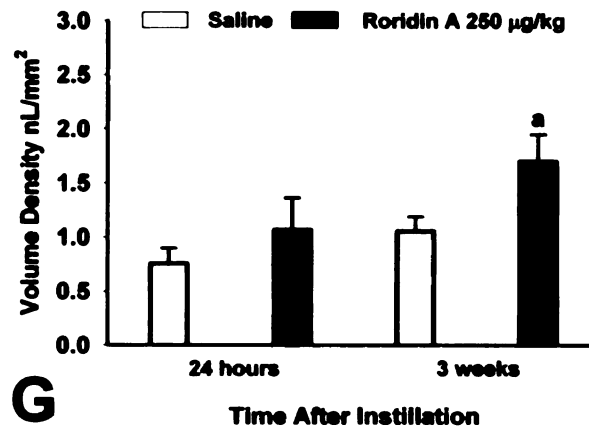


Figure 16 cont'd. Morphometric analysis of the volume density (V_s) of mucus in Bowman's Glands (G), RE lining the NPM (H), and mucus in the LNG (I) at 24h and 3 wks following instillation. Bars represent group means \pm standard error of the mean (SEM). a indicates significantly different from respective saline control group, ($p \leq 0.05$); b indicates significantly different from comparably instilled group sacrificed at 24h, ($p \leq 0.05$).

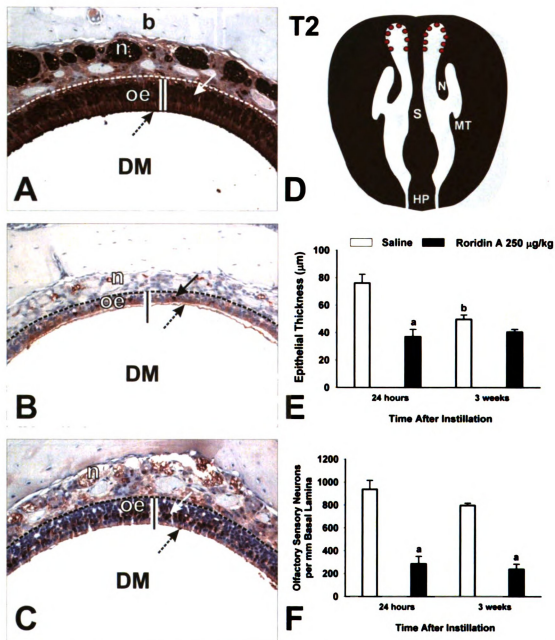


Figure 17. Persistence of loss of OSNs in the DM. (A-C) Photomicrographs of OMP-stained sections from mice instilled with saline (A) or 250 $\mu\text{g}/\text{kg}$ at 24h (B) or 3 wks (C) post-exposure. DM, dorsal meatus; oe, olfactory epithelium; n, nerve bundle; b, bone. Arrows indicate OMP-stained nuclei. Bar = thickness of OE in saline control mouse. (D) Diagrammatic representation of T2. Red dots indicate location of photomicrographs and morphometric analyses. DM, dorsal meatus; N, nasoturbinates; S, septum; MT, maxilloturbinates; HP, hard palate. (E) Atrophy of OE and (F) loss of OSNs in the DM. Bars represent group means \pm standard error of the mean (SEM). a indicates significantly different from respective saline control group, ($p \leq 0.05$); b indicates significantly different from comparably instilled group sacrificed at 24h, ($p \leq 0.05$).

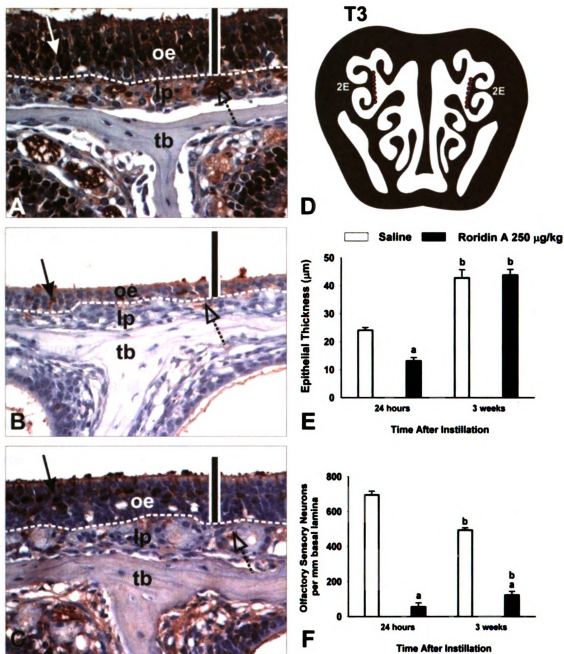


Figure 18. Persistence of loss of OSNs in OE lining ET2. (A-C) Photomicrographs of OMP-stained sections from mice instilled with saline (A) or 250 µg/kg at 24h (B) or 3 wks (C) post-exposure. oe, olfactory epithelium; lp, lamina propria; tb, turbinate bone. Arrows indicate OMP-stained nuclei. Bar = 50 µm. (D) Diagrammatic representation of T3. Yellow dots indicate location of photomicrographs and morphometric analyses. 2E, ethmoid turbinate 2. (E) Atrophy of OE and (F) loss of OSNs in the DM. Bars represent group means ± standard error of the mean (SEM). a indicates significantly different from respective saline control group, ($p \leq 0.05$); b indicates significantly different from comparably instilled group sacrificed at 24h, ($p \leq 0.05$).

addition, there was no neutrophilic encephalitis in the OB at three weeks following RA exposure.

DISCUSSION

Recent reviews and reports (Pestka et al. 2008, Institute of Medicine, 2004) indicate that multiple factors contribute to the etiology of DBRI and may include exposure to the spores and macrocyclic trichothecene mycotoxins of *S. chartarum* and other such molds. The nose is a likely target of inhaled spores and toxins, as particles of various sizes ($>5 \mu\text{m}$ to $< 10 \text{ nm}$ in diameter) have been shown to deposit in the noses of humans and laboratory animals in aerosol studies (Cheng et al., 1990, 1991, 1996). Distinct types of epithelium line the nasal passages of mammals, including squamous epithelium, ciliated, pseudostratified, respiratory epithelium (RE), nonciliated transitional epithelium (NTE), and OE lining the turbinates in the dorsocaudal nasal cavity. OE includes OSNs, sustentacular support cells, and basal cells (Harkema et al., 2006).

Repeated instillations of RA induced marked, widespread inflammation throughout the nasal cavity, hypersecretion of mucosubstances, atrophy of OE and loss of OSNs, atrophy and loss of OMP staining in the OB, and necrosis and exfoliation of NTE and RE. We previously found that single, intranasal instillations of RA caused atrophy of OE, loss of OSNs, and atrophy of the OB (Islam et al., 2007). Single instillations of RA also resulted in neutrophil infiltration in the affected OE and associated lamina propria. We are unaware of

other studies describing the additional changes we observed following repeated exposures to RA.

The neutrophilic inflammation induced by repeated exposures to RA was significantly more widespread and severe than that seen with single instillations of RA. No effects were observed in T1 and T2 with single instillations of RA. Here we observed significant inflammation and edema in the MNT accompanied by bone loss in the MT. Large numbers of neutrophils were also observed in the secreted mucus found in the airways. Proinflammatory cytokine levels in the nasal lavage of mice instilled with the high dose of RA as well as the proinflammatory gene expression we observed support the presence of an active inflammatory response consisting primarily of neutrophil infiltration 24h following the last RA exposure. The neutrophilic infiltration we observed was likely present during intranasal instillations of RA as well. Further work could investigate whether any of these genes remain upregulated in mice weeks after the last exposure to RA when visible evidence of inflammation is lacking.

The loss of stored product in mucus-secreting epithelial cells in both the airway surface epithelium and the LNG, along with the accumulation of excess mucus in the airway lumens, suggested that intranasal instillation of RA induced widespread mucus hypersecretion. These morphologic changes are consistent with those previously described in human subjects (Williams et al., 2006; Rogers, 2007) and laboratory animals (Nikula and Green, 2000; Reader et al., 2003) with chronic hypersecretory conditions in either the upper or lower respiratory tract (e.g., rhinitis, asthma, chronic bronchitis). The accumulation of airway mucus

reflects a protective reaction in response to the inflammatory and tissue damaging effects of the repeated instillations of RA. It is unclear why Bowman's glands in the lamina propria of ET2 were unaffected 24h after the last RA instillation. This would seem to indicate that these glands were not significantly contributing to the volume of mucus being released into the airway. It is also unclear why Bowman's glands would then have mucus overproduction at three weeks post-instillation. The overproduction of mucus we observed in Bowman's glands, the RE lining the NPM, and the LNG three weeks after the last RA instillation is likely an attempt to prevent further tissue injury. It is interesting that this response persisted three weeks after the last RA instillation.

RA may induce mucus hypersecretion by induction of proinflammatory cytokines IL-1 β , IL-6, and TNF- α , which have been shown to cause mucus secretion and MUC gene expression. (Rogers, 2007). Additionally, TNF- α and proteinases can induce mucus secretion and goblet cell hyperplasia (Rogers, 2007). Many molds including *S. chartarum* and other black mold species produce a variety of proteinases (Nielsen et al., 2002; Yike et al., 2007). We observed significant neutrophilic inflammation throughout the nasal cavities of RA-exposed mice. Neutrophils have been shown to release proteinases and cytokines that contribute to pathways involved in COPD, including potent stimulation of release of mucus from goblet cells (Kim and Nadel, 2004). Cigarette smoke-induced inflammation has been shown to play a role in mucus cell metaplasia and mucus hypersecretion (Yoshida and Tuder, 2007). Ozone, another irritant gas, induces mucus cell metaplasia and secretion that is partially

dependent on neutrophilic inflammation (Wagner et al., 2001). Damage to surrounding epithelial cells resulting in cytokine and growth factor release may also play a role in the mucus responses we observed (Rogers, 2007). Additional studies are needed to better understand the mechanisms behind the mucus changes we observed and to determine whether long-lasting changes in mucus production would result from repeated exposures to RA.

Unlike our observations in the present study, single intranasal instillations did not result in atrophy and loss of OSNs in the OE lining the DM (Islam et al., 2007). We suggested that the DM might have been spared from the effects of a single intranasal instillation of SG because of distinct populations of odorant receptors found in the nose (Islam et al., 2006). Ressler et al. (1993) described specific zones of odorant receptors in the OE, one of which was found in the dorsal meatus.

We previously speculated that macrocyclic trichothecenes might bind to specific odorant receptors and initiate apoptosis in OSNs (Islam et al., 2007). Our results suggest that this is not the case. It is possible that macrocyclic trichothecenes interact with the odorant receptors on OSNs, but that no binding specificity exists. Another potential explanation is that macrocyclic trichothecenes interact with the odorant receptors in the DM, but that this area is less sensitive than the areas in which we observed effects after a single intranasal instillation of SG or RA (Islam et al., 2006; Islam et al., 2007). It is possible that a higher overall dose of toxin is required for adverse effects in the DM, and that the overall amount of RA instilled via repeated instillations reached

a sufficiently high dose to cause effects in this area. Repeated instillations might also saturate the receptors in the OE lining areas such as ET2 and result in interaction with, and apoptosis of, OSNs in the DM.

RA might induce apoptosis in OSNs by a variety of mechanisms. We have previously demonstrated that RA induces expression of p53, BAX, and PKR mRNA 24 hours after instillation (Islam et al., 2007). SG causes upregulation of the pro-apoptotic genes Fas, FasL, p75, p53, BAX, caspase 3, and caspase-activated DNase (CAD) in the OE lining the ethmoid turbinates following a single intranasal instillation (Islam et al., 2006). Activation of mitogen-activated protein kinases (MAPK) such as p38 and p53 by trichothecene mycotoxins, C-Jun N-terminal kinase (JNK) and extracellular signal-related kinase (ERK) have also been observed in response to trichothecenes (Shifrin and Anderson, 1999; Yang et al., 2000; Chung et al., 2003; Zhou et al., 2005).

Other mechanisms might be involved as well, such as the extended inflammatory response we observed with repeated instillations. *In vitro* studies have shown that TNF- α induces apoptosis in OSNs (Suzuki and Farbman, 2000), and the extended release of this proinflammatory cytokine might contribute to the more extensive apoptosis of OSNs we observed in this study via death receptors and the extrinsic apoptotic pathway. Fas is also involved in the extrinsic pathway (Cowan and Roskams, 2002). We showed that RA induces expression of Fas and TNF- α mRNA prior to or concurrent with expression and activation of caspase 3 (Islam et al., 2007). Here we observed that IL-1 β , TNF- α , IL-6, iNOS, MCP-1 and MIP-2 mRNA expression were significantly upregulated at 24 hours

in the ET and MNT. We also observed significantly increased TNF- α , MCP-1, and IL-6 in nasal lavage fluid. These proinflammatory cytokines and the primarily neutrophilic cellular infiltrate indicate an active inflammatory process that may contribute to cell death. Macrocyclic trichothecenes might also cause production of reactive oxygen species (Yang et al., 2000), contributing to a ribotoxic stress response (Zhou et al. 2005) and leading to apoptosis of OSNs and tissue damage.

The OSNs in OE are unique among the populations of neuronal cells within the body in that mature OSNs undergo a regular cycle of apoptosis and regeneration via basal cell proliferation and differentiation. OSNs have a typical lifespan of 30-40 days or longer, a short duration compared to other neurons (Graziadei and Graziadei, 1978). Loss of OSNs persisted 3 weeks after the last RA instillation while atrophy of OE did not. It is possible that the cells present at 3 weeks after the instillations were immature OSNs, and thus would not be expressing OMP. It is also possible that the cells accounting for the OE thickness are sustentacular cells.

Intranasal perfusion with ZnSO₄ has been used to induce death of OSNs in mice and rats to study the recovery of OSNs following chemical lesion (Burd, 1993; Herzog and Otto, 1999) Ducray et al. (2002) showed that mice could differentiate water and butanol in a behavioral test maze approximately 18 days following intranasal instillation of ZnSO₄, indicating that an intact sense of smell was present. ZnSO₄ is a common chemical used to induce death of OSNs. The

authors of this study noted that OMP staining was significantly reduced at 25 and 35 days after instillation in treated mice in spite of the recovery of olfactory-mediated behavior at 18 days. Many of the cells observed in the OE were immature OSNs, suggesting that only a limited number of mature OSNs are needed to restore olfactory function (Ducray et al., 2002). Further studies are needed to determine the duration of the loss of OSNs we observed 3 weeks post-exposure. Studies to investigate whether these mice have retained or recovered their ability to detect odors might shed some light on the disparity between OE thickness and the number of OSNs. The effects of macrocyclic trichothecenes on basal and sustentacular cells in the OE should also be investigated. A small increase in OSNs was observed 3 weeks after the last instillation, which suggests that some sustentacular and basal cells must be intact. Significant damage to sustentacular and basal cells might result in an inability of OSNs to recover from the effects of repeated exposure to RA. We could speculate that the incomplete recovery of the OSNs 3 weeks after the last instillation is due to damage to sustentacular and basal cells, particularly globose basal cells. Globose basal cells proliferate rapidly compared to horizontal basal cells (Schwob, 2002), and it is possible that the globose basal cells are damaged by RA, leaving the more slowly proliferating horizontal cells to produce replacement OSNs. Further studies are needed to characterize the effects of single and repeated exposures to macrocyclic trichothecenes on these olfactory cell populations.

We observed atrophy and loss of OMP staining in the OB 24h after the last RA instillation. At three weeks post-exposure, no evidence of OB atrophy was observed. We also found upregulation of IL-1 β , TNF- α , and MCP-1 expression in the OB 24 hours after the last instillation of RA. Shipley (1985) reported retrograde and anterograde transport of wheat germ agglutinin-horseradish peroxidase between the OSNs and the OB. This type of transport suggests that inhaled environmental toxins could potentially travel along the axons of OSNs and reach the OB. It is possible that the toxicity we observed in the OB results from such a transport mechanism. Unlike the OE, loss of OMP staining did not persist three weeks after the last RA instillation in the OB. It is unclear whether this return to normality in the OB relates to recovery of OE. If transport via the axons of the OSNs is indeed the route by which the RA reached the OB to cause toxicity, it is possible that a gradient was established and the OB actually received a lower dose of RA than the OSNs. It is also possible that RA ascends to the OB shortly after instillation and results in neutrophilic inflammation, but further instillations of RA do not have significant effect on the OB. If RA is traveling to the OB via the axons of the OSNs, this connection may be lost as the OSNs undergo apoptosis. Studies in the future could further investigate the mechanisms of toxicity in the OB and determine what, if any, relationship exists between recovery of the OB and OSNs.

The atrophy and exfoliation of NTE and RE induced by repeated instillations of RA has not been previously reported. We previously speculated that the slower mucociliary clearance rate of OE, which is lined by immotile cilia,

might account for the susceptibility of OSNs to RA that we observed (Islam et al., 2007). Repeated exposures to RA resulted in loss of cilia and death of ciliated cells. This may account for the effects of repeated RA exposures on the RE, which is normally lined by motile cilia with a high beat frequency (Morgan et al., 1984). Additional factors affecting mucosal clearance, such as metabolism and blood flow, may be impacted such that existing differences that may have accounted for the specific effects noted with a single instillation are overcome, leading to more widespread toxicity. The prolonged inflammatory response caused by repeated instillations of RA might account for the damage to other epithelial tissues in the nose.

Studies should determine the effects of more chronic exposures to macrocyclic trichothecenes on all cell populations in the OE and OB, and investigate whether a threshold of injury exists beyond which recovery of normal olfaction and OMP staining do not occur. Based on the results of this study, it is likely that repeated exposures to macrocyclic trichothecenes like RA would result in more severe and long-lasting effects than single, acute exposures. Long-lasting or permanent loss of the sense of smell or the potential effects associated with atrophy and inflammation of the OB could have significant consequences for human health, and thus further studies are needed to determine the risk of such effects in humans. Aerosol inhalation studies of macrocyclic trichothecenes in mice could be undertaken to better model the route of exposure expected in people and would help to frame the results presented here in the context of human risk.

CHAPTER 3 BIBLIOGRAPHY

- Andersson, M. A., Nikulin, M., Koljalg, U., Andersson, M. C., Rainey, F., Reijula, K., Hintikka, E. L., and Salkinoja-Salonen, M. (1997) Bacteria, molds, and toxins in water-damaged building materials. *Appl. Environ. Microbiol.* **63**, 387-93.
- Audige, A., Yu, Z. R., Frey, B. M., Uehlinger, D. E., Frey, F. J., and Vogt, B. (2003) Epithelial sodium channel (ENaC) subunit mRNA and protein expression in rats with puromycin aminonucleoside-induced nephrotic syndrome. *Clin. Sci. (Lond)* **104**, 389-95.
- Boutin-Forzano, S., Charpin-Kadouch, C., Chabbi, S., Bennedjai, N., Dumon, H., and Charpin, D. (2004) Wall relative humidity: a simple and reliable index for predicting *Stachybotrys chartarum* infestation in dwellings. *Indoor Air* **14**, 196-99.
- Brasel, T. L., Douglas, D. R., Wilson, S. C., and Straus, D. C. (2005) Detection of airborne *Stachybotrys chartarum* macrocyclic trichothecene mycotoxins on particulates smaller than conidia. *Appl. Environ. Microbiol.* **71**, 114-22.
- Burd, G. D. (1993) Morphological study of the effects of intranasal zinc sulfate irrigation on the mouse olfactory epithelium and olfactory bulb. *Microsc. Res. Tech.* **24**, 195-213.
- Cheng, Y. S., Hansen, G. K., Su, Y. F., Yeh, H. C., and Morgan, K. T. (1990) Deposition of ultrafine aerosols in rat nasal molds. *Toxicol. Appl. Pharmacol.* **106**, 222-233.
- Cheng, Y. S., Yeh, H. C., Swift, D. L. (1991) Aerosol deposition in human nasal airway for particles 1 nm to 20 μ m: a model study. *Radiat. Prot. Dosimetry.* **38**, 41-47.
- Cheng, Y. S., Yeh, H. C., Guilmette, R. A., Simpson, S. Q., Cheng, K. H., and Swift, D. L. (1996) Nasal deposition of ultrafine particles in human volunteers and its relationship to airway geometry. *Aerosol. Sci. Technol.* **25**, 274-291.
- Chung, Y., Zhou, H., and Pestka, J. J. (2003) Transcriptional and posttranscriptional roles for p38 mitogen-activated protein kinase in upregulation of TNF- α expression by deoxynivalenol (vomitoxin). *Toxicol. Appl. Pharmacol.* **193**, 188-201.
- Chung, K. F. (2005) Inflammatory mediators in chronic obstructive pulmonary disease. *Curr. Drug Targets Inflamm. Allergy* **4**(6), 619-625.
- Cowan, C. M., and Roskams, A. J. (2002) Apoptosis in the mature and developing olfactory neuroepithelium. *Microsc. Res. Tech.* **58**, 204-215.

Ducray, A., Bondier, J., Michel, G., Bon, K., Propper, A., and Kastner, A. (2002) Recovery following peripheral destruction of olfactory neurons in young and adult mice. *Eur. J. Neurosci.* **15**, 1907-1917.

Nielsen, K. F. (2003) Mycotoxin production by indoor molds. *Fungal Genet. Biol.* **39**, 103-117.

Fung, F., Clark, R., and Williams, S. (1998) *Stachybotrys*, a mycotoxin-producing fungus of increasing toxicologic importance. *J. Toxicol. Clin. Toxicol.* **36**, 79-86.

Gordon, W. A. (1999) Cognitive impairment associated with exposure to toxigenic fungi. In: *Bioaerosols, Fungi and Mycotoxins: Health Effects, Assessment, Prevention and Control* (E. Johannig, ed.), Chapter I, pp. 94-98. Eastern New York Occupational and Environmental Health Center, Albany, New York.

Gregory, L., Pestka, J. J., Dearborn, D. G., and Rand, T. G. (2004) Localization of satratoxin-G in *Stachybotrys chartarum* spores and spore-impacted mouse lung using immunocytochemistry. *Toxicol. Pathol.* **32**, 26-34.

Grove, J. F. (1988) Non-macrocylic trichothecenes. *Nat. Prod. Rep.* **5**, 187-209.

Grove, J. F. (1993) Macrocylic trichothecenes. *Nat. Prod. Rep.* **10**, 429-48.

Grove, J. F. (2000) Non-macrocylic trichothecenes. Part 2. *Prog. Chem. Org. Nat. Prod.* **69**, 1-70.

Harkema, J. R., Carey, S. A., and Wagner, J. G. (2006) The nose revisited: a brief review of the comparative structure, function, and toxicologic pathology of the nasal epithelium. *Toxicol. Pathol.* **34**, 252-269.

Harkema, J. R., Plopper, C. G., Hyde, D. M., St George, J. A., and Dungworth, D. L. (1987) Effects of an ambient level of ozone on primate nasal epithelial mucosubstances. Quantitative histochemistry. *Am. J. Pathol.* **127**, 90-6.

Herzog, C. and Otto, T. (1999) Regeneration of olfactory receptor neurons following chemical lesion: time course and enhancement with growth factor administration. *Brain Res.* **849**, 155-161.

Hinkley, S. F., and Jarvis, B. B. (2001) Chromatographic method for *Stachybotrys* toxins. *Methods Mol. Biol.* **157**, 173-94.

Hossain, M. A., Ahmed, M. S., and Ghannoum, M. A. (2004) Attributes of *Stachybotrys chartarum* and its association with human disease. *J. Allergy Clin. Immunol.* **113**, 200-08.

Hyde, D. M., Magliano, D. J., and Plopper, C. G. (1991) Morphometric assessment of pulmonary toxicity in the rodent lung. *Toxicol. Pathol.* **19**, 428-446.

Hyde, D. M., Plopper C. G., St. George, J. A., and Harkema, J. R. (1990) Morphometric cell biology of air space epithelium. In: Schraufnagel, D. E. (Ed.), *Electron Microscopy of the Lung*. Marcel Dekker, New York, pp.71-120.

Institute of Medicine (2004) *Damp Indoor Spaces and Health*, pp. 1-355. National Academies Press, Washington, D.C.

Islam, Z., Harkema, J. R., and Pestka, J. J. (2006) Satratoxin G from the black mold *Stachybotrys chartarum* evokes olfactory sensory neuron loss and inflammation in the murine nose and brain. *Environ. Health Perspect.* **114**, 1099-107.

Jarvis, B. B., Lee, Y. W., Comezoglu, S. N., and Yatawara, C. S. (1986) Trichothecenes produced by *Stachybotrys atra* from Eastern Europe. *Appl. Environ. Microbiol.* **51**, 915-18.

Jarvis, B. B., Sorenson, W. G., Hintikka, E. L., Nikulin, M., Zhou, Y., Jiang, J., Wang, S., Hinkley, S., Etzel, R. A., and Dearborn, D. (1998) Study of toxin production by isolates of *Stachybotrys chartarum* and *Memnoniella echinata* isolated during a study of pulmonary hemosiderosis in infants. *Appl. Environ. Microbiol.* **64**, 3620-25.

Johanning, E., Biagini, R., Hull, D., Morey, P., Jarvis, B., and Landsbergis, P. (1996) Health and immunology study following exposure to toxigenic fungi (*Stachybotrys chartarum*) in a water-damaged office environment. *Int. Arch. Occup. Environ. Health* **68**, 207-18.

Kilburn, K. H. (2004) Role of molds and mycotoxins in being sick in buildings: neurobehavioral and pulmonary impairment. *Adv. Appl. Microbiol.* **55**, 339-59.

Kim, S., and Nadel, J. A. (2004) Role of neutrophils in mucus hypersecretion in COPD and implications for therapy. *Treat. Respir. Med.* **3**(3), 147-159.

Kream, R. M., and Margolis, F. L. (1984) Olfactory marker protein: turnover and transport in normal and regenerating neurons. *J. Neurosci.* **4**, 868-79.

Mery, S., Gross, E. A., Joyner, D. R., Godo, M., and Morgan, K. T. (1994) Nasal diagrams: a tool for recording the distribution of nasal lesions in rats and mice. *Toxicol. Pathol.* **22**, 353-72.

Morgan, K. T., Jiang, X. Z., Patterson, D. L., and Gross, E. A. (1984) The nasal mucociliary apparatus. Correlation of structure and function in the rat. *Am. Rev. Respir. Dis.* **130**, 275-281.

Nielsen, K. F., Huttunen, K., Hyvärinen, A., Andersen, B., Jarvis, B. B., Hirvonen, M. (2002) Metabolite profiles of *Stachybotrys* isolates from water-damaged buildings and their induction of inflammatory mediators and cytotoxicity in macrophages. *Mycopathologia* **154**, 201-205.

Nikula, K. J. and Green, F. H. (2000) Animal models of chronic bronchitis and their relevance to studies of particle-induced disease. *Inhalation Toxicology* **12**(S4), 123-153.

Rand, T. G., Mahoney, M., White, K., and Oulton, M. (2002) Microanatomical changes in alveolar type II cells in juvenile mice intratracheally exposed to *Stachybotrys chartarum* spores and toxin. *Toxicol. Sci.* **65**, 239-45.

Reader, J. R., Tepper, J. S., Schelegle, E. S., Aldrich, M. C., Putney, L. F., Pfeiffer, J. W., Hyde, D. M. (2003) Pathogenesis of mucous cell metaplasia in a murine asthma model. *American Journal of Pathology* **162**, 2069-2078.

Ressler, K. J., Sullivan, S. L., and Buck, L. B. (2003) A zonal organization of odorant receptor gene expression in the olfactory epithelium. *Cell* **73**, 597-609.

Rogers, D. F. (2007) Physiology of mucus secretion and pathophysiology of hypersecretion. *Respiratory Care* **52**, 1134-1149.

Schwob, J. E. (2002) Neural regeneration and the peripheral olfactory system. *Anat. Rec.* **269**, 33-49.

Shifrin, V. I., and Anderson, P. (1999) Trichothecene mycotoxins trigger a ribotoxic stress response that activates c-Jun N-terminal kinase and p38 mitogen-activated protein kinase and induces apoptosis. *J. Biol. Chem.* **274**, 13985-13992.

Shiple, M. T. (1985) Transport of molecules from nose to brain: transneuronal anterograde and retrograde labeling in the rat olfactory system by wheat germ agglutinin-horseradish peroxidase applied to the nasal epithelium. *Brain Res. Bull.* **15**, 129-142.

Sorenson, W. G., Frazer, D. G., Jarvis, B. B., Simpson, J., and Robinson, V. A. (1987) Trichothecene mycotoxins in aerosolized conidia of *Stachybotrys atra*. *Appl. Environ. Microbiol.* **53**, 1370-75.

Suzuki, Y., and Farbman, A. I. (2000) Tumor necrosis factor- α -induced apoptosis in olfactory epithelium in vitro: possible roles of caspase 1 (ICE), caspase 2 (ICH-1), and caspase 3 (CPP32). *Exp. Neurol.* **165**, 35-45.

Steiger, D., Hotchkiss, J., Bajaj, L., Harkema, J., and Basbaum, C. (1995) Concurrent increases in the storage and release of mucin-like molecules by rat airway epithelial cells in response to bacterial endotoxin. *Am. J. Respir. Cell. Mol. Biol.* **12**, 307-14.

Tuomi, T., Reijula, K., Johnsson, T., Hemminki, K., Hintikka, E. L., Lindroos, O., Kalso, S., Koukila-Kahkola, P., Mussalo-Rauhamaa, H., and Haahtela, T. (2000) Mycotoxins in crude building materials from water-damaged buildings. *Appl. Environ. Microbiol.* **66**, 1899-1904.

Tuomi, T., Saarinen, L., and Reijula, K. (1998) Detection of polar and macrocyclic trichothecene mycotoxins from indoor environments. *Analyst* **123**, 1835-41.

Wagner, J. G., Van Dyken, S. J., Hotchkiss, J. A., and Harkema, J. R. (2001) Endotoxin enhancement of ozone-induced mucus cell metaplasia is neutrophil-dependent in rat nasal epithelium. *Toxicol. Sci.* **60**, 338-347.

Williams, O. W., Sharafkhaneh, A., Kim, V., Dickey, B. F., and Evans, C. M. (2006) Airway mucus from production to secretion. *American Journal of Respiratory Cell and Molecular Biology* **34**, 527-536.

Yang, G., Jarvis, B. B., Chung, Y., and Pestka, J. J. (2000) Apoptosis induction by the Satratoxins and other trichothecene mycotoxins: relationship to ERK, p38 MAPK, and SAPK/JNK activation. *Toxicol. Appl. Pharmacol.* **164**, 149-160.

Yike, I., and Dearborn, D. G. (2004) Pulmonary effects of *Stachybotrys chartarum* in animal studies. *Adv. Appl. Microbiol.* **55**, 241-73.

Yike, I., Miller, M. J., Sorenson, W. G., Walenga, R., Tomaszefski, J. F., Jr., and Dearborn, D. G. (2002) Infant animal model of pulmonary mycotoxicosis induced by *Stachybotrys chartarum*. *Mycopathologia* **154**, 139-52.

Yike, I., Rand, T. G., and Dearborn, D. G. (2005) Acute inflammatory responses to *Stachybotrys chartarum* in the lungs of infant rats: time course and possible mechanisms. *Toxicol. Sci.* **84**, 408-17.

Yike, I., Rand, T. G., and Dearborn, D. G. (2007) The role of fungal proteinases in pathophysiology of *Stachybotrys chartarum*. *Mycopathologia* **164**, 171-181.

Yoshida, T., and Tuder, R. M. (2007) Pathobiology of cigarette smoke-induced chronic obstructive pulmonary disease. *Physiol. Rev.* **87**, 1047-1082.

Zhou, H., Islam, Z., and Pestka, J. J. (2005) Induction of competing apoptotic and survival signaling pathways in the macrophage by the ribotoxic trichothecene deoxynivalenol. *Toxicol. Sci.* **87**, 113-122.

CHAPTER 4

Nasal Toxicity in Weanling and Adult Mice Repeatedly Exposed to the Macrocyclic Trichothecene Mycotoxin, Satratoxin G

ABSTRACT

Satratoxin G (SG) is a macrocyclic trichothecene mycotoxin produced by *Stachybotrys chartarum*, the black mold suggested to contribute to illnesses associated with water-damaged buildings. We have previously reported that acute SG exposure causes nasal toxicity in adult mice. The purpose of the present study was to determine the susceptibility of weanling mice to SG-induced nasal injury as compared to adults. Female C57BL/6 mice, 3-4 wks (weanling) or 10-12 wks (adult) of age, were intranasally instilled once daily with 250 $\mu\text{g}/\text{kg}$ SG in saline (30 μl) or saline alone (0 $\mu\text{g}/\text{kg}$ SG) for 3 consecutive days. Mice were sacrificed 24 h after the last instillation. Nasal tissues were processed for microscopic examination and morphometric analysis. SG induced a neutrophilic rhinitis, atrophy of olfactory epithelium (OE), and loss of olfactory sensory neurons (OSNs) in both weanling and adult mice. The severity of toxicant-induced rhinitis (mucosal density of neutrophils) was significantly greater (approximately 1.5x) in weanling mice compared to adults. The severity of SG-induced OE injury (epithelial atrophy and loss of OSNs), however, was similar in both age groups. These findings in mice suggest that neurotoxicity and inflammation are potential adverse health effects of exposure to SG-laden *S. chartarum* in both infants and adults. The long-term consequences of early life exposure are yet to be investigated.

INTRODUCTION

Numerous adverse human health effects have been attributed to damp indoor environments caused by water damage, and there are strong associations between exposure to damp buildings and upper respiratory tract symptoms, such as nasal congestion, sneezing, runny or itchy nose, and throat irritation. (Institute of Medicine, 2004) In addition, lower respiratory symptoms such as cough, wheeze, and exacerbation of asthma have also been linked to damp indoor environments. Other symptoms reported in suspected damp building-related illnesses include immunological and neurological effects, but supporting evidence for these is lacking (Pestka et al., 2008).

Damp building-related illnesses are often linked to the moisture-promoted presence of *Stachybotrys chartarum*, a saprophytic black mold which grows on water-damaged materials containing high amounts of cellulose (Andersson et al., 1997; Boutin-Forzano et al., 2004; Tuomi et al., 1998; Tuomi et al., 2000). Macrocytic trichothecene mycotoxins produced by the fungus might potentially contribute to adverse associations with *S. chartarum* (Fung et al., 1998; Hossain et al., 2004; Kilburn 2004; Rosenblum et al., 2006). These compounds bind to ribosomes and inhibit protein synthesis (Ueno, 1984; Ehrlich and Daigle, 1987; Shifrin and Anderson, 1999; Bennett and Klich, 2003; Li and Pestka, 2008) and have been shown to cause pulmonary toxicity in laboratory mice (Hossain et al., 2004). Satratoxin G (SG), a macrocytic trichothecene produced by *S. chartarum*, is found in both spores and mycelial fragments (Gregory et al., 2004) that may become airborne and could potentially be inhaled. Macrocytic

trichothecenes produced by *S. chartarum* have been detected in the indoor air of mold-contaminated buildings (Brasel et al., 2005), and have been found on small particles, such as house dust (Brasel et al., 2005). Both fungal spores and mycelial fragments may become airborne and inhaled under the right conditions. The linkage between *S. chartarum* and damp building-related illness is complex and requires further study (Institute of Medicine, 2004; Pestka et al., 2008).

Studies of idiopathic pulmonary hemorrhage (IPH) in infants sparked concern about both the general health effects of exposure to *S. chartarum* and the unique susceptibility of children to this fungal organism. 37 infants in the Cleveland, Ohio area presented for respiratory distress attributed to pulmonary hemorrhage between 1993 and 1998. The Centers for Disease Control and Prevention (CDC) led case-control investigations of the reported cases of IPH and found that the homes of affected infants were more likely to have experienced water damage than those of control children. A higher quantity of airborne mold, including *S. chartarum*, was detected in air samples collected in the homes of affected infants compared to air samples from control homes (CDC, 1994; CDC, 1996; Dearborn et al., 1999). Similar results were reported following identification of another cluster of IPH cases in Chicago (CDC, 1995). Flappan et al. (1999) conducted an investigation of a case of IPH in an infant living in a water-damaged home in Missouri and identified *S. chartarum* and several other mold species in the residence. Dearborn et al. (1999) suggested that *S. chartarum*, and particularly Satratoxins G and H, might be involved in the pathogenesis of IPH in infants. The authors also observed that none of the

adults residing in the homes of affected infants experienced respiratory symptoms. In 1999, a CDC panel of experts reassessed the existent evidence from investigations of IPH and determined that further work was needed to prove a connection between exposure to *S. chartarum* in water-damaged buildings and IPH (CDC, 2000).

The effects of other trichothecene mycotoxins have been compared in young and adult mice. The effects of oral exposure to the trichothecenes T-2 toxin, nivalenol, and deoxynivalenol (DON) were compared in young and adult mice. The author observed that infant and immature mice were significantly more susceptible to the effects of these mycotoxins than adults (Ueno, 1984). It was recently shown that weanling mice are more susceptible than adult mice to oral exposure to DON (Pestka and Amuzie, 2008). While clearance of DON was similar in weanling and adult mice, tissue burdens in weanlings were twice that of adults. IL-1 α , IL-6, and TNF- α were evaluated to compare proinflammatory cytokine induction in weanling and adult mice. At 60 minutes, cytokine mRNA levels were similar in weanlings and adults, but the cytokine expression in weanlings was twice that in adults at 120 minutes. The results of these studies indicate that trichothecenes may impact children and adults differently. We are unaware of other studies comparing the nasal effects of intranasal exposure to trichothecenes, particularly SG, in young and adult mice. In a recent study, we demonstrated that mice intranasally instilled once with 250 ng of SG develop rapid and significant loss of olfactory sensory neurons (OSNs) through apoptosis in both the nose and brain (Islam et al., 2006). In a following study, we found

that Roridin A (RA), another macrocyclic trichothecene of similar chemical structure, also induced rapid apoptosis and marked loss of OSNs in the nasal airways and the olfactory bulb (OB) of mice after a single intranasal instillation (Islam et al. 2007). The purpose of the present study was to compare the effects of SG on the epithelial and inflammatory responses in the nasal passages of weanling mice to those in adult mice.

MATERIALS AND METHODS

Experimental Design

Pathogen-free female weanling (3-4 wk) or adult (10-12 wk) mice (C57BL/6, Charles River, Portage, MI) were randomly assigned to 4 experimental groups by age at arrival (n = 6). Mice were housed in polycarbonate cages containing *Cell-Sorb Plus* bedding (A & W products, Cincinnati, OH) and covered with filter bonnets. Room lights were set on a 12-hour light/dark cycle.

Temperature and relative humidity were maintained between 21-24°C and 40-55% humidity, respectively. This study was carried out in accordance with National Institutes of Health guidelines and approved by the All University Committee on Animal Use and Care at Michigan State University.

SG was isolated from *S. chartarum* as previously described (Hinkley and Jarvis, 2001; Islam et al., 2006). The identity of the toxin was confirmed using electrospray ionization and collision-induced dissociation tandem mass spectroscopy (Tuomi et al., 1998). For instillation, mice were lightly anesthetized using 3.5% Isoflurane (Abbott Laboratories, IL) and 96.5% oxygen. Mice

received intranasal instillations of saline (0 µg/kg) or 250 µg/kg SG in 30 µL of pyrogen-free saline (Abbott Laboratories, IL; 15 µL per nostril), once daily for three consecutive days.

Animal Necropsies and Tissue Processing

At the designated time of sacrifice, mice were deeply anesthetized with an intraperitoneal (ip) injection of 0.1 ml of 12% sodium pentobarbital and euthanized by exsanguination via cutting of the abdominal aorta and vena cava. After death, the head of each mouse was immediately removed and the lower jaw, skin, and muscles were removed. The dorsal cranium was opened to allow for greater fixation of brain tissues. The nasal cavities were flushed with 500 mL of 10% neutral buffered formalin (Fischer Scientific, Fair Lawn, NJ) using a 1 mL syringe and 20-gauge cannula, retrograde through the nasopharyngeal meatus. The nasal cavities were then immersed in a large volume of the same fixative and stored for 24 hours prior to further processing. Following fixation, the heads were decalcified in 13% formic acid (Mallinckrodt Baker, Phillipsburg, MD) for 7 days and then rinsed in running tap water for four hours.

Transverse tissue blocks were selected from the heads of the mice for light microscopy as previously described. (Islam et al., 2006) Transverse blocks were taken at four specific anatomic locations as previously described (Young, 1981; Harkema et al., 2006). Briefly, the proximal section (T1) was taken immediately caudal to the upper incisor teeth; the middle section (T2) was taken at the level of the incisive papilla of the hard palate; the third nasal section (T3)

was taken at the level of the second palatal ridge; and the most caudal nasal section (T4) was taken at the level of the intersection of the hard and soft palates, through the proximal portion of the olfactory bulb (OB) of the brain. Nasal tissue blocks were processed for histopathologic, immunohistochemical and morphometric analyses. All blocks were embedded in paraffin, and the anterior face of each block was sectioned at a thickness of five microns and stained with hematoxylin and eosin for routine light microscopic examination. **Figure 19** illustrates these four transverse tissue sections, the location of specific nasal epithelial injury, the intranasal airways, and the specific site used for morphometric analyses.

Immunohistochemistry (IHC)

Tissue sections were immunohistochemically stained to identify neutrophils in the nasal mucosa, a cellular marker of inflammation, and mature olfactory sensory neurons (OSNs) in olfactory epithelium (OE). Sections T1-T4 were incubated with a nonspecific protein blocking solution of normal sera (Vector Laboratories Inc., Burlingame, CA). Tissue sections designated for anti-neutrophil IHC were transferred to a 1:2500 dilution of primary polyclonal antibody directed against neutrophils (AbD Serotec, Raleigh, NC). After primary antibody incubation, tissue sections were incubated in biotinylated anti-species IgG. Anti-neutrophil immunoreactivity was visualized using anti-rabbit IgG, Streptavidin-Phosphatase complex (KPL Laboratories, Gaithersburg, MD) and

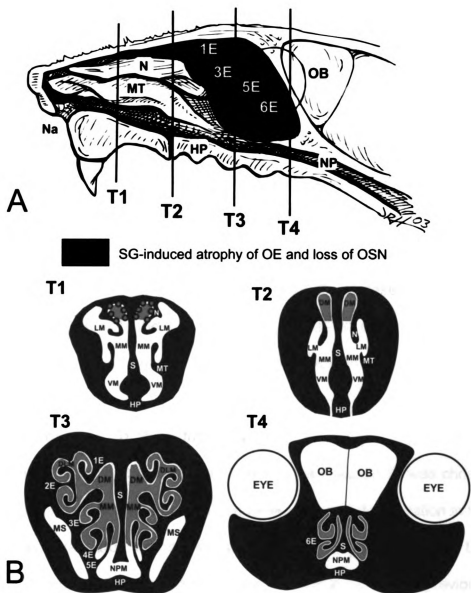


Figure 19. Location of SG-induced OE injury and morphometric analyses. (A) Right nasal passage of the murine nose with septum removed, exposing nasoturbinates (N), maxilloturbinate (MT), and ethmoid turbinates (E1-6); vertical lines indicate anterior surfaces of transverse tissue blocks (T1-T4) that were selected for microscopic examination. (B) Cross-sectional views of T1-4. Blue dots indicate location chosen for morphometric analyses. Na, naris; NP, nasopharynx; NPM, nasopharyngeal meatus; OB, olfactory bulb; HP, hard palate; DM, dorsal medial meatus; DLM, dorsal lateral meatus; LM, lateral meatus; MM, middle medial meatus; VM, ventral meatus; NPM, nasopharyngeal meatus; MS, maxillary sinus; S, septum.

Fast Red chromagen. Following IHC, tissue sections were lightly counterstained with hematoxylin.

Tissues sections designated for olfactory marker protein (OMP; marker of mature OSNs) IHC were pretreated with 3% H₂O₂ in methanol to eliminate endogenous peroxidase prior to transfer to a 1:4000 dilution of primary polyclonal antibody directed against OMP-containing olfactory sensory neurons (goat anti-OMP antibody, Wako Chemicals USA, Richmond, VA). Immunoreactivity of OMP was visualized using Vector R.T.U. Elite ABC-Peroxidase Reagent (Vector Laboratories Inc., Burlingame, CA) followed by Nova Red chromagen. The sections were also lightly counterstained with hematoxylin.

Light Microscopy and Morphometric Analysis

The OE lining the dorsal meatus (DM) in nasal section T1 was chosen as the location for morphometric analysis because of its proximal location in the nasal airway. Standard morphometric techniques were used to estimate the numeric cell density of OSNs in the OE lining the dorsal meatus as previously reported (Islam et al., 2006). Cell counts were determined using light microscopy at a final magnification of 790X. To determine the numeric cell density, the number of nuclear profiles of OMP-positive cells were counted and divided by the length of the underlying basal lamina. The length of the basal lamina was determined by measuring the contour of the basal lamina on a digital image using Scion Image software (Scion Corporation, Fredrick, MD) and a Dell XPS 400 computer (Dell, Austin, TX).

To morphometrically estimate the severity of the neutrophilic inflammatory response, the nuclei of immunohistochemically stained neutrophils were counted in the OE and lamina propria lining the DM in section T1. The numeric cell density of neutrophils was calculated in the same manner used for OMP-positive cells and expressed as the number of neutrophils per length of basal lamina.

Thickness of OE lining the DM was morphometrically estimated using a standard cycloid grid overlay and computer software specifically designed for point and intercept counting (Stereology Toolbox, Davis, CA) as previously described in detail (Hyde et al., 1990; Hyde et al., 1991; Islam et al., 2006). Briefly, microscopic measurements were made at a final magnification of 1920X using a light microscope coupled to a 3.3 megapixel digital camera (Q-color 3 Camera, Quantitative Imaging Corp., Burnaby, BC, Canada) and a Dell Dimension 8200 (Dell, Austin, TX). The thickness (τ) of OE, as measured by volume (μm^3) of OE per unit area (μm^2) of basal lamina, was estimated from point and intercept counts with a 136-point, 35-curve cycloid grid by the equation: $\tau = (3.2 \times Pp)/(2 \times Io)$, where Pp is the number of points counted for the OE and Io is the number of intercepts of the basal lamina. OE thickness was calculated for each mouse from point and intercept counts covering the entire DM in both the right and left nasal airways.

Statistics

All data were analyzed using SigmaStat v. 3.1 and graphed using SigmaPlot 6.0 (Jandel Scientific, San Rafael, CA). Criterion for significance was

set at $p \leq 0.05$. Morphometric data were analyzed using Two-Way analysis of variance (ANOVA) with Student-Newman-Keuls post hoc test.

RESULTS

Nasal Histopathology

The most noticeable age-related difference in nasal morphology, besides the overall size of nasal airways and intranasal septal and turbinate structures, was a thicker and more cellular OE in the saline-instilled control weanling mice as compared to that of adult control mice also instilled with only the saline vehicle. Otherwise the character and distribution of nasal epithelial populations were similar between the two ages of mice.

Both weanling and adult mice that were repeatedly instilled with SG and sacrificed one day after the last instillation had bilateral nasal epithelial and inflammatory lesions that were restricted to the OE lining the dorsocaudal half of the nasal passages (**Figure 19**). These lesions were not present in saline-instilled control mice. SG-related alterations were not histologically evident in nasal airways (meatus) lined by squamous, transitional or respiratory epithelium. SG-instilled mice, both weanlings and adults, had widespread atrophy of OE with conspicuous loss of nuclear and cytoplasmic profiles of OMP-positive OSNs with marked attenuation of the dendritic ciliated layer along the luminal surface of this markedly atrophic epithelium. A few widely scattered pyknotic nuclei and apoptotic bodies were present in toxicant-induced atrophic epithelium.

There was also an associated attenuation of OMP-positive olfactory nerves (axons of OSNs) in the lamina propria beneath the atrophic OE. SG-induced epithelial atrophy was diffuse and affected all olfactory surfaces in both the proximal (T1, T2) and distal (T3, T4) airways, with only minor variations in lesion severity among mice of similar ages. Likewise, there was no microscopically apparent difference in the severity of toxicant-induced epithelial atrophy between weanlings and adults. **Figure 19** illustrates the distribution of the SG-induced OE lesions in both weanling and adult mice.

Associated with the SG-induced OE atrophy, there was a mixed inflammatory cell infiltrate composed mainly of neutrophils with lesser numbers of lymphocytes and monocytes (neutrophilic rhinitis). This induced inflammatory response in SG-instilled mice was restricted to the olfactory mucosa, with no or minimal neutrophilic inflammation in non-olfactory mucosa containing respiratory, transitional or squamous epithelium. Interestingly, SG-exposed weanling mice had a slightly more severe neutrophilic rhinitis compared to similarly treated adult mice.

SG induces loss of OSNs and atrophy of OE in weanling and adult mice

OMP is a peptide specific for mature olfactory sensory neurons (Kream and Margolis, 1984), and loss of OMP-staining is indicative of loss of OSNs. SG induced marked loss of OMP-staining in the DM of both weanling and adult mice, with an approximate decrease of 83% in the number of OMP-stained cells being observed in both treatment groups as compared to saline control animals (**Figure**

20). Interestingly, when the saline control weanling animals were compared to saline control adult animals, weanling controls had a significantly higher (49%) number of OSNs per millimeter of basal lamina (**Figure 21**).

Decreased thickness of OE lining the dorsal meatus in SG-treated mice was observed in both weanling and adults instilled with SG (**Figure 22**).

Weanling mice had a decrease in OE thickness of approximately 35%, while adult mice had a decrease in OE thickness of approximately 41%, compared to weanling and adult control animals, respectively. No statistically significant differences were observed between weanling and adult mice instilled with SG (**Figure 23**).

SG induces an increase in mucosal neutrophils in weanling and adult mice

The number of neutrophils in the OE and lamina propria in the DM were assessed to estimate the inflammatory response induced by SG. Weanling and adult mice both had significant increases in the number of neutrophils in the mucosa of the DM (**Figure 24**). Weanling mice had an increase in neutrophils of approximately 158% compared to saline controls, while adults had an increase in neutrophils of approximately 260% compared to saline controls. A statistically significant difference ($p \leq 0.05$) in the number of mucosal neutrophils was observed in SG-treated weanling and adult mice (**Figure 25**). However, both saline and SG-instilled weanling mice had larger numbers of neutrophils in the mucosa of the DM than saline and SG-instilled adults, respectively.

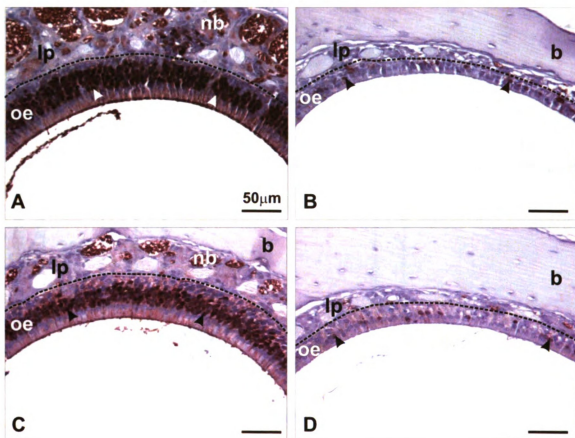


Figure 20. Light photomicrographs of the DM in nasal section T1 (OMP). Weanling (A,B) and Adult mice (C,D) were exposed to either saline alone (A,C) or 250 $\mu\text{g}/\text{kg}$ SG (B,D). Sections were immunohistochemically stained with olfactory marker protein (OMP, marker of mature OSNs). lp, lamina propria; nb, nerve bundle; oe, olfactory epithelium; b, bone; dotted line = basal lamina; black arrowheads = OSN nuclei stained with OMP.

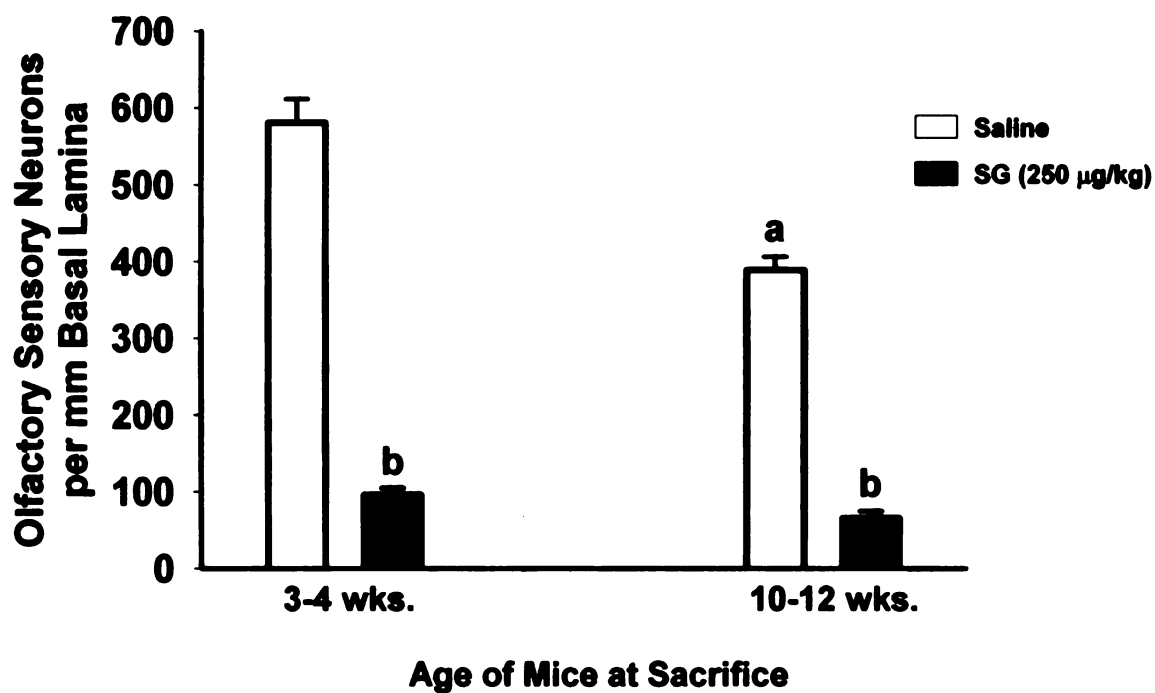


Figure 21. Loss of OSNs in the DM in T1. Both weanling and adult mice instilled with 250 µg/kg SG had 83% decreases in the number of OSNs per mm basal lamina. a, significantly different from weanling saline control mice; b, significantly different from respective saline control group ($p \leq 0.05$).

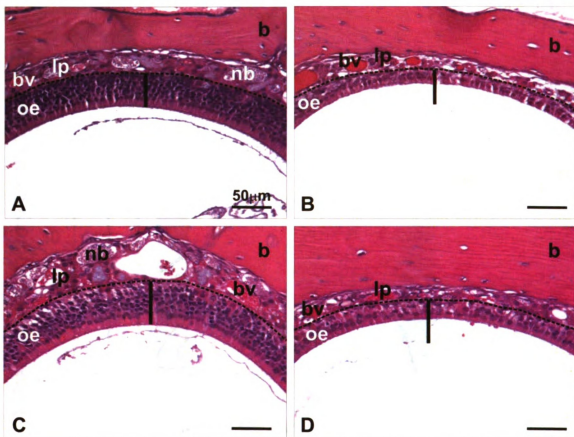


Figure 22. Light photomicrographs of the DM in nasal section T1 (H & E). Weanling (A,B) and Adult mice (C,D) were exposed to either saline alone (A,C) or 250 $\mu\text{g}/\text{kg}$ SG (B,D). Sections were stained with hematoxylin and eosin. bv, blood vessel; lp, lamina propria; nb, nerve bundle; oe, olfactory epithelium; b, bone; dotted line, basal lamina.

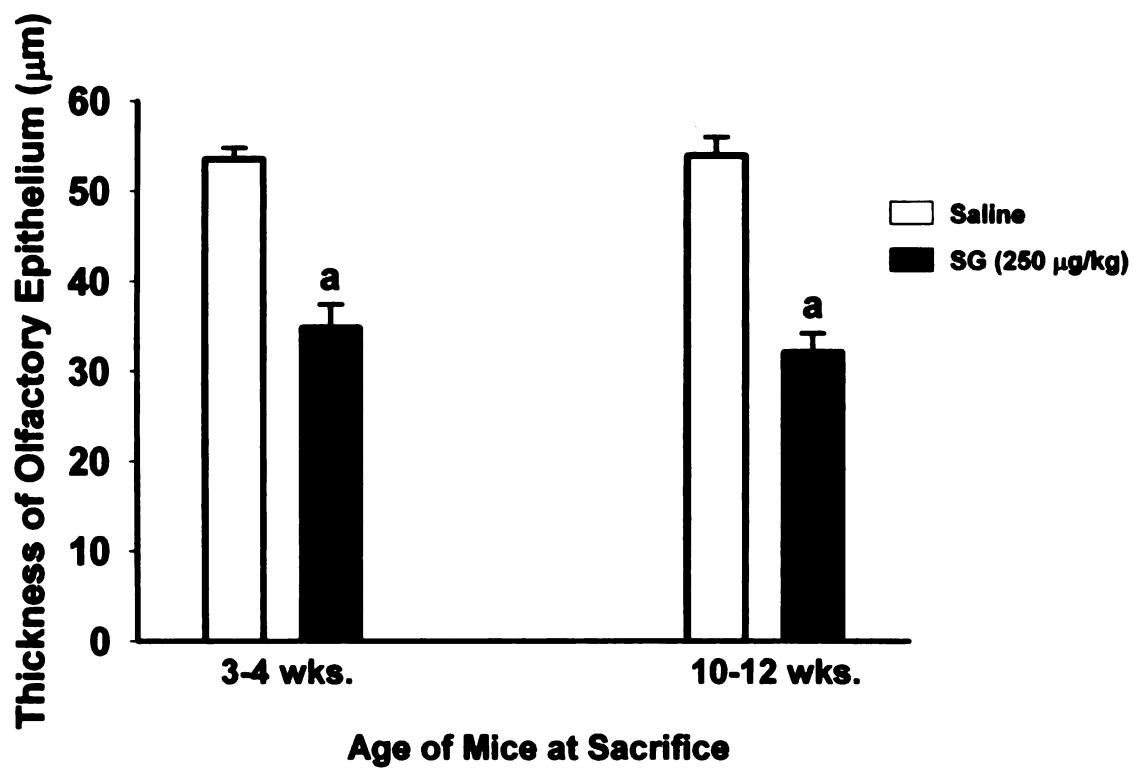


Figure 23. Atrophy of OE in the DM in T1. Weanling and adult mice had 35% and 41% decreases in the thickness of OE, respectively. a, significantly different from respective saline control group ($p \leq 0.05$).

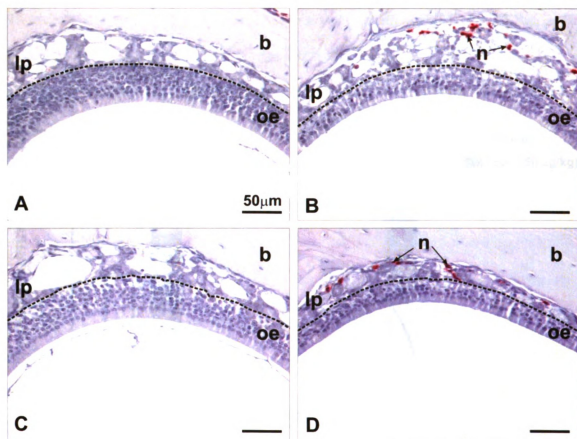


Figure 24. Light photomicrographs of the DM in nasal section T1 (Neutrophils). Weanling (A,B) and Adult mice (C,D) were exposed to either saline alone (A,C) or 250 µg/kg SG (B,D). Sections were immunohistochemically stained with anti-neutrophil antibody. b, bone ; lp, lamina propria; n, neutrophils; oe, olfactory epithelium; dotted line, basal lamina.

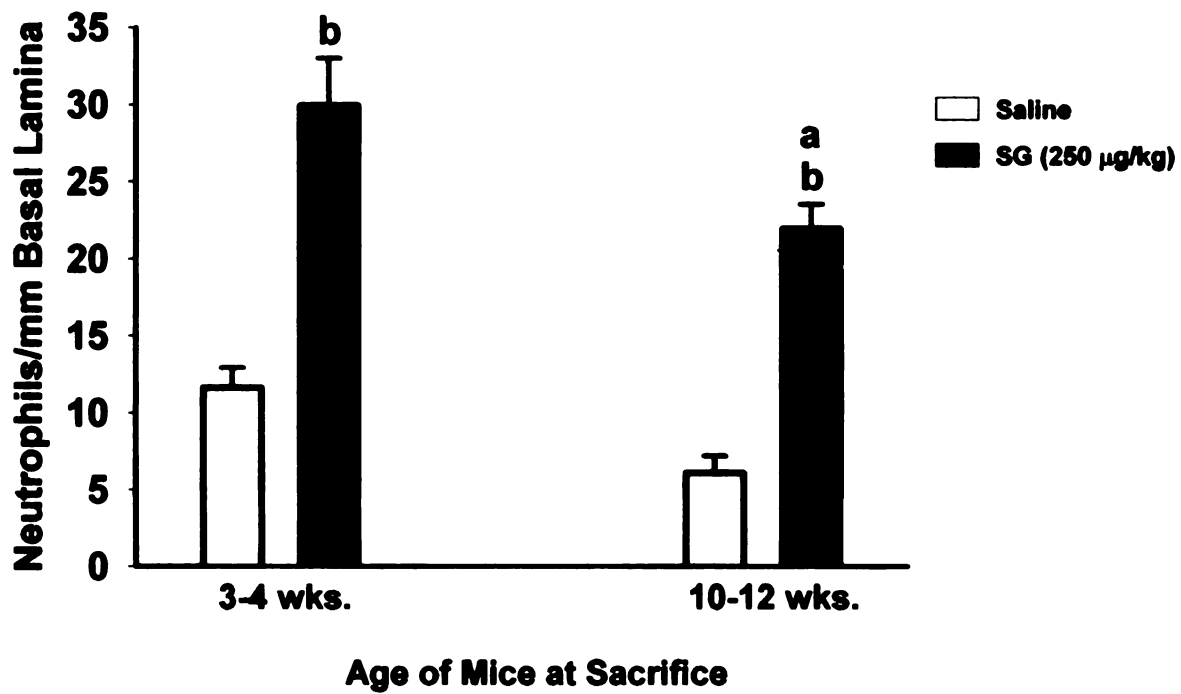


Figure 25. Neutrophilic inflammation in the DM in T1. Weanling and adult mice had 158% and 260% increases in the number of neutrophils per mm basal lamina, respectively. a, significantly different from weanling SG-instilled group. b, significantly different from respective saline control group ($p \leq 0.05$).

DISCUSSION

Damp building-related illness is a current public health concern and is poorly understood, though recent studies have suggested that *S. chartarum* and its secondary, toxic metabolite SG might contribute to some of the adverse effects (Dearborn et al., 1999; Dearborn et al., 2002; Fung et al., 1998; Hossain et al., 2004; Jarvis et al., 1998; Kilburn et al., 2004). The nose presents a logical target for inhaled toxins due to the tendency of airborne particles of various sizes, particularly those larger than 5 μm , to deposit in the nasal passages (Cheng et al., 1990; Cheng et al., 1991; Yeh et al., 1997). The toxin-containing spores of *S. chartarum* have been shown to be 7-12 X 4-6 μm (Jarvis et al., 1998; Tucker et al., 2007) and have a mean respirable diameter of 5 μm (Jarvis et al., 1998; Yike and Dearborn, 2004), making it feasible that some inhaled spores would lodge in the nose. A computer model of particle deposition in an adult male and a 3-month-old infant and showed that 65-90% of inhaled *S. chartarum* spores lodged in the nose of both adults and infants (Cho et al., 2005). Deposition of Satratoxin-containing spores in the nose provides a route of toxin exposure to the OSNs.

OSNs undergo a cycle of normal turnover throughout the life of an animal, with mature OE undergoing apoptosis and being replaced through regeneration (Graziadei and Graziadei, 1978). OSNs have been induced to die by a variety of means in laboratory animals, such as transection of the olfactory nerve or intranasal exposure to methyl bromide, a chemical known to be toxic to OE (Cowan and Roskams, 2002). Most of these methods induce necrosis of OSNs

rather than apoptosis. Kai et al. (2004) reported that the chemotherapeutic agent vincristine caused apoptosis of OSNs when administered systemically, though nasal inflammation was absent.

Recently we observed that single intranasal instillations of SG induced loss of OSNs and atrophy of OE through apoptosis, as well as neutrophilic rhinitis in adult mice (Islam et al., 2006). Here we demonstrate that repeated, intranasal instillations result in specific loss of OSNs with atrophy of OE and neutrophilic rhinitis in both adult and weanling mice.

The mechanism by which SG causes apoptosis of OSNs may involve many factors from both the intrinsic and extrinsic apoptotic pathways. We recently found upregulation of the pro-apoptotic genes Fas, FasL, p75, p53, Bax, caspase 3, and caspase-activated DNase (CAD) in the OE lining the ethmoid turbinates following a single intranasal instillation of SG (Islam et al., 2006). RA, another macrocyclic trichothecene, induced expression of double-stranded RNA-activated protein kinase (PKR), CAD, Bax, and p53 mRNA in the ethmoid turbinates 24 hours following intranasal instillation. Expression of the proinflammatory cytokine TNF- α and Fas mRNA occurred between 6 and 24 hours following instillation, indicating that these extrinsic pathway factors may be inducing apoptosis (Islam et al., 2007). TNF- α has been shown to induce apoptosis of OSNs *in vitro* (Suzuki and Farbman, 2000). Others have shown activation of mitogen-activated protein kinases (MAPK) such as p38 and p53 by trichothecene mycotoxins. C-Jun N-terminal kinase (JNK) and extracellular signal-related kinase (ERK) have also been implicated in apoptosis signaling in

response to trichothecenes (Shifrin and Anderson, 1999; Yang et al., 2000; Chung et al., 2003; Zhou et al., 2005). Further work is needed to determine the exact apoptotic mechanisms involved in apoptosis induced by macrocyclic trichothecenes.

Our findings here contrast with the results of single intranasal instillations of SG or RA, which did not induce loss of OSNs in the DM. Ressler et al. (1993) demonstrated a zone-specific expression of odorant receptors, with one population lining the dorsal meatus. We previously hypothesized that macrocyclic trichothecenes may interact only with specific receptors on populations of OSNs, thus sparing the dorsal meatus from injury (Islam et al., 2006; Islam et al., 2007). It is still feasible that SG is interacting with odorant receptors to cause apoptosis, but it is unclear why the DM would be spared with single instillations but affected when repeated instillations were administered. It is possible that repeated instillations prolong the inflammatory response, which could lead to more widespread tissue damage and a longer duration of proinflammatory cytokine expression. There may also be other currently undiscovered mechanisms involved. Further work is needed to determine if macrocyclic trichothecenes are capable of interacting with receptors on OSNs and to investigate cellular and molecular mechanisms of toxicity following repeated exposures to SG.

The cluster of idiopathic pulmonary hemorrhage cases in infants residing in an area of Cleveland in the early 1990's resulted in great concern about the overall health effects of exposure to *S. chartarum*, but also raised questions

about the susceptibility of infants and children to such exposures. Interestingly, none of the adults living with the affected infants in these cases were affected (Dearborn et al., 1999). Recent publications have noted that infants and young children have behavioral and physiological differences from adults that make them more susceptible to exposure to environmental toxicants (Faustman et al., 2000; Landrigan et al., 2004). When weanling mice were recently used to model humans at 1-2 years of age, it was determined that young mice were more susceptible to the trichothecene DON than adult mice (Pestka and Amuzie, 2008).

In the present study, we observed that weanling and adult mice are relatively similar in their susceptibility to the toxic effects of SG with respect to OE atrophy, loss of OSNs, and neutrophilic inflammation. Weanling mice receiving 250 µg/kg SG had a proportionally smaller increase in neutrophils in the mucosa lining the DM compared to SG-treated adult mice, though control weanling mice had a larger number of neutrophils in the mucosa of the dorsal meatus than adult control mice. The reasons for the disparity in the number of neutrophils in saline control weanling and adult mice, as well as the difference in the increase in mucosal neutrophils between weanling and adult mice, are unclear. It is possible that there are age-related differences in neutrophils, secretion of inflammatory cytokines, and a variety of other mediators that are involved in inflammatory responses that have not been described that may explain the differences we observed. We are unaware of any previous reports comparing normal levels of neutrophils in weanling and adult mice or in infant and adult humans. There are

no previous reports comparing infant and adult inflammatory responses with respect to cellular components and cytokine expression in the nose. Elder et al. (2000) reported that inhalation of carbon ultrafine particles or endotoxin resulted in a greater increase in neutrophils in BALF from the lungs of old (22 mo. old) rats compared to young (10 wk. old) rats, but that the overall response (overall number of neutrophils) in young rats was higher than the overall response in old rats. The animals used in this study are of different ages than those used in our study, with 22 mo. old rats representing elderly adult humans rather than adults. However, their results appear to parallel our observations and may reflect a difference in the inflammatory responses of young and old animals.

We observed an interesting difference in the number of OSNs in saline control weanling and adult mice. A number of possible explanations for this exist. Tian and Ma (2008) recently found that OSNs expressing multiple odorant receptors are eliminated postnatally in response to sensory stimuli. Adult mice (8 wks.) had significantly fewer OSNs expressing multiple receptors than 4 wk. old mice, and the authors suggested that apoptosis might mechanistically explain the decrease in these OSNs. Others have reported an age-related decrease in proliferation of OE in spite of an increase in the total surface area occupied by OE (Weiler and Farbman, 1997). They observed that the number of OSNs per unit area of OE increased in rats until approximately 3 wks. of age, after which the number of OSNs decreased until reaching a plateau at approximately 15 wks. of age. It is therefore possible that our 3-4 wk. old mice were still undergoing postnatal development in response to sensory input and that they would

eventually eliminate OSNs until reaching a number similar to that we observed in the adult mice. It is also possible that a combination of sensory-driven apoptosis of some OSNs and a decrease in proliferation may explain the differences we observed in weanling and adult mice.

Our observations suggest that the nasal neurotoxicity and inflammation induced by SG exposure are of concern in both adults and infants. In considering the risk of *S. chartarum* exposure to children, it is useful to point out that young children crawl across carpet and other floor surfaces (Faustman et al., 2000). Such activity could potentially disturb settled fungal spores, fungal fragments, or house dust, which have been shown to contain SG (Gregory et al., 2004; Brasel et al., 2005; Brasel et al., 2005). Also, a resting infant inhales twice the air that a resting adult takes in per unit body weight (National Academy of Sciences, 1993), which could lead to a proportionally larger exposure to inhaled toxicants. Further studies are needed to establish dose-response effects of SG in weanling mice and evaluate the regenerative abilities of OSNs in 3-4 wk-old mice. A particularly interesting direction is the comparison of inflammatory cytokines and apoptotic gene expression in weanling and adult mice exposed to SG. Specific investigations of the risk of children and infants being exposed to *S. chartarum* should be undertaken to allow contextual evaluation of the results of animal studies. A variety of methods have been described for assessing mold exposure in children (Dillon et al., 1999). Quantitative assessments of potential human exposure to *S. chartarum* and satratoxins are currently ongoing (Portnoy et al., 2004; Bloom et al., 2007; Bloom et al., 2007), and should include separate

values for infants and children, taking into consideration the differences in potential for exposure, possible routes of exposure, and physiology.

CHAPTER 4 BIBLIOGRAPHY

Andersson, M. A., Nikulin, M., Koljalg, U., Andersson, M. C., Rainey, F., Reijula, K., Hintikka, E. L., and Salkinoja-Salonen, M, 1997. Bacteria, molds, and toxins in water-damaged building materials. *Appl Environ Microbiol*. 63, 387-93.

Bennett, J. W., and Klich, M., 2003. Mycotoxins. *Clin Microbiol.Rev* 16, 497-516.

Bloom, E., Bal, K., Nyman, E., and Larsson, L., 2007. Optimizing a GC-MS method for screening of *Stachybotrys* mycotoxins in indoor environments. *J Environ Monit* 9, 151-156.

Bloom, E., Bal, K. Nyman, E., Must, A., and Larsson, L., 2007. Mass-spectrometry-based strategy for direct detection and quantification of some mycotoxins produced by *Stachybotrys* and *Aspergillus* spp. in indoor environments. *Appl Environ Microbiol* 73, 4211-4217.

Boutin-Forzano, S., Charpin-Kadouch, C., Chabbi, S., Bennedjai, N., Dumon, H., and Charpin, D., 2004. Wall relative humidity: a simple and reliable index for predicting *Stachybotrys chartarum* infestation in dwellings. *Indoor Air* 14, 196-99.

Brasel, T. L., Douglas, D. R., Wilson, S. C., Straus, D. C., 2005. Detection of Airborne *Stachybotrys chartarum* Macrocylic Trichothecene Mycotoxins on particulates Smaller than Conidia. *Appl Environ Microbiol* 71, 114-122.

Brasel, T. L., Martin, J. M., Carriker, C. G., Wilson, S. C., Straus, D. C., 2005. Detection of Airborne *Stachybotrys chartarum* Macrocylic Trichothecene Mycotoxins in the Indoor Environment *Appl Environ Microbiol* 71, 7376-7388.

CDC, 1994. Acute pulmonary hemorrhage/hemosiderosis among infants – Cleveland, January 1993-November 1994. *MMWR* 43, 881-883.

CDC, 1995. Acute pulmonary hemorrhage among infants –Chicago, April 1992-1994. *MMWR* 44, 67; 73-74.

CDC, 1997. Update: pulmonary hemorrhage/hemosiderosis among infants – Cleveland, Ohio 1993-1996. *MMWR* 46, 33-35.

CDC, 2000. Update: pulmonary hemorrhage/hemosiderosis among infants – Cleveland, Ohio 1993-1996. *MMWR* 49, 180-184.

Cheng, Y. S., Hansen, G. K., Su, Y. F., Yeh, H. C., and Morgan, K. T., 1990. Deposition of ultrafine aerosols in rat nasal molds. *Toxicol Appl Pharmacol* 106, 222-233.

- Cheng, Y. S., Yeh, H. C., Swift, D. L., 1991. Aerosol deposition in human nasal airway for particles 1 nm to 20 μ m: a model study. *Radiat Prot Dosimetry* 38, 41-47.
- Chung, Y., Zhou, H., and Pestka, J. J., 2003. Transcriptional and posttranscriptional roles for p38 mitogen-activated protein kinase in upregulation of TNF- α expression by deoxynivalenol (vomitoxin). *Toxicol Appl Pharmacol* 193, 188-201.
- Cowan, C. M., and Roskams, A. J., 2002. Apoptosis in the mature and developing olfactory neuroepithelium. *Microsc Res Tech* 58, 204-215.
- Dearborn, D. G., Yike, I., Sorenson, W. G., Miller, M. J., Etzel, R. A., 1999. Overview of Investigations into Pulmonary Hemorrhage among Infants in Cleveland, Ohio. *Environ Health Perspect* 107(S3), S495-499.
- Dearborn, D. G., Smith, P. G., Dahms, B. B., Allan, T. M., Sorenson, W. G., Montana, E., and Etzel, R. A., 2002. Clinical profile of 30 infants with acute pulmonary hemorrhage in Cleveland. *Pediatrics* 110, 627-637.
- Dillon, H. K., Miller, J. D., Sorenson, W. G., Douwes, J., and Jacobs, R. R., 1999. Review of methods applicable to the assessment of mold exposure to children. *Environ Health Perspect* 107 (S3), S473-480.
- Ehrlich, K. C., and Daigle, K. W., 1987. Protein synthesis inhibition by 8-oxo-12,13-epoxytrichothecenes. *Biochim Biophys Acta* 923, 206-213.
- Elder, A. C. P., Gelein, R., Finkelstein, J. N., Cox, C., and Oberdörster, G., 2000. Pulmonary inflammatory response to inhaled ultrafine particles is modified by age, ozone exposure, and bacterial toxin. *Inhalation Toxicology* 12(S4), 227-246.
- Faustman, E. M., Silbernagel, S. M., Fenske, R. A., Burbacher, T. M., and Ponce, R. A., 2000. Mechanisms underlying children's susceptibility to environmental toxicants. *Environ Health Perspect* 108(S1), S13-21.
- Flappan, S. M., Portnoy, J., Jones, P., Barnes, C., 1999. Infant Pulmonary Hemorrhage in a Suburban Home with Water Damage and Mold (*Stachybotrys atra*). *Environ Health Perspect* 107, 927-930.
- Nielsen, K. F., 2003. Mycotoxin production by indoor molds. *Fungal Genet Biol* 39, 103-117.
- Fung, F., Clark, R., and Williams, S., 1998. *Stachybotrys*, a mycotoxin-producing fungus of increasing toxicologic importance. *J Toxicol Clin Toxicol* 36, 79-86.

Graziadei P., and Graziadei G. A., 1978. The olfactory system: a model for the study of neurogenesis and axon regeneration in mammals. In: Cotman, C. W. (Ed.), *Neuronal Plasticity*. Raven Press, New York, pp. 131-153.

Gregory, L., Pestka, J. J., Dearborn, D. G., Rand, T. G., 2004. Localization of Satratoxin-G in *Stachybotrys chartarum* Spores and Spore-Impacted Mouse Lung Using Immunocytochemistry. *Toxicol Pathol* 32, 26-34.

Hinkley, S. F., and Jarvis, B. B., 2001. Chromatographic method for *Stachybotrys* toxins. *Methods Mol Biol* 157, 173-194.

Hossain, M. A., Ahmed, M. S., and Ghannoum, M. A., 2004. Attributes of *Stachybotrys chartarum* and its association with human disease. *J Allergy Clin Immunol* 113, 200-08.

Hyde, D. M., Magliano, D. J., and Plopper, C. G., 1991. Morphometric assessment of pulmonary toxicity in the rodent lung. *Toxicol Pathol* 19, 428-446.

Hyde, D. M., Plopper C. G., St. George, J. A., and Harkema, J. R., 1990. Morphometric cell biology of air space epithelium. In: Schraufnagel, D. E. (Ed.), *Electron Microscopy of the Lung*. Marcel Dekker, New York, pp.71-120.

Institute of Medicine, 2004. *Damp Indoor Spaces and Health*. National Academies Press, Washington DC.

Islam, Z., Harkema, J. R., Pestka, J. J., 2006. Satratoxin G from the Black Mold *Stachybotrys chartarum* Evokes Olfactory Sensory Neuron Loss and Inflammation in the Murine Nose and Brain. *Environ Health Perspect* 114, 1099-1107.

Islam, Z., Amuzie, C. J., Harkema, J. R., and Pestka, J. J., 2007. Neurotoxicity and inflammation in the nasal airways of mice exposed to the macrocyclic trichothecene Roridin A: kinetics and potentiation by bacterial lipopolysaccharide coexposure. *Toxicol Sci* 98, 526-541.

Jarvis, B. B., Sorenson, W. G., Hintikka, E. L., Nikulin, M., Zhou, Y., Jiang, J., Wang, S., Hinkley, S., Etzel, R. A., and Dearborn, D., 1998. Study of toxin production by isolates of *Stachybotrys chartarum* and *Memnoniella echinata* isolated during a study of pulmonary hemosiderosis in infants. *Appl Environ Microbiol* 64, 3620-3625.

Kai, K., Satoh, H., Kajimura, T., Kato, M., Uchida, K., Yamaguchi, R., Tateyama, S., and Furuhashi, K., 2004. Olfactory epithelial lesions induced

by various cancer chemotherapeutic agents in mice. *Toxicol Pathol* 32, 701-709.

Kilburn, K. H., 2004. Role of molds and mycotoxins in being sick in buildings: neurobehavioral and pulmonary impairment. *Adv Appl Microbiol* 55, 339-59.

Kream, R. M., and Margolis, F. L., 1984. Olfactory marker protein: turnover and transport in normal and regenerating neurons. *J Neurosci* 4, 868-79.

Landrigan, P. L., Kimmel, C. A., Correa, A., and Eskenazi, B., 2004. Children's health and the environment: public health issue and challenges for risk assessment. *Environ Health Perspect* 112, 257-265.

Li, M. and Pestka, J. J., 2008. Comparative induction of 28S ribosomal RNA cleavage by ricin and the trichothecenes deoxynivalenol and T-2 toxin in the macrophage. *Toxicol Sci* 105, 67-78.

National Academy of Sciences, 1993. Pesticides in the diets of infants and children. National Academies Press, Washington DC.

Pestka, J. J., and Amuzie, C. J., 2008. Tissue distribution and proinflammatory cytokine gene expression following acute oral exposure to deoxynivalenol: comparison of weanling and adult mice. *Food Chem Toxicol* 46, 2826-2831.

Pestka, J. J., Yike, I., Dearborn, D. G., Ward, M. D. W., and Harkema, J. R., 2008. *Stachybotrys chartarum*, trichothecene mycotoxins, and damp building-related illness: new insights into a public health enigma. *Toxicol Sci* 104, 4-26.

Portnoy, J. M., Barnes, C. S., and Kennedy, K., 2004. Sampling for indoor fungi. *J Allergy Clin Immunol* 113, 189-198.

Ressler, K. J., Sullivan, S. L., and Buck, L. B., 1993. A zonal organization of odorant receptor gene expression in the olfactory epithelium. *Cell* 73, 597-609.

Rosenblum Lichtenstein, J. H., Molina, R. M., Donaghey, T. C., Brain, J. D., 2006. Strain differences influence murine pulmonary responses to *Stachybotrys chartarum*. *Am J Respir Cell Mol Biol* 35, 415-423.

Shifrin, V. I., and Anderson, P., 1999. Trichothecene mycotoxins trigger a ribotoxic stress response that activates c-Jun N-terminal kinase and p38 mitogen-activated protein kinase and induces apoptosis. *J Biol Chem* 274, 13985-13992.

- Suzuki, Y., and Farbman, A. I., 2000. Tumor necrosis factor- α -induced apoptosis in olfactory epithelium in vitro: possible roles of caspase 1 (ICE), caspase 2 (ICH-1), and caspase 3 (CPP32). *Exp Neurol* 165, 35-45.
- Tian, H., and Ma, M., 2008. Activity plays a role in eliminating olfactory sensory neurons expressing multiple odorant receptors in the mouse septal organ. *Mol Cell Neurosci* 38, 484-488.
- Tucker, K., Stolze, J. L., Kennedy, A. H., and Money, N. P., 2007. Biomechanics of conidial dispersion in the toxic mold *Stachybotrys chartarum*. *Fungal Genet Biol* 44, 641-647.
- Tuomi, T., Reijula, K., Johnsson, T., Hemminki, K., Hintikka, E. L., Lindroos, O., Kalso, S., Koukila-Kahkola, P., Mussalo-Rauhamaa, H., and Haahtela, T., 2000. Mycotoxins in crude building materials from water-damaged buildings. *Appl Environ Microbiol* 66, 1899-1904.
- Tuomi, T., Saarinen, L., and Reijula, K., 1998. Detection of polar and macrocyclic trichothecene mycotoxins from indoor environments. *Analyst* 123, 1835-41.
- Ueno, Y., 1984. General toxicology. In: Ueno, Y. (Ed.), *Trichothecenes: Chemical, Biological, and Toxicological Aspects*. Elsevier, New York, pp. 135-145.
- Ueno, Y., 1984. Toxicological features of T-2 toxin and related trichothecenes. *Fundam Appl Toxicol* 4, S124-132.
- Weiler, E., and Farbman, A. I., 1997. Proliferation in the rat olfactory epithelium: age-dependent changes. *J Neurosci* 17, 3610-3622.
- Yang, G., Jarvis, B. B., Chung, Y., and Pestka, J. J., 2000. Apoptosis induction by the Satratoxins and other trichothecene mycotoxins: relationship to ERK, p38 MAPK, and SAPK/JNK activation. *Toxicol Appl Pharmacol* 164, 149-160.
- Yeh, H. C., Muggenburg, B. A., Harkema, J. R., 1997. In vivo deposition of inhaled ultrafine particles in the respiratory tract of rhesus monkeys. *Aerosol Sci Technol* 27, 465-470.
- Yike, I., and Dearborn, D. G., 2004. Pulmonary effects of *Stachybotrys chartarum* in animal studies. *Adv Appl Microbiol* 55, 241-273.
- Zhou, H., Islam, Z., and Pestka, J. J., 2005. Induction of competing apoptotic and survival signaling pathways in the macrophage by the ribotoxic trichothecene deoxynivalenol. *Toxicol Sci* 87, 113-122.

CHAPTER 5

**Nasal Toxicity and Pulmonary Inflammation in Mice Exposed to the Spores and
Macrocyclic Trichothecene Mycotoxin, Satratoxin G, of *Stachybotrys chartarum***

ABSTRACT

Stachybotrys chartarum is a ubiquitous, saprophytic fungus suggested to contribute to adverse health effects associated with water-damaged buildings. Satratoxin G (SG) is a macrocyclic trichothecene mycotoxin that is found in the spores and mycelial fragments of *S. chartarum*. We have previously reported that single and repeated intranasal instillations of SG cause nasal toxicity in mice. The purpose of the present study was to characterize and compare the effects of SG, *S. chartarum* spores, and exposure to a combination of SG and spores in the nose and lungs of mice. Female C57BL/6 mice 6-8 weeks of age were intranasally instilled once daily for four consecutive days with: i) Saline (0 $\mu\text{g}/\text{kg}$ bw SG and 0 spores), ii) 25 $\mu\text{g}/\text{kg}$ bw SG and 0 spores, iii) 100 $\mu\text{g}/\text{kg}$ bw SG and 0 spores, iv) 0 $\mu\text{g}/\text{kg}$ bw SG and 5×10^5 spores v) 25 $\mu\text{g}/\text{kg}$ bw SG and 5×10^5 spores, or vi) 100 $\mu\text{g}/\text{kg}$ bw SG and 5×10^5 spores. Mice similar in strain, age, and weight were intranasally instilled once daily for 2 consecutive days with: vii) 0 $\mu\text{g}/\text{kg}$ bw SG and 2×10^6 spores, viii) 25 $\mu\text{g}/\text{kg}$ bw SG and 2×10^6 spores, or ix) 100 $\mu\text{g}/\text{kg}$ bw SG and 2×10^6 spores. Mice were sacrificed 24 hours after the last instillation, at which time bronchoalveolar lavage fluid (BALF) was collected. Nasal and lung tissues were processed for microscopic examination and morphometric analysis. Inflammatory cell infiltration and flow cytometric determination of proinflammatory cytokines were characterized using BALF. SG induced dose-dependent atrophy of olfactory epithelium (OE) and loss of olfactory sensory neurons (OSNs). *S. chartarum* spores had no effect on

nasal pathology. Trends of increasing total cells, eosinophils, and neutrophils in BALF were observed with increasing dose of spores. All groups receiving 5×10^5 spores demonstrated a significant increase in the number of lymphocytes in BALF. SG had no effect on the cells detected in BALF. A trend of increasing levels of IL-6, MCP-1, and TNF- α was seen with increasing dose of spores. Interestingly, a trend of decreasing levels of INF- γ was seen with increasing dose of SG at all spore doses. Significant differences in the levels of IL-12 were detected in mice receiving 2×10^6 spores and 25 or 100 $\mu\text{g}/\text{kg}$ SG. No significant differences were detected in the levels of IL-10 present in BALF from any mice. These results indicate that the murine nose is susceptible to the toxic effects of SG but not to exposure to toxin-free spores, while the lung is affected by exposure to both SG and *S. chartarum* spores.

INTRODUCTION

Stachybotrys chartarum, a saprophytic black mold that grows on cellulose-containing materials, has been linked to damp building-related illnesses (Andersson et al., 1997; Boutin-Forzano et al., 2004; Tuomi et al., 1998; Tuomi et al., 2000). Adverse health effects involving the upper and lower respiratory tracts (nasal congestion, runny or itchy nose; throat irritation, cough, wheeze, exacerbation of asthma symptoms) have been associated with damp indoor environments (Institute of Medicine, 2004). In addition to those symptoms found by the Institute of Medicine Committee to be linked to damp indoor environments, evidence is lacking to confirm a link between water-damaged buildings and other reported symptoms, including neurobehavioral and immunological alterations. The etiological role of *S. chartarum* in health effects associated with water-damaged buildings has not been completely established (Institute of Medicine, 2004; Pestka et al., 2008).

The spores and macrocyclic trichothecene mycotoxins produced by *S. chartarum* might contribute to the health effects associated with exposure to the fungus in damp indoor environments (Fung et al., 1998; Dearborn et al., 1999; Flappan et al., 1999; Hossain et al., 2004; Kilburn 2004; Rosenblum et al., 2006). Macrocyclic trichothecene mycotoxins have been localized to the outer plasmalemma and inner cell wall of the spores and also found in mycelial fragments (Gregory et al., 2004). They have been identified in experimentally aerosolized cultures of *S. chartarum* (Sorenson et al., 1987). Macrocyclic trichothecenes are potent inhibitors of protein synthesis (Ueno, 1984; Ehrlich and

Daigle, 1987; Shifrin and Anderson, 1999; Bennett and Klich, 2003; Li and Pestka, 2008). These mycotoxins have been isolated in damp indoor environments and have also been located on particulates smaller than *S. chartarum* spores (Brasel et al., 2005; Brasel et al., 2005). Macrocyclic trichothecenes have been shown to displace out of spores and into aqueous solutions, and these solutions are capable of inhibiting protein synthesis (Jarvis et al., 1998; Karunasena et al., 2004). The spores of a macrocyclic trichothecene-producing strain of *S. chartarum*, JS5817, have been estimated to contain approximately 1 picogram of Satratoxin G (SG) (Yike et al., 2002; Yike and Dearborn, 2004). Residing or working in a water-damaged building supporting *S. chartarum* growth could therefore result in exposure to spores as well as macrocyclic trichothecenes.

The pulmonary effects of exposure to *S. chartarum* have been investigated in rats and mice. A single intratracheal (IT) instillation of 1×10^4 spores resulted in neutrophilic alveolitis and spores on lung histopathology, while repeated instillations of 1×10^5 spores led to infiltration of neutrophils, eosinophils, macrophages, and multinucleated giant cells in alveoli 4 days after exposure (Ochiai et al., 2005). BALF from rat pups contained primarily alveolar macrophages but included neutrophils and lymphocytes 3 days following IT instillation of 1.1×10^5 spores per gram body weight (bw). The proinflammatory cytokines TNF- α and IL-1 β were also increased in BALF (Gregory et al., 2004). IT instillations of 7×10^4 spores led to granulomatous inflammation, cellular

debris, hemosiderin-laden macrophages, and occasional lymphocytes in alveolar spaces. Similar instillation of isosatratoxin F, a macrocyclic trichothecene, did not result in significant pulmonary changes (Rand et al., 2002). Alcohol extraction was shown to decrease the toxicity of *S. chartarum* by removing macrocyclic trichothecenes (Rao et al., 2000). The pulmonary toxicities of intact and ethanol-extracted spores were compared using IT instillations of 1×10^5 spores. The authors found that the most significant pulmonary changes were induced by intact, toxin-containing spores but concluded that spore proteins could also contribute to toxicity. Changes in inflammatory cell infiltration and proinflammatory cytokines similar to those previously reported were also noted (Yike et al., 2005). IT instillations of spores or isosatratoxin F have also been shown to affect alveolar macrophages, type II alveolar cells, and surfactant production (Mason et al., 1998; Rand et al., 2002).

Intranasal instillation has been used in a number of studies to evaluate pulmonary toxicity due to *S. chartarum* exposure. Nikulin et al. (1997) compared the two chemotypes of *S. chartarum*, one producing macrocyclic trichothecenes and the other producing the atranone class of mycotoxins. Single and repeated instillations of spores resulted in significantly greater pulmonary inflammation and pathology in mice exposed to the chemotype producing macrocyclic trichothecenes. In contrast, Leino et al. (2003) did not detect any differences in the pulmonary changes induced by exposure to 2 *S. chartarum* strains, only one of which produced macrocyclic trichothecenes. We recently showed that single instillations of SG resulted in loss of OSNs and atrophy of OE through apoptosis,

and that a neutrophilic rhinitis was present 24 hours following exposure. Exposures to 100 µg/kg SG for 5 consecutive days resulted in similar changes (Islam et al., 2006). A single intranasal instillation of Roridin A (RA), a commercially available macrocyclic trichothecene used as a surrogate for SG, also resulted in apoptosis of OSNs, atrophy of OE, and neutrophilic rhinitis (Islam et al., 2007). The purpose of the present study was to compare the effects of intranasal instillations of spores, SG, and combinations thereof in the noses and lungs of mice, specifically focusing on OE effects in the nose and inflammatory effects in the lung thus allowing a single macrocyclic trichothecene-producing strain of *S. chartarum* to be utilized for all spore instillations. Toxin was removed by suspension in several aqueous solution washes, previously shown to remove macrocyclic trichothecenes (Jarvis et al., 1998; Rao et al, 2000; Karunasena et al., 2004). This allowed specific investigation of the effects of macrocyclic trichothecene-free spores without the use of a strain producing atranone mycotoxins, which have been observed to induce proinflammatory mediators in BALF (Nielsen et al., 2002).

MATERIALS AND METHODS

Experimental Design

Pathogen-free female 6-8 week-old mice (C57BL/6, Charles River, Portage, MI) were randomly assigned to experimental groups (n = 6). Mice were housed in polycarbonate cages containing *Cell-Sorb Plus* bedding (A & W products, Cincinnati, OH) and covered with filter bonnets. Room lights were set

on a 12-hour light/dark cycle. Temperature and relative humidity were maintained between 21-24°C and 40-55% humidity, respectively. Studies were carried out in accordance with National Institutes of Health guidelines and overseen by the All University Committee on Animal Use and Care at Michigan State University.

SG was isolated from *S. chartarum* as previously described (Hinkley and Jarvis, 2001; Islam et al., 2006). The identity of the toxin was confirmed using electrospray ionization and collision-induced dissociation tandem mass spectroscopy (Tuomi et al., 1998). The doses of SG and spores were chosen based on the observation that approximately 1 pg of SG is contained within each spore (Yike et al., 2002). 25 µg/kg is the approximate dose of SG from 5×10^5 spores, and 100 µg/kg is the approximate dose of SG from 2×10^6 spores.

Spores of *S. chartarum* strain 29-58-17 NIOSH (JS5817) were grown on a Nytran supercharge nylon membrane (Sigma-Aldrich, St. Louis, MO) centered on a sterile potato dextrose agar plate (Difco Potato Dextrose Agar, BD Biosciences, Franklin Lakes, NJ). 5×10^4 spores were suspended in endotoxin-free water and dropped in the center of the membrane. Plates were incubated at room temperature in the dark for four weeks. Spores were harvested on autoclaved circular head swabs (Fischer Scientific, Fair Lawn, NJ) by pressing into the growth on the surface of the Nytran membrane. Three swabs were collected from each plate and stored at 4°C. To prepare spore suspensions for intranasal instillation, 3 swabs were used per dose of spores. The first swab was vortexed

for 5 minutes in 15 mL of sterile phosphate buffered saline (PBS, Abbott Laboratories, IL), followed by similar vortexing of the second and third swabs in the same tube. The spores were counted on a hemocytometer and final concentrations of 5×10^5 or 2×10^6 spores were made by adding PBS as needed. Mycotoxins including SG were removed from the spores by washing the required number of spores 3 times in equal volumes of PBS (5×10^5 or 2×10^6 spores in 50 μ L PBS). Spore suspensions were vortexed for 5 minutes during each washing, and the supernatant was removed by pipette after each washing. After the third washing, the spore pellet was resuspended in 50 μ L of PBS and stored at 4°C overnight.

For instillation, mice were lightly anesthetized with 3.5% Isoflurane (Abbott Laboratories, Chicago, IL) and 96.5% oxygen. Mice received intranasal instillations of saline (0 μ g/kg bw SG and 0 spores), 25 μ g/kg bw SG and 0 spores, 100 μ g/kg bw SG and 0 spores, 0 μ g/kg bw SG and 5×10^5 spores, 25 μ g/kg bw SG and 5×10^5 spores, or 100 μ g/kg bw SG and 5×10^5 spores for four consecutive days. Mice similar in strain, age, and weight received intranasal instillations of 0 μ g/kg bw SG and 2×10^6 spores, 25 μ g/kg bw SG and 2×10^6 spores, or 100 μ g/kg bw SG and 2×10^6 spores for two consecutive days. Mice instilled with 2×10^6 spores were sacrificed after 2 instillations due to health concerns. All mice were sacrificed 24 hours after the last instillation. **Table 2** lists the experimental groups and the number of animals in each group, and

differentiates the animals receiving 4 instillations from those receiving 2 instillations.

Table 2. Experimental Groups for spores and SG instillations. Six animals were randomly assigned to each of the experimental groups. Asterisk = sacrificed after two instillations. All other animals sacrificed after four instillations.

Experimental Groups	Control (0 Spores)	5 X 10⁵ Spores	2 X 10⁶ Spores
Saline (0 µg/kg SG)	6	6	6 *
25 µg/kg SG	6	6	6 *
100 µg/kg SG	6	6	6 *

Animal Necropsies and Tissue Processing

At the designated time of sacrifice, mice were deeply anesthetized with an intraperitoneal (ip) injection of 0.1 ml of 12% sodium pentobarbital and euthanized by exsanguination via the abdominal aorta. After death, the head of each mouse was immediately removed and the lower jaw, skin, and muscles were removed. The dorsal cranium was opened to allow greater fixation of brain tissues. The nasal cavities were flushed with 500 µL of 10% neutral buffered formalin (NBF; Fischer Scientific, Fair Lawn, NJ) using a 1 mL syringe and 20-gauge cannula, retrograde through the nasopharyngeal meatus. The nasal cavities were then immersed in a large volume of NBF and stored for 24 hours prior to further processing.

Transverse tissue blocks from the heads of the mice were selected as previously described. (Steiger et al., 1995; Islam et al., 2006) Following fixation, the heads were decalcified in 13% formic acid (Mallinckrodt Baker, Phillipsburg,

MD) for 7 days and then rinsed in running tap water for 4 hours. The nasal sections were taken at four specific anatomic locations as previously described (Young, 1981; Harkema et al., 2006). The proximal section (T1) was taken immediately caudal to the upper incisor teeth; the middle section (T2) was taken at the level of the incisive papilla of the hard palate; the third nasal section (T3) was taken at the level of the second palatal ridge; and the most caudal nasal section (T4) was taken at the level of the intersection of the hard and soft palates, through the proximal portion of the olfactory bulb (OB) of the brain. Nasal tissue blocks were processed for histopathologic, immunohistochemical and morphometric analyses. All blocks were embedded in paraffin, and the anterior face of each block was sectioned at a thickness of five microns and stained with hematoxylin and eosin for routine light microscopic examination. **Figure 26** illustrates the locations of the T1-T4 nasal sections and the specific site used for morphometric analyses.

Immunohistochemistry (IHC)

Nasal tissue sections were immunohistochemically stained to identify mature olfactory sensory neurons (OSNs) in olfactory epithelium (OE). Sections T1-T4 were incubated with a nonspecific protein blocking solution of normal sera (Vector Laboratories Inc., Burlingame, CA) and were pretreated with 3% H₂O₂ in methanol to eliminate endogenous peroxidase. The sections were then transferred to a primary polyclonal antibody directed against OMP-containing olfactory sensory neurons (1:4000 dilution, goat anti-OMP antibody, Wako

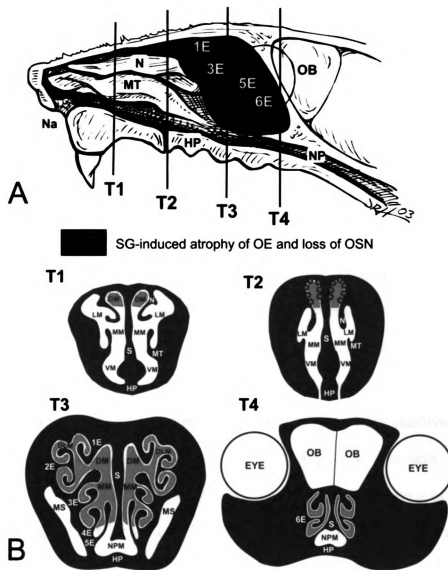


Figure 26. Location of SG-induced OE injury and morphometric analyses. (A) Diagrammatic representation of the lateral aspect of the right nasal passage of the murine nose. Nasal septum has been removed to expose the turbinates. N, nasoturbinate; MT, maxilloturbinate; 1-6E, ethmoid turbinates). Vertical lines represent the rostral surfaces of sections T1-T4 taken for histopathology and light microscopic examination. Red indicates areas of damage caused by RA. (B) Cross-sections of T1-T4. Red indicates areas of atrophy of Olfactory Epithelium (OE) and loss of Olfactory Sensory Neurons (OSN) induced by SG exposure. Blue dots indicate location of morphometric analyses. DM, dorsal medial meatus; N, nasoturbinate; LM, lateral meatus; MM, medial meatus; MT, maxilloturbinate; S, septum; VM, ventral meatus; HP, hard palate; 1E-6E, ethmoid turbinates; MS, maxillary sinus; NPM, nasopharyngeal meatus; OB, olfactory bulb of brain.

Chemicals USA, Richmond, VA). Immunoreactivity of OMP was visualized using Vector R.T.U. Elite ABC-Peroxidase Reagent (Vector Laboratories Inc., Burlingame, CA) followed by Nova Red chromagen. Following IHC, tissue sections were lightly counterstained with hematoxylin.

Light Microscopy and Morphometric Analysis

The OE lining the dorsal meatus (DM) in nasal section T2 was chosen as the representative location for morphometric analyses. Standard morphometric techniques were used to estimate the numeric cell density of OSNs in the OE lining the DM as previously described (Islam et al., 2007). Cell counts were determined using light microscopy at a final magnification of 790X. To determine the numeric cell density, the number of nuclear profiles of OMP-positive cells were counted and divided by the length of the underlying basal lamina. The length of the basal lamina was determined by measuring the contour of the basal lamina on a digital image using Scion Image software (Scion Corporation, Fredrick, MD) and a Dell XPS 400 computer (Dell, Austin, TX).

Thickness of OE lining the DM was morphometrically estimated using a standard cycloid grid overlay and computer software specifically designed for point and intercept counting (Stereology Toolbox, Davis, CA) as previously described in detail (Hyde et al., 1990; Hyde et al., 1991; Islam et al., 2006). Briefly, microscopic measurements were made at a final magnification of 1920X using a light microscope coupled to a 3.3 megapixel digital camera (Q-color 3 Camera, Quantitative Imaging Corp., Burnaby, BC, Canada) and a Dell

Dimension 8200 (Dell, Austin, TX). The thickness (τ) of OE, as measured by volume (μm^3) of OE per unit area (μm^2) of basal lamina, was estimated from point and intercept counts with a 136-point, 35-curve cycloid grid by the equation: $\tau = (3.2 \times Pp)/(2 \times Io)$, where Pp is the number of points counted for the OE and Io is the number of intercepts of the basal lamina. OE thickness was calculated for each mouse from point and intercept counts covering the entire DM in both the right and left nasal airways.

BALF and Flow Cytometry

The lungs of the mice were lavaged immediately after death and prior to tissue fixation with 1 mL of saline two times (total volume of 2 mL) via the trachea using a 20 gauge cannula and a 1 mL syringe. For each animal, 100 μL of the collected BALF was taken for cytopsin, 10 μL was taken for hemocytometry, and 50 μL was taken for Flow Cytometric analysis. After cytopsin was complete, the slides were prepared and stained using a standard Diff Quick staining protocol (Dade Behring, Newark, DE). Differential cell counts were used to quantify cells on stained slides.

The concentrations of TNF- α , INF- γ , MCP-1, IL-6, IL-10, and IL-12 in BALF were determined using a Cytometric Bead Array Mouse Inflammation Kit (BD Biosciences, San Diego, CA). Measurements were carried out according to manufacturer's instructions using a FACSCalibur and BD CBA Analysis software (BD Biosciences, San Jose, CA). Cytokine concentrations are expressed as pg/ml.

Statistics

All data were analyzed using SigmaStat v. 3.1 and graphed using SigmaPlot 6.0 (Jandel Scientific, San Rafael, CA). Criterion for significance was set at $p \leq 0.05$. Morphometric data were analyzed using One-Way or Two-Way analysis of variance (ANOVA) with Student-Newman-Keuls post hoc test. Flow Cytometry data were analyzed using One-Way or Two-Way ANOVA with Student-Newman-Keuls post hoc test or ANOVA on Ranks with Dunn's post hoc test.

RESULTS

Nasal Histopathology

Instillation of the saline-vehicle alone induced no nasal airway lesions that were detectable by light microscopic examination. In contrast, mice that received four instillations of either the low or high dose of SG alone, without spores, and sacrificed one day post-exposure had bilateral atrophy of OE throughout the nasal airways (T1-T4). Severity of this toxicant-induced epithelial change was dose-dependent with greater atrophy in mice receiving the high dose of SG. With both the low and high dose of SG, OE lining the dorsolateral meatus in T3 appeared to be the most severely affected intranasal site.

A mixed inflammatory cell infiltrate composed mainly of polymorphonuclear cells (neutrophils) with lesser numbers of mononuclear cells (lymphocytes and monocytes) was associated with the induced OE atrophy. This inflammatory cell infiltrate was restricted to the olfactory mucosa lined by atrophic

OE and the severity of this inflammatory response corresponded to the severity of the SG-induced epithelial lesions.

Atrophy of the OE was primarily due to the loss of OMP-positive OSNs. A few OMP-positive cells with pyknotic nuclei and apoptotic bodies were also present in some areas of atrophic OE. Basal and sustentacular cell numbers in the altered OE appeared to be unaffected. Sustentacular cells, however, were low columnar to cuboidal with the SG-induced epithelial atrophy, compared to tall columnar phenotype in the normal OE of saline-instilled control mice. SG instillations also caused corresponding attenuation and loss of the OMP-positive dendritic ciliated layer lining the luminal surface of the atrophic OE. Likewise there was attenuation and loss of OMP-positive, olfactory nerve bundles (proximal axonal portions of OSNs) in the lamina propria underlying the atrophic OE. Mild bilateral atrophy the OMP-positive olfactory neuronal layer (distal aspects of OSNs) and attenuation of OMP-positive staining in the more inner glomerular layer of the OB was present in the high dose SG-treated mice that received four instillations.

Mice that received only two instillations of SG (high or low doses) also had conspicuous nasal epithelial and inflammatory lesions that were restricted to the OE. The distribution of these lesions was similar to those induced by four instillations of the toxin (**Figure 26**). However, the phenotypic character of the SG-induced OE lesions in these mice consisted of numerous individual epithelial cells with morphologic features characteristic of apoptosis with only mild to moderate atrophy. The severity of SG-induced apoptosis in these mice was also

dose-dependent with greater severity in mice that received the higher daily dose. SG-induced apoptosis was defined by condensation and shrinkage of individual epithelial cells; clumping, fragmentation, margination of nuclear chromatin, and numerous widely scattered cellular fragments (apoptotic bodies). Apoptosis was restricted to OMP-positive OSNs whose cell bodies and nuclei reside in the middle nuclear layers of the OE, below the distinct apical row of sustentacular cell nuclei and above basal cell nuclei near the basal lamina.

Mice that were instilled with the low dose of spores had minimal to no nasal epithelial or inflammatory lesions. A few mice had single or small focal accumulations of 2-3 spores in the dorsolateral meatus in T3 and/or T4 surrounded closely by a small inflammatory cell accumulation of mainly neutrophils and lesser numbers of monocytes/macrophages. OE immediately adjacent to these airway spores had a similar inflammatory cell infiltrate with minimal apical, vacuolar degeneration and occasional superficial necrosis.

In mice that received both SG (high or low doses) and the low dose instillations of spores, the severity of SG-induced OE atrophy was not enhanced by the co-exposure with the spores. There was only slight enhancement of neutrophilic inflammation in the OE adjacent to areas where spores had accumulated in the meatus.

A few mice that were instilled with only two instillations of the high dose of spores (no SG) had minimal focal inflammatory and epithelial lesions, associated directly with intranasal airway accumulations of single or small clusters of spores, like those described above for mice that were instilled with only the lower dose of

spores. In contrast, all the mice that were instilled with two instillations of the high daily dose of spores plus SG (low or high dose) had moderate to marked epithelial and inflammatory nasal lesions that were of greater severity than in mice that received either spores or toxin alone. Mice that received the high dose of both toxin and spores had the most profound nasal lesions. These co-exposed mice had a severe neutrophilic rhinitis with marked nasal airway accumulations of mucopurulent material, small clusters of spores (2-6), and epithelial cellular debris that was most prominent in the dorsolateral meatus in T3 and T4. These mice also had enhanced OE degeneration, apoptosis, and exfoliation in these distal nasal airways. Toxicant-induced epithelial changes (apoptosis and atrophy) in the more proximal nasal airways (T1 and T2) were not enhanced by the instillations of the high dose of spores.

SG induces loss of OSNs and atrophy of OE in the DM

OMP is a marker of mature OSNs (Kream and Margolis, 1984). Mice receiving 25 or 100 µg/kg SG had marked loss of OSNs compared to animals receiving saline (**Figure 27**). Mice that were instilled with 100 µg/kg SG showed significantly more loss than those instilled with 25 µg/kg SG. Animals in groups instilled with 0 spores and 25 or 100 µg/kg SG had 57% and 96% fewer OMP-stained OSNs in the DM compared to mice receiving saline. Those instilled with 5×10^5 spores and 25 or 100 µg/kg SG had 58% and 95% fewer OMP-stained OSNs in the DM compared to mice instilled with 5×10^5 spores and saline (**Figure 28**).

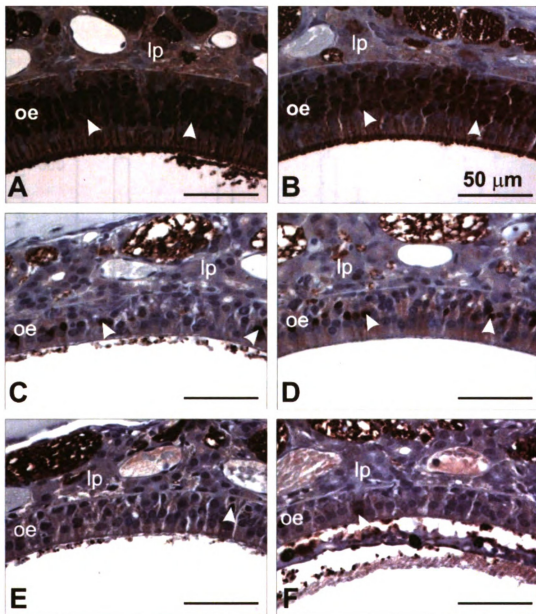


Figure 27. Photomicrographs of the DM from mice instilled with (A) saline, (B) 5×10^5 spores, (C) 25 $\mu\text{g}/\text{kg}$ SG, (D) 25 $\mu\text{g}/\text{kg}$ SG + 5×10^5 spores, (E) 100 $\mu\text{g}/\text{kg}$ SG, or (F) 100 $\mu\text{g}/\text{kg}$ SG + 5×10^5 spores. Loss of OMP staining was evident in mice instilled with SG (C,D,E,F) but not in mice receiving only spores (B). Spores were found in the DM of mice instilled with 100 $\mu\text{g}/\text{kg}$ SG + 5×10^5 spores (F). oe, olfactory epithelium; lp, lamina propria. Arrowheads = OMP-stained nuclei.

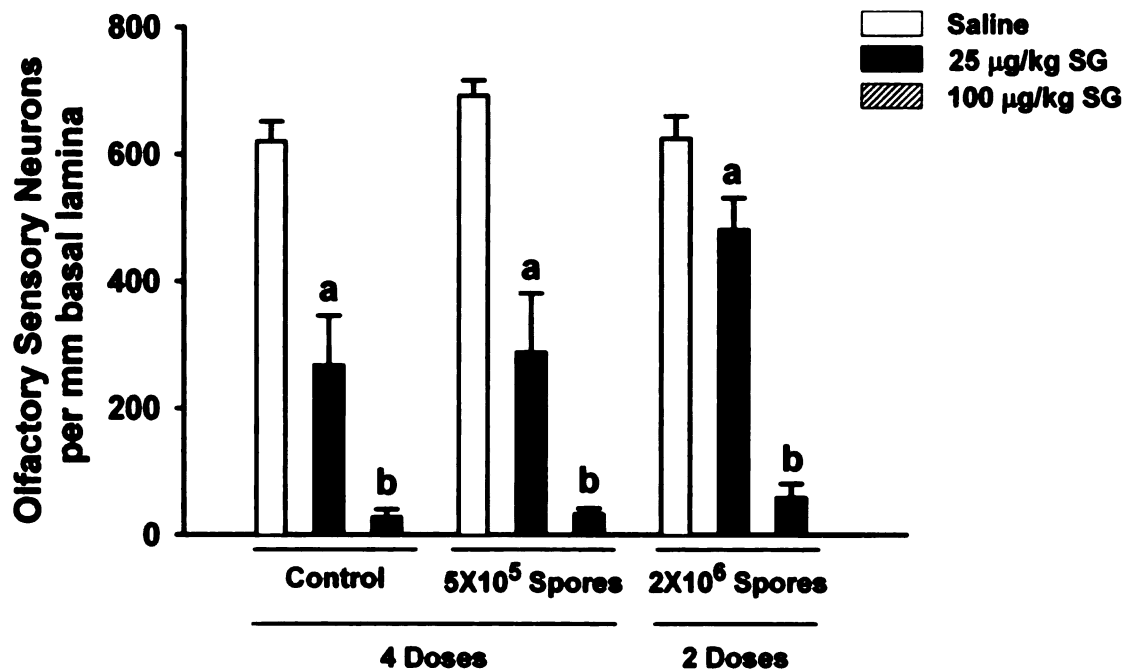


Figure 28. Loss of OSNs in the DM of T2. Loss of OSNs occurred in a dose-dependent manner based on the dose of SG. a indicates significantly different from respective saline (0 µg/kg SG) control group; b indicates significantly different from respective 25 µg/kg SG and saline (0 µg/kg SG) control groups ($p \leq 0.05$).

Mice in groups instilled with 2×10^6 spores and 25 or 100 $\mu\text{g}/\text{kg}$ SG had OSN decreases of approximately 23% and 91%, respectively, compared to those receiving 2×10^6 spores and saline. No statistically significant difference was found between spore-instilled mice and control mice (**Figure 28**).

Similarly, mice instilled with 25 or 100 $\mu\text{g}/\text{kg}$ SG had significant loss of thickness of OE compared to animals receiving only saline, and those instilled with 100 $\mu\text{g}/\text{kg}$ had significantly more OE atrophy than mice receiving 25 $\mu\text{g}/\text{kg}$ (**Figure 29**). Among groups of mice receiving 0 spores, those dosed with 25 or 100 $\mu\text{g}/\text{kg}$ SG had 22% and 43% reductions in the thickness of OE, respectively, compared to saline-instilled animals. Among groups receiving 5×10^5 spores, those animals instilled with 25 or 100 $\mu\text{g}/\text{kg}$ SG had reductions in the thickness of OE of 31% and 55% compared to animals exposed to 5×10^5 spores and saline.

No significant differences between animals instilled with saline, 25 or 100 $\mu\text{g}/\text{kg}$ SG in groups also instilled with 2×10^6 were observed. No statistically significant difference was detected between spore-instilled mice and control mice (**Figure 30**). **Table 3** summarizes the results of the OE analyses.

S. chartarum spores induce inflammatory cell infiltration in the lung

Statistically significant trends of increasing total cells, neutrophils, and eosinophils per mL of BALF were seen with increasing dose of *S. chartarum* spores. All mice instilled with 5×10^5 spores had a 6-fold increase in the number

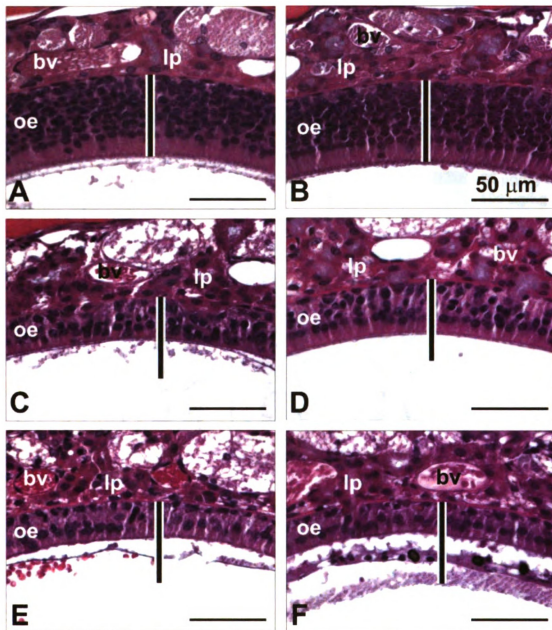


Figure 29. Photomicrographs of the DM from mice instilled with (A) saline, (B) 5×10^5 spores, (C) $25 \mu\text{g}/\text{kg}$ SG, (D) $25 \mu\text{g}/\text{kg}$ SG + 5×10^5 spores, (E) $100 \mu\text{g}/\text{kg}$ SG, or (F) $100 \mu\text{g}/\text{kg}$ SG + 5×10^5 spores. A decrease in the thickness of OE was evident in mice instilled with SG (C,D,E,F) but not in mice receiving only spores (B). Spores were found in the DM of mice instilled with $100 \mu\text{g}/\text{kg}$ SG + 5×10^5 spores (F). oe, olfactory epithelium; lp, lamina propria; bv, blood vessel. Vertical bar = thickness of OE in the DM of saline instilled mice.

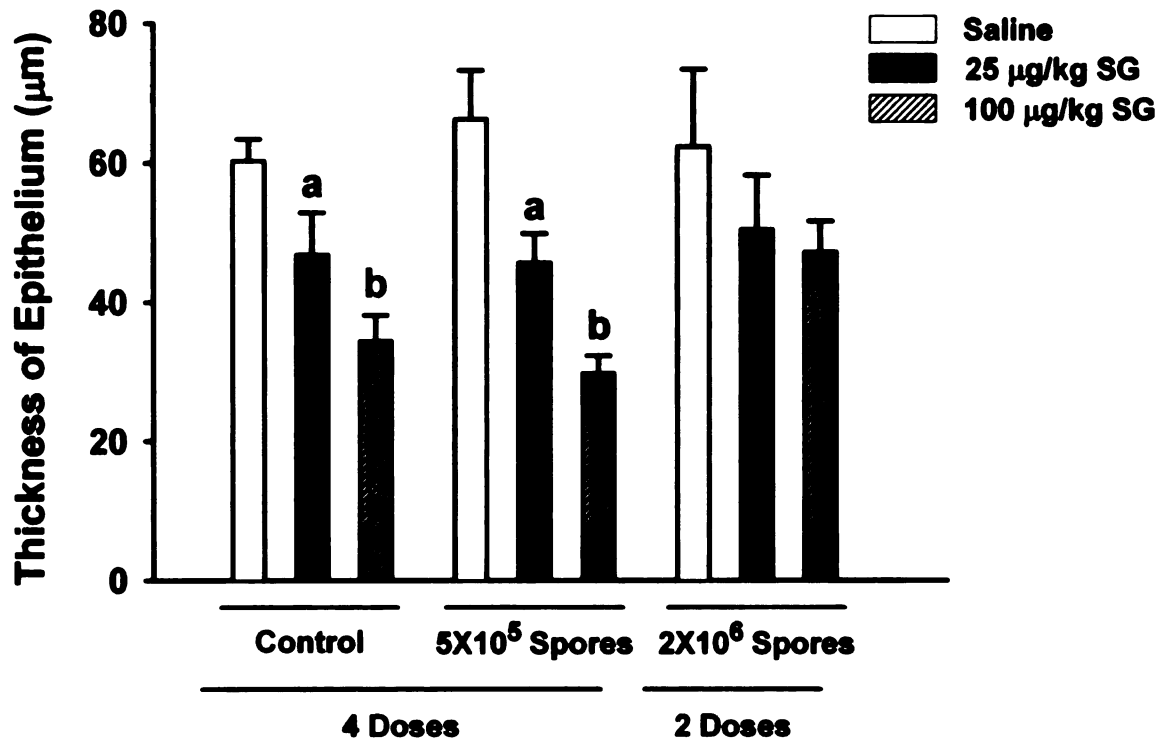


Figure 30. Atrophy of OE in the DM of T2. OE atrophy occurred in a dose-dependent manner based on the dose of SG. a indicates significantly different from respective saline (0 µg/kg SG) control group; b indicates significantly different from respective 25 µg/kg SG and saline (0 µg/kg SG) control groups ($p \leq 0.05$).

Table 3. Summary of changes in the OE of all groups. Values are the percent decrease in OE thickness or number of OSNs per mm basal lamina, compared to respective saline control animals.

OE Lesions Induced by SG and <i>S. chartarum</i> Spores									
	Saline	5 X 10 ⁵ spores	2 X 10 ⁶ spores	25 µg/kg	100 µg/kg	25 µg/kg 5 X 10 ⁵	100 µg/kg 5 X 10 ⁵	25 µg/kg 2 X 10 ⁶	100 µg/kg 2 X 10 ⁶
OE Atrophy, DM (T2)	-	-	-	22%	43%	31%	55%	-	-
Loss of OSNs, DM (T2)	-	-	-	57%	96%	58%	95%	23%	91%

of total cells per mL BALF compared to respective control (0 spores) mice. A trend of increased total cells in BALF was observed in mice instilled with 2×10^6 spores and saline (16-fold), 25 $\mu\text{g}/\text{kg}$ SG (10-fold), and 100 $\mu\text{g}/\text{kg}$ SG (11-fold) compared to respective control mice. Mice instilled with 5×10^5 spores and saline (39-fold), 25 $\mu\text{g}/\text{kg}$ SG (80-fold), or 100 $\mu\text{g}/\text{kg}$ SG (58-fold) had significant increases in the number of neutrophils in BALF compared to respective control mice. Animals instilled with 5×10^5 spores and saline (23-fold), 25 $\mu\text{g}/\text{kg}$ SG (39-fold), or 100 $\mu\text{g}/\text{kg}$ SG (25-fold) had significant increases in the number of eosinophils in BALF compared to respective control mice. **(Figure 31)**.

We observed a trend, though not statistically significant, of increased neutrophils in the BALF of mice instilled with 2×10^6 spores and saline (130-fold), 25 $\mu\text{g}/\text{kg}$ SG (130-fold), or 100 $\mu\text{g}/\text{kg}$ SG (110-fold) compared to respective control mice. A trend, though not statistically significant, of increased eosinophils in BALF was also observed in mice instilled with 2×10^6 spores and saline (38-fold), 25 $\mu\text{g}/\text{kg}$ SG (50-fold), or 100 $\mu\text{g}/\text{kg}$ SG (30-fold) compared to respective control mice **(Figure 31)**.

All mice instilled with 5×10^5 spores had significant increases in the number of lymphocytes per mL BALF compared to control animals receiving 0 spores, with animals receiving saline, 25 or 100 $\mu\text{g}/\text{kg}$ SG having 99-fold, 27-fold, and 129-fold increases in the number of lymphocytes per mL BALF, respectively. A similar increase was not observed in animals instilled with $2 \times$

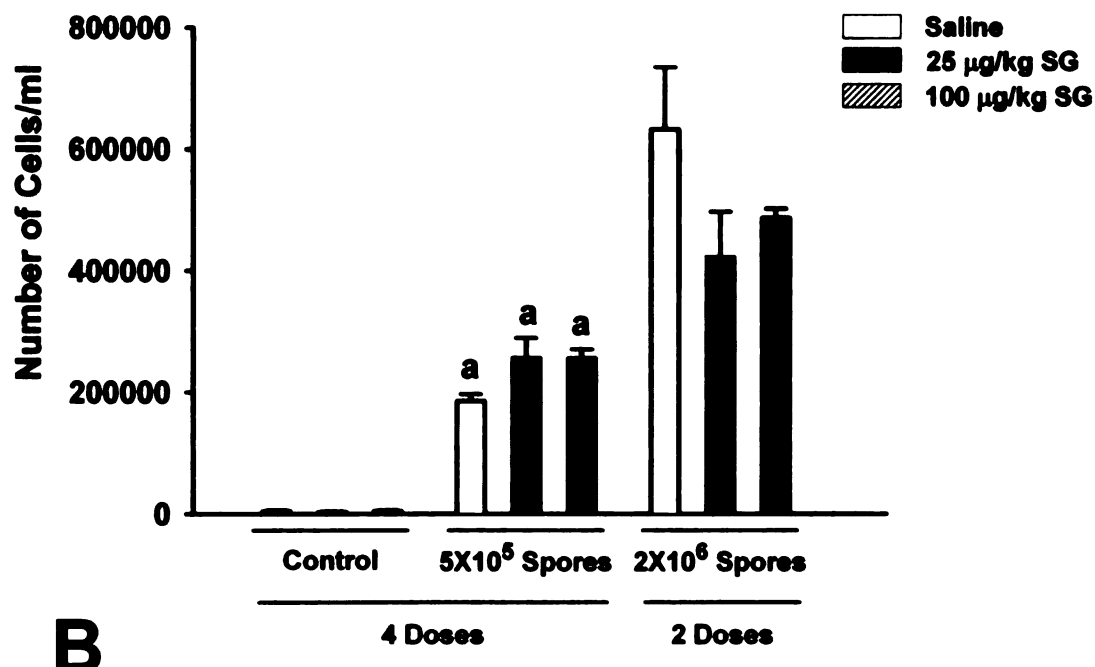
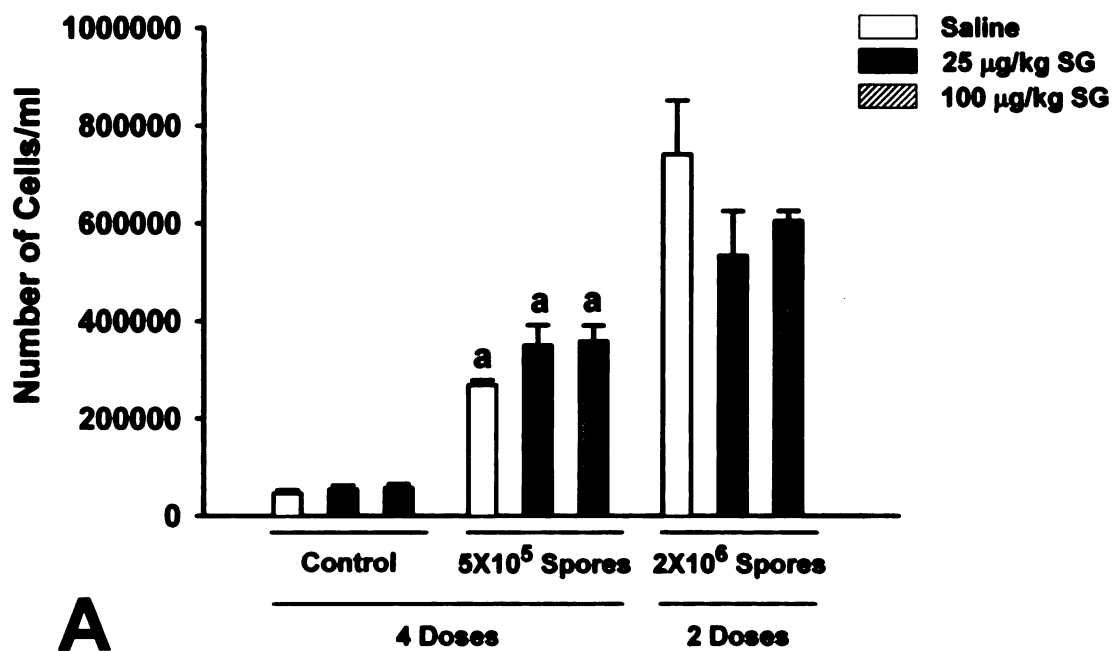
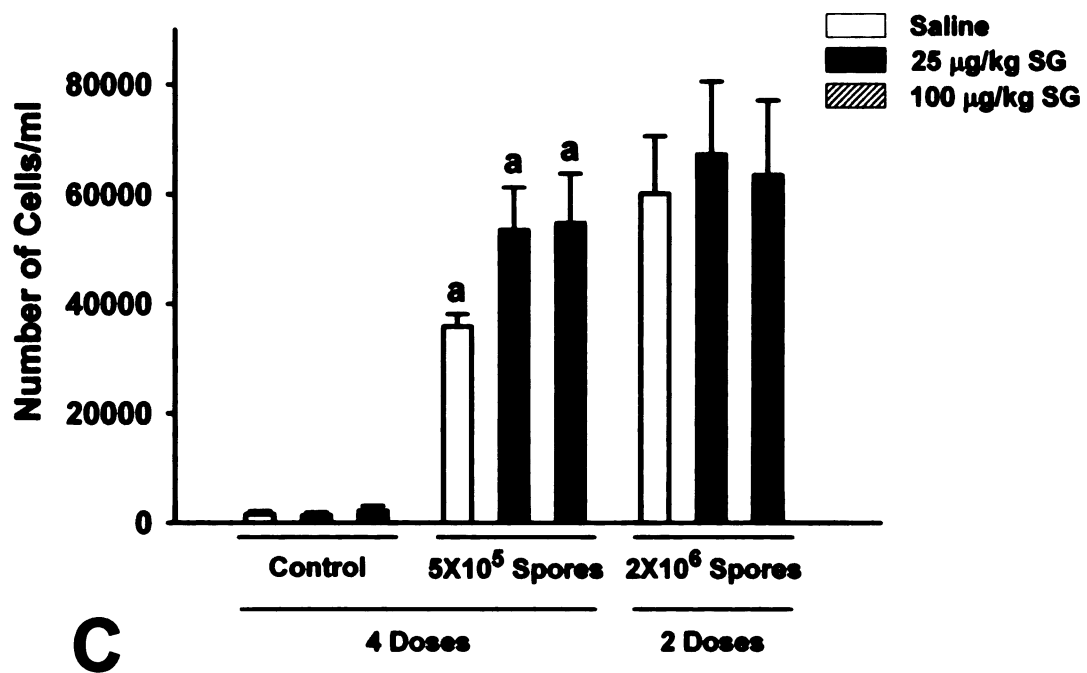


Figure 31. (A) Total cells, (B) neutrophils, and (C) eosinophils in BALF. a indicates significantly different from control (0 spores) mice ($p \leq 0.05$).

Figure 31 continued.



C

10^6 spores (**Figure 32**). The numbers of macrophages per mL of BALF of the animals instilled with 5×10^5 spores and 25 or 100 $\mu\text{g}/\text{kg}$ SG were significantly different from respective control animals receiving 25 or 100 $\mu\text{g}/\text{kg}$ SG and 0 spores. Both groups had 2-fold fewer macrophages in their BALF compared to the BALF of control animals (**Figure 32**). No significant differences between the doses of SG were detected for any cell type in BALF at all doses of spores.

S. chartarum spores and SG influence changes in proinflammatory cytokine levels in BALF

Flow cytometric analysis of proinflammatory cytokine levels in BALF revealed trends of increasing TNF- α , MCP-1, and IL-6 concentrations with increasing dose of spores (**Figure 33**). The levels of TNF- α in the BALF of mice instilled with 5×10^5 spores and saline, 25 $\mu\text{g}/\text{kg}$ SG, or 100 $\mu\text{g}/\text{kg}$ SG were 54-fold, 75-fold, and 95-fold higher than the concentrations in BALF from respective control (0 spore) mice. A non-significant trend of increasing MCP-1 concentration was observed in animals instilled with 5×10^5 spores. Mice receiving 5×10^5 spores and saline, 25 $\mu\text{g}/\text{kg}$ SG, or 100 $\mu\text{g}/\text{kg}$ SG had 3-fold, 3-fold, and 5-fold higher levels of MCP-1 in BALF, respectively, compared to respective control mice. Mice instilled with 5×10^5 spores and saline (16-fold), 25 $\mu\text{g}/\text{kg}$ SG (9-fold), or 100 $\mu\text{g}/\text{kg}$ SG (6-fold) had significant increases in the concentration of IL-6 in BALF compared to respective control mice.

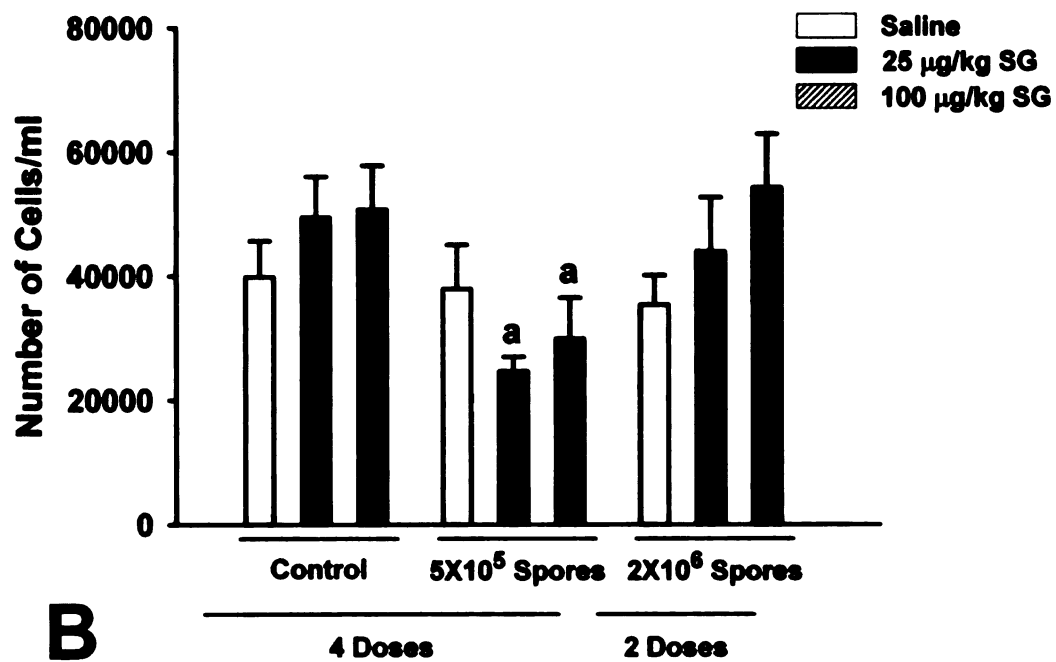
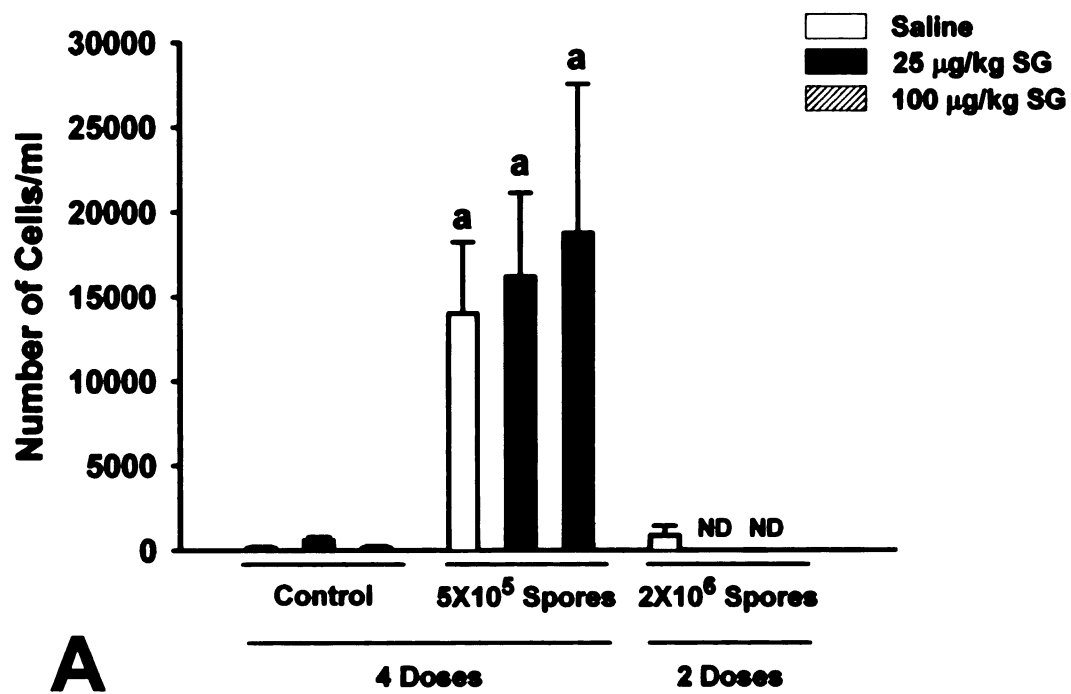
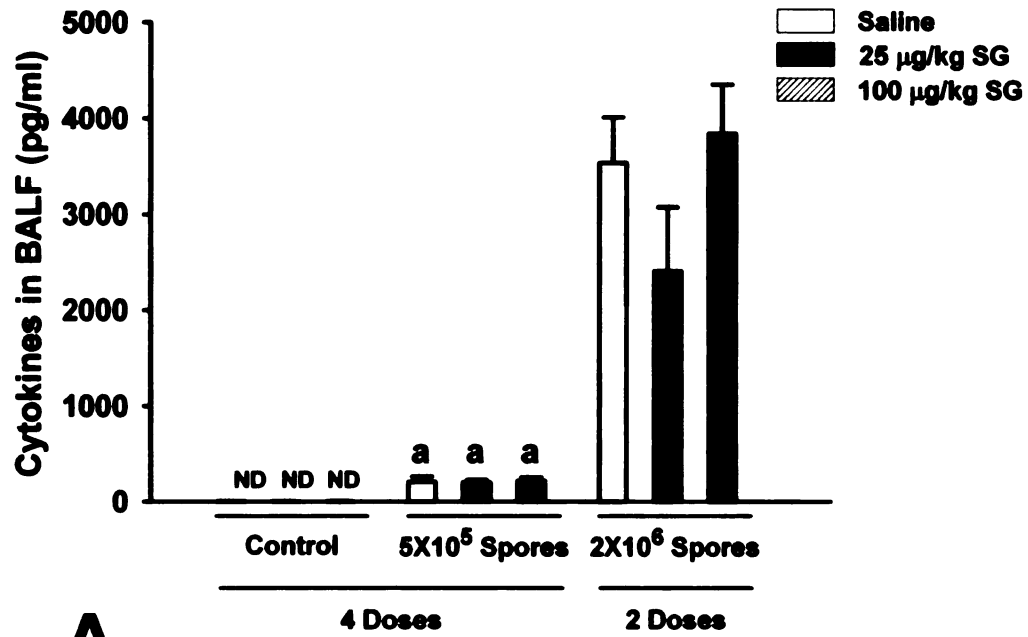
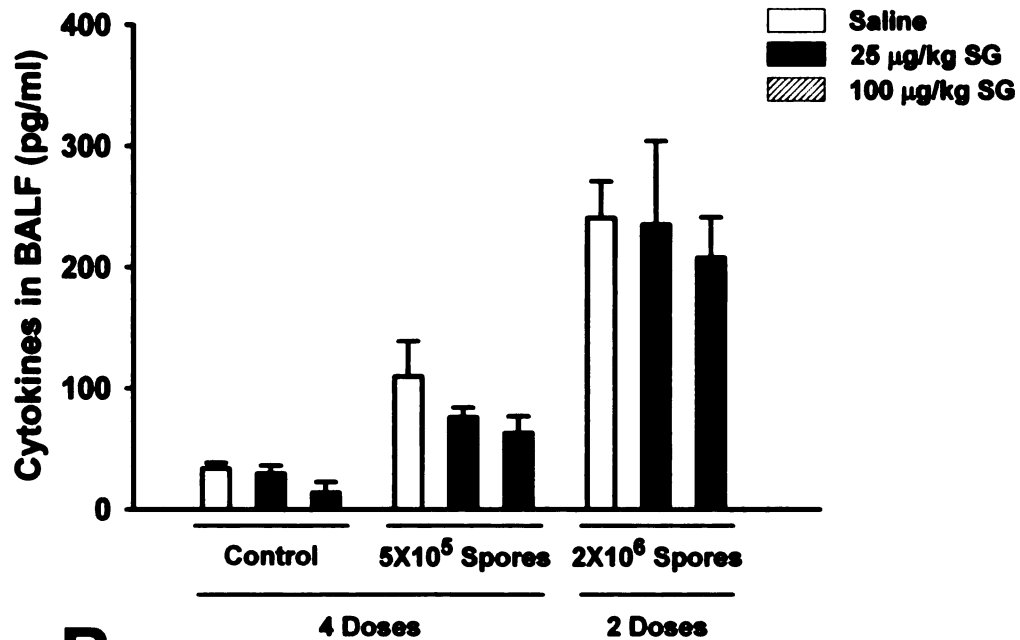


Figure 32. (A) Lymphocytes and (B) macrophages in BALF. a indicates significantly different from control (0 spores) mice, ($p \leq 0.05$). ND, not detected.



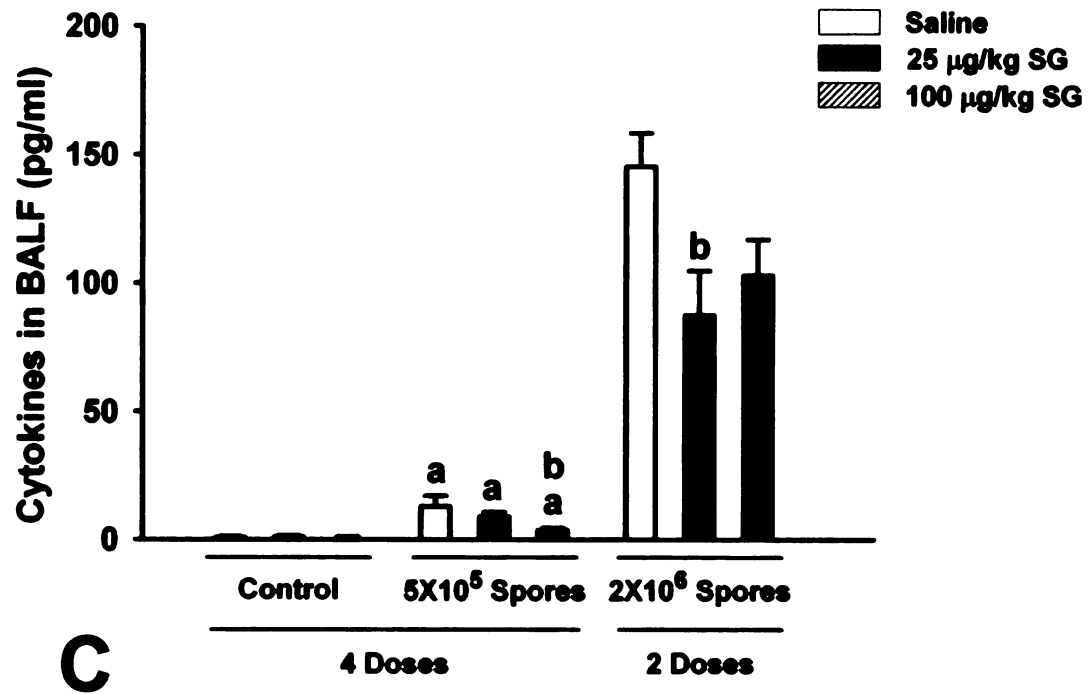
A



B

Figure 33. (A) TNF- α , (B) MCP-1, and (C) IL-6 in BALF. a indicates significantly different from control (0 spores) mice; b indicates significantly different from respective saline (0 μ g/kg SG) mice ($p \leq 0.05$). ND, not detected.

Figure 33 continued.



Non-significant trends of increased TNF- α , MCP-1, and IL-6 were also detected in the BALF of mice instilled with 2×10^6 spores. Mice in these groups instilled with saline (940-fold), 25 $\mu\text{g}/\text{kg}$ SG (890-fold), or 100 $\mu\text{g}/\text{kg}$ SG (1700-fold) had large increases in TNF- α in BALF compared to control animals. Mice receiving 2×10^6 spores and saline, 25 $\mu\text{g}/\text{kg}$ SG, or 100 $\mu\text{g}/\text{kg}$ SG had 7-fold, 8-fold, and 15-fold higher concentrations of MCP-1 in BALF compared to respective control mice. Mice instilled with 2×10^6 spores and saline (190-fold), 25 $\mu\text{g}/\text{kg}$ SG (87-fold), or 100 $\mu\text{g}/\text{kg}$ SG (160-fold) compared to respective control animals.

There were no significant differences between doses of SG at any concentration of spores for MCP-1 and TNF- α . However, two groups had concentrations of IL-6 in their BALF that were statistically significantly different from their respective saline (0 $\mu\text{g}/\text{kg}$ SG) controls. The level of IL-6 in the BALF of mice receiving 5×10^5 spores and 100 $\mu\text{g}/\text{kg}$ SG was 3-fold lower than that found in the BALF of mice instilled with 5×10^5 spores and saline. BALF from animals instilled with 2×10^6 spores and 25 $\mu\text{g}/\text{kg}$ SG had an IL-6 concentration 2-fold lower than mice receiving 2×10^6 spores and saline.

The concentration of INF- γ in mice instilled with 5×10^5 spores and saline (2-fold), 25 $\mu\text{g}/\text{kg}$ SG (3-fold), or 100 $\mu\text{g}/\text{kg}$ SG (3-fold) was significantly increased compared to respective control animals (0 spores) at all doses of SG.

A similar, non-significant trend of increased INF- γ was observed in all mice instilled with 2×10^6 (Figure 34).

Within both the control group of mice (0 spores) and the group receiving 5×10^5 spores, animals instilled with 100 $\mu\text{g}/\text{kg}$ SG had significantly less INF- γ in BALF than animals receiving saline. Both groups had 2-fold less INF- γ in their BALF than respective groups receiving saline and 0 or 5×10^5 spores.

Only in groups instilled with 2×10^6 spores was a significant difference in the levels of IL-12 detected (Figure 34). Those receiving 2×10^6 spores and 25 or 100 $\mu\text{g}/\text{kg}$ SG had 5-fold and 3-fold lower concentrations of IL-12 than animals instilled with saline and 2×10^6 spores. Mice instilled with 2×10^6 spores and saline had 5-fold higher concentrations of IL-12 in their BALF than saline control animals. No significant differences in the concentrations of IL-10 were detected in any groups (data not shown).

DISCUSSION

S. chartarum spores have been shown to be 7-12 X 4-6 μm (Jarvis et al., 1998; Tucker et al., 2007). The tendency for particles to deposit in the nose makes it a potential target of the effects of both the spores of *S. chartarum* and the secondary metabolite toxins found within the spores (Cheng et al., 1990; Cheng et al., 1991; Yeh et al., 1997). Particles less than 10 μm in diameter may also reach the lungs when inhaled (Salvi and Holgate, 1999). It has been

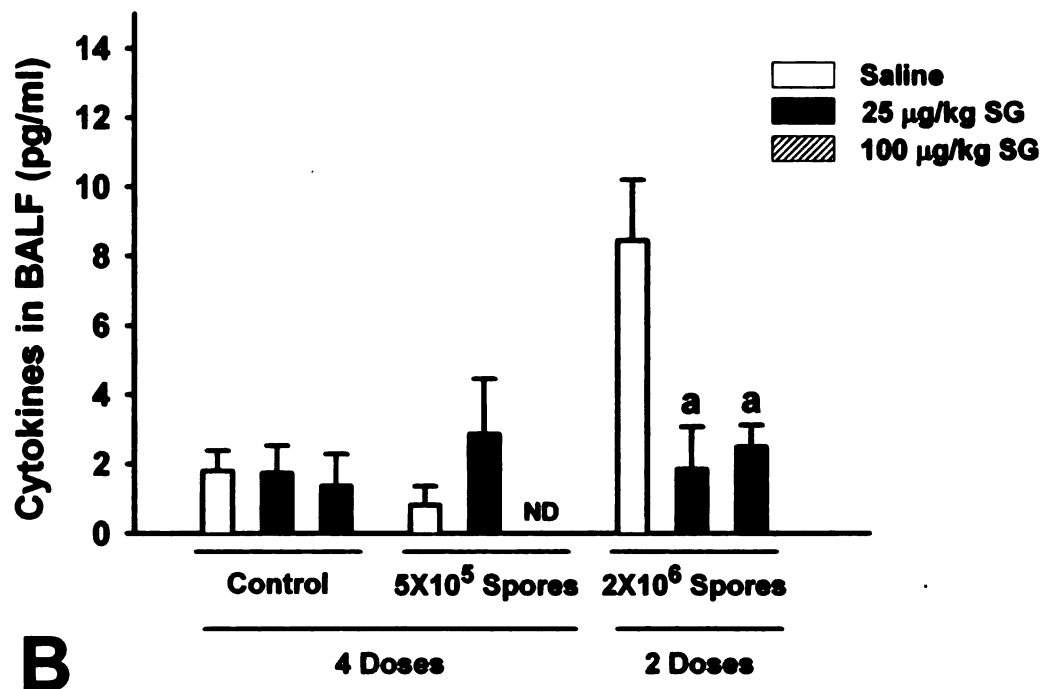
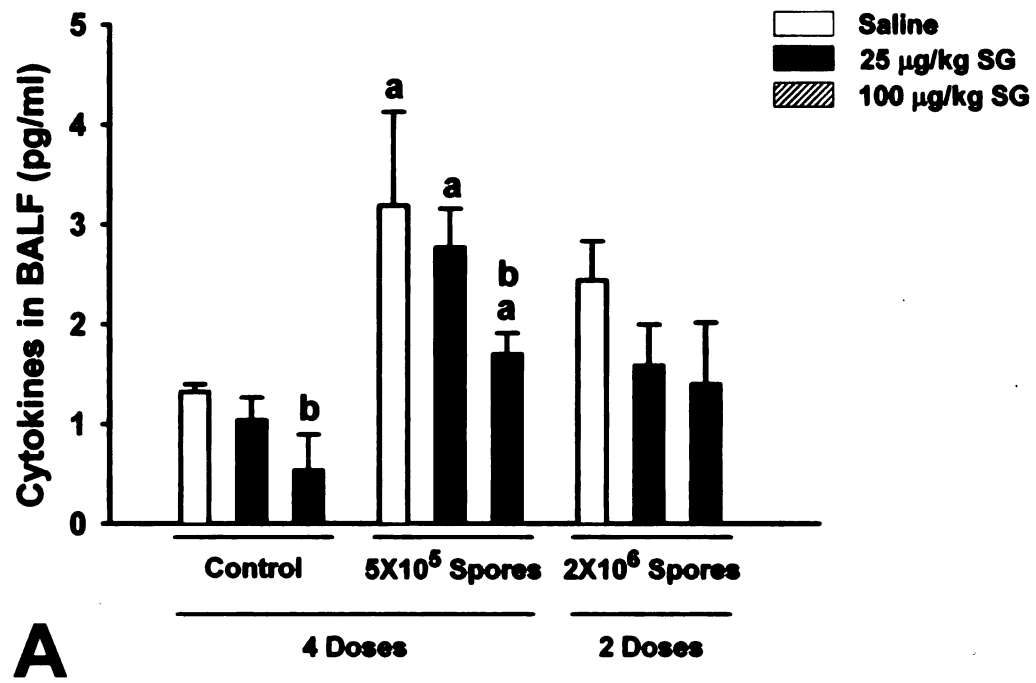


Figure 34. (A) INF- γ and (B) IL-12 in BALF. a indicates significantly different from control (0 spores) mice; b indicates significantly different from saline (0 $\mu\text{g/kg}$ SG) mice, ($p \leq 0.05$). ND, not detected.

postulated that the spores of *S. chartarum* would not readily aerosolize due to the polysaccharide “slime” in which they grow (Hossain et al., 2004), or reach the lungs when inhaled due to their size (Wilkins et al., 1998). However, the dry spores have been shown to aerosolize and have a mean respirable diameter of 5 μm (Jarvis et al., 1998; Yike and Dearborn, 2004), indicating that some inhaled spores may reach the lungs in addition to lodging in the nose.

The existence of two chemotypes of *S. chartarum* presents the possibility that exposure to spores may contribute to adverse effects in the absence of macrocyclic trichothecenes. Additionally, the observation of macrocyclic trichothecenes on particulates such as house dust (Brasel et al., 2005) and in mycelial fragments (Gregory et al., 2004) provides a route of exposure to macrocyclic trichothecenes in both the nose and the lungs that is not dependent on exposure to spores.

In this study, we observed that repeated intranasal instillations containing 25 or 100 $\mu\text{g}/\text{kg}$ resulted in a dose-dependent loss of OSNs and atrophy of OE, regardless of the presence or absence of spores. In addition to areas we previously observed to be affected by single intranasal instillations of SG, the OE in the DM was atrophic due to loss of OSNs. We observed slightly less severe changes in mice instilled with 2×10^6 spores. The lack of change in the thickness of OE and the smaller decrease in OSNs is likely due to the fact that these mice received fewer instillations than those in other experimental groups. However, we previously observed that a single intranasal instillation of 25 $\mu\text{g}/\text{kg}$ SG represented the lowest adverse effect level on histopathology scoring (Islam

et al., 2006). Signs of apoptosis in the OE in DM are apparent on histopathology. The only interaction between spores and SG observed in the nose was enhancement of the inflammatory response. This was most apparent in the group of mice instilled with 2×10^6 spores. Areas of OE in the immediate vicinity of spores were affected by the additional inflammatory infiltrates present at those sites, but other effects of spores on the OE were not observed. This indicates that components of the spores are capable of inciting an inflammatory response independently of macrocyclic trichothecenes, but that the apoptosis observed in the OE was caused by SG.

The OSNs in the OE of the nose are unique in that they undergo turnover similar to many epithelial populations in the body. Cycles of apoptosis and regeneration result in regular replacement of mature OSNs (Graziadei and Graziadei, 1978). A variety of experimental methods have been employed to induce death of OSNs *in vivo*, such transection of the olfactory nerve at the cribriform plate, olfactory bulbectomy, and exposure to chemicals toxic to OE, such as zinc sulfate. The majority of chemicals that result in OE toxicity cause necrotic cell death rather than inducing apoptosis (Cowan and Roskams, 2002). Chemotherapeutic agents such as vinca alkaloids induce apoptosis in OSNs that resembles the selective death we observed in mice exposed to a single intranasal instillation of SG (Kai et al., 2004).

SG may contribute to apoptosis of OSNs by inducing expression of a variety of factors involved in apoptotic mechanisms. Trichothecenes including SG have been shown to activate c-Jun N-terminal kinase (JNK), mitogen-

activated protein kinases (MAPK) such as p38 and p53, and extracellular signal-related kinase (ERK) (Shifrin and Anderson, 1999; Yang et al., 2000; Chung et al., 2003; Zhou et al., 2005). We recently showed that a single intranasal instillation of SG induces upregulation of the pro-apoptotic genes Fas, FasL, p75, p53, Bax, caspase 3, and caspase-activated DNase (CAD) in the OE lining the ethmoid turbinates (Islam et al., 2006). Intranasal instillation of RA induced expression of Fas and TNF- α , followed by expression of double-stranded RNA-activated protein kinase (PKR), CAD, Bax, and p53 mRNA in the ethmoid turbinates (Islam et al., 2007). TNF- α has been used to experimentally induce apoptosis in OSNs (Suzuki and Farbman, 2000). Exposure to SG resulted in DNA fragmentation and expression of pro-apoptotic genes in a neural crest-derived pheochromocytoma cell line (PC-12). Double-stranded RNA-activated protein kinase (PKR), CAD, Bax, and p53 expression were significantly increased in SG-treated cells, while caspase 3 remained unchanged. Application of PKR inhibitors prevented apoptosis and expression of pro-apoptotic genes, indicating it may have a significant role in apoptosis induced by SG (Islam et al., 2008). However, PKR inhibitors failed to prevent apoptosis and pro-apoptotic gene expression in OP-6 cells, a cell line representing a late-developmental stage of OSNs (Pestka, Unpublished Data). This indicates that further elucidation of apoptotic mechanisms is needed to clarify the effects of SG at the cellular level in OE. We previously hypothesized that macrocyclic trichothecenes might interact with specific odorant receptors on OSNs to induce apoptosis (Islam et al., 2006; Islam et al., 2007). Ressler et al. (1993) described area-specific expression of

odorant receptors, with one population lining the DM. We postulated that this receptor organization might explain the lack of apoptosis in the dorsal meatus that we observed with a single intranasal instillation of SG. It is unclear why the repeated instillations employed in this study resulted in significant apoptosis in the DM. Macrocyclic trichothecenes may interact with all odorant receptor types but have greater affinity for certain receptors. Repeated exposures might result in saturation of those receptors for which SG has the greatest affinity, then bind to other populations of receptors. This would potentially explain the unique sensitivity of OSNs to SG-induced apoptosis. On the other hand, repeated instillations of SG might cause increased release of cytokines from leukocytes, resulting in prolonged inflammation and greater tissue injury and may contribute to greater apoptosis of OSNs. It is also possible that other mechanisms that have not yet been investigated are responsible for apoptosis of OSNs in response to macrocyclic trichothecene exposure.

In this study, we observed neutrophil influx and increased proinflammatory cytokines in BALF. The marked increases in IL-6 and TNF- α concentrations in BALF in animals instilled twice compared to those instilled four times are logical given that these cytokines are involved in the acute phase of inflammation and thus would be substantially increased early in the inflammatory response (Mitchell and Cotran, 2003). Eosinophil infiltration was present in the lungs of mice exposed four times to 5×10^5 and twice to 2×10^6 spores. Ochiai et al. (2005) previously reported influx of eosinophils into the lungs of mice with repeated exposures but not with single instillations of spores of *S. chartarum*. It

is possible that repeated instillations of spores result in sensitization and a shift in the Th1/Th2 balance, changing the character of the inflammatory profile with repeated exposure to *S. chartarum*. Analysis of BALF from mice instilled with spores for Th1/Th2 cytokines such as IL-5 should be undertaken to further clarify the mechanisms behind the changes we observed. A variety of cytokines involved with asthma and allergic responses have been shown to activate eosinophils and stimulate release of eotaxin, a chemokine that specifically attracts eosinophils (Foster et al., 2001). It is unclear whether this response is allergic in nature, as many authors have reported a lack of IgE antibodies in the serum of animals and humans exposed to *S. chartarum* (Johanning et al., 1996; Leino et al., 2003).

Mice exposed to 5×10^5 spores had marked influx of lymphocytes into BALF, though no significant difference between the doses of SG were seen. The appearance of lymphocytes in animals exposed to spores for 4 days but not in those exposed for 2 days, even at a higher dose of spores, is not surprising given that lymphocytes are not significantly involved in the acute inflammatory response and are typically considered to be involved in inflammation that is more chronic in nature (Mitchell and Cotran, 2003). The changes in IL-12 that we observed would seem to fit this conclusion as well. IL-12 is important in the differentiation of Th1 and Th2 CD4⁺ lymphocytes and is a potent inducer of INF- γ release by those cells (Mitchell and Cotran, 2003; Mitchell and Kumar, 2003). This pattern, like the pattern in lymphocyte infiltration, is likely a result of the duration of exposure rather than the dose of spores. It may be that IL-12 was

secreted at 2 days, hence a significant increase appears only in the groups instilled twice, and the resultant significant increases in INF- γ concentration and lymphocytes in BALF are seen in animals instilled for 4 days. We noted a trend of decreased INF- γ concentration with increasing dose of SG at all levels of spore dose.

We also observed non-significant increases in MCP-1. MCP-1 is primarily produced by lymphocytes and is chemoattractant for macrophages, but is also capable of attracting activated T-lymphocytes (Carr et al., 1994; Mitchell and Kumar, 2003). The large increase in MCP-1 increase seen in the group instilled twice may be reflective of a switch from the acute inflammatory phase to a more chronic, macrophage- and lymphocyte- dominated infiltrate. Interestingly, we did not observe a difference in the number of macrophages between the different spore doses. This may be reflective of a lack of increase in macrophages or may represent the resident population of alveolar macrophages. It may also be due to death of macrophages that have been exposed to SG, as was suggested by *in vitro* work examining the effect of mycotoxins on macrophages (Sorenson et al., 1986).

Other authors have compared the pulmonary effects of the two chemotypes of *S. chartarum* and have found that strains producing macrocyclic trichothecenes cause significantly more inflammatory and pathological changes (Nikulin et al., 1997; Flemming et al., 2004), while others have found no difference in the effects caused by exposure to the two chemotypes (Leino et al., 2003). Our results contrast with those of Yike et al. (2005), which indicated that

spores containing macrocyclic trichothecenes induced significantly more inflammation than the spores of the same toxin-producing strain lacking SG. In this study, we did not observe a statistically significant effect of increasing doses of SG on inflammatory cell infiltrates in the lungs. There are a number of possible explanations for this, including the difference in exposure method. IT instillation provides a more direct route into the lungs and would ensure that the entire dose of spores arrives at the lung parenchyma. Our method of separating spores and toxin was intended to allow differentiation of the effects of both and to allow confirmation of the exact dose of each being instilled. A lack of response to SG alone in the lung parallels the results reported by Rand et al. (2002), who observed no effect of IT instillation of pure isosatratoxin F. It is therefore feasible that deposition of spores in the lung may allow localized release of SG and other macrocyclic trichothecenes that may enhance the response to the spores or cause separate effects that add to the cumulative changes in the lung. Yike et al. (2005) noted that SG is rapidly released from spores upon IT instillation and then eliminated such that only very small amounts are detectable in BALF 15 minutes after instillation. Perhaps macrocyclic trichothecenes are cleared even more quickly without the protection of the spore, thus preventing obvious pulmonary effects. Other spore contents, such as Stachylysin, a hemolysin identified in both chemotypes of *S. chartarum*, atranones, and proteinases have been suggested as possible players in the etiology of pulmonary pathology (Nielsen et al., 2002; Vesper and Vesper, 2002; Yike et al., 2007). Regardless of the factors involved,

it appears that macrocyclic trichothecenes do not cause significant gross changes in the lungs of mice independent of spore exposure.

Based on these results, we concluded that the adverse effects observed in the OE in the noses of mice in this study are dependent on macrocyclic trichothecene mycotoxins, and macrocyclic trichothecene-free spores did not contribute to adverse olfactory effects in the nose resulting from exposure to *S. chartarum*. The spores of *S. chartarum* clearly contributed to a more severe inflammatory response. It is therefore possible that exposure to both spores and macrocyclic trichothecenes could result in more severe nasal tissue damage. We are unaware of studies investigating the effects of intranasal exposure to toxins or spores of the atranone-producing chemotype of *S. chartarum* on the noses of mice. Given the ability of atranones to induce inflammation in the lungs (Nielsen et al., 2002), it is possible that intranasal exposure would result in inflammation in the nose. However, we previously showed that the ability of SG to induce apoptosis in OSNs is highly chemical structure-dependent (Islam et al., 2006), and it is therefore unlikely that atranones would have a similar effect on OE based on their structures (Andersen et al., 2002).

Our observations of the result of intranasal exposure to spores and SG indicate that macrocyclic trichothecenes influence proinflammatory cytokines in the lungs. It is likely, based on our results and the results of others (Ochiai et al., 2005), that longer-term exposure would result in more significant injury in the lungs and that significant differences between macrocyclic trichothecene-containing spores and those lacking the toxins would be observed. These results

also indicate that *S. chartarum* spores are capable of inducing pulmonary pathology in the absence macrocyclic trichothecenes. We therefore concluded that pulmonary pathology is not dependent on macrocyclic trichothecenes, though these mycotoxins are likely to contribute to pulmonary pathology induced by more chronic exposures to *S. chartarum*. Further studies are needed to investigate the interactions between the macrocyclic trichothecenes and spores of *S. chartarum*. Flow cytometric analysis of Th1/Th2-related cytokines in BALF could be used to further explain the eosinophilic infiltration we observed in this study. Studies investigating the effects of intranasal instillations of atranones on the OE in the nose as well as effects in the lung would be useful in further characterizing the results of exposures to the two chemotypes of *S. chartarum*. Exposure to both chemotypes is environmentally feasible (Andersen et al., 2002), and investigations should begin attempting to characterize any interactions resulting from a co-exposure. Time course and dose-response studies could be undertaken to investigate the cellular and proinflammatory cytokine changes associated with chronic exposures. Aerosol inhalation studies utilizing both macrocyclic trichothecenes and spores may shed further light on the effects of exposure to *S. chartarum*, and should include comparisons of the effects of both acute and chronic inhalation exposures in the lungs and nose.

CHAPTER 5 BIBLIOGRAPHY

- Andersen, B., Nielsen, K. F., and Jarvis, B.B., 2002. Characterization of *Stachybotrys* from water-damaged buildings based on morphology, growth, and metabolite production. *Mycologia* 94, 392-403.
- Andersson, M. A., Nikulin, M., Koljalg, U., Andersson, M. C., Rainey, F., Reijula, K., Hintikka, E. L., and Salkinoja-Salonen, M, 1997. Bacteria, molds, and toxins in water-damaged building materials. *Appl. Environ. Microbiol.* 63, 387-93.
- Bennett, J. W., and Klich, M., 2003. Mycotoxins. *Clinical Microbiology Reviews* 16, 497-516.
- Boutin-Forzano, S., Charpin-Kadouch, C., Chabbi, S., Bennedjai, N., Dumon, H., and Charpin, D., 2004. Wall relative humidity: a simple and reliable index for predicting *Stachybotrys chartarum* infestation in dwellings. *Indoor Air* 14, 196-99.
- Brasel, T. L., Douglas, D. R., Wilson, S. C., Straus, D. C., 2005. Detection of Airborne *Stachybotrys chartarum* Macrocylic Trichothecene Mycotoxins on particulates Smaller than Conidia. *Applied and Environmental Microbiology* 71, 114-122.
- Brasel, T. L., Martin, J. M., Carriker, C. G., Wilson, S. C., Straus, D. C., 2005. Detection of Airborne *Stachybotrys chartarum* Macrocylic Trichothecene Mycotoxins in the Indoor Environment *Applied and Environmental Microbiology* 71, 7376-7388.
- Carr, M. W., Roth, S. J., Luther, E., Rose, S. S., and Springer, T. A., 1994. Monocyte chemoattractant protein 1 acts as a T-lymphocyte chemoattractant. *Proc Natl Acad Sci USA* 91, 3652-3656.
- Cheng, Y. S., Hansen, G. K., Su, Y. F., Yeh, H. C., and Morgan, K. T., 1990. Deposition of ultrafine aerosols in rat nasal molds. *Toxicol. Appl. Pharmacol.* 106, 222-233.
- Cheng, Y. S., Yeh, H. C., Swift, D. L., 1991. Aerosol deposition in human nasal airway for particles 1 nm to 20 mm: a model study. *Radiat. Prot. Dosimetry* 38, 41-47.
- Chung, Y., Zhou, H., and Pestka, J. J., 2003. Transcriptional and posttranscriptional roles for p38 mitogen-activated protein kinase in upregulation of TNF- α expression by deoxynivalenol (vomitoxin). *Toxicology and Applied Pharmacology* 193, 188-201.
- Cowan, C. M., and Roskams, A. J., 2002. Apoptosis in the mature and developing olfactory neuroepithelium. *Microsc Res Tech* 58, 204-215.

Dearborn, D. G., Yike, I., Sorenson, W. G., Miller, M. J., Etzel, R. A., 1999. Overview of Investigations into Pulmonary Hemorrhage among Infants in Cleveland, Ohio. *Environmental Health Perspectives* 107(Supplement 3), 495-499.

Dearborn, D. G., Smith, P. G., Dahms, B. B., Allan, T. M., Sorenson, W. G., Montana, E., and Etzel, R. A., 2002. Clinical profile of 30 infants with acute pulmonary hemorrhage in Cleveland. *Pediatrics* 110, 627-637.

Ehrlich, K. C., and Daigle, K. W., 1987. Protein synthesis inhibition by 8-oxo-12,13-epoxytrichothecenes. *Biochimica et biophysica acta* 923, 206-213.

Flappan, S. M., Portnoy, J., Jones, P., Barnes, C., 1999. Infant Pulmonary Hemorrhage in a Suburban Home with Water Damage and Mold (*Stachybotrys atra*). *Environmental Health Perspectives* 107, 927-930.

Flemming, J., Hudson, B., and Rang, T. G., 2004. Comparison of inflammatory and cytotoxic lung responses in mice after intratracheal exposure to spores of two different *Stachybotrys chartarum* strains. *Toxicological Sciences* 78, 267-275.

Foster, P. S., Mould, A. W., Yang, M., Mackenzie, J., Mattes, J., Hogan, S. P., Mahalingham, S., Mckenzie, A. N. J., Rothenberg, M. E., Young, I. G., Matthaei, K. I., and Webb, K. I., 2001. Elemental signals regulating eosinophil accumulation in the lung. *Immunol Rev* 179, 173-181.

Fung, F., Clark, R., and Williams, S., 1998. *Stachybotrys*, a mycotoxin-producing fungus of increasing toxicologic importance. *J. Toxicol. Clin. Toxicol.* 36, 79-86.

Graziadei P., and Graziadei G. A., 1978. The olfactory system: a model for the study of neurogenesis and axon regeneration in mammals. In: Cotman, C. W. (Ed.), *Neuronal Plasticity*. Raven Press, New York, pp. 131-153.

Gregory, L., Pestka, J. J., Dearborn, D. G., Rand, T. G., 2004. Localization of Satratoxin-G in *Stachybotrys chartarum* Spores and Spore-Impacted Mouse Lung Using Immunocytochemistry. *Toxicol. Pathol.* 32, 26-34.

Hossain, M. A., Ahmed, M. S., and Ghannoum, M. A., 2004. Attributes of *Stachybotrys chartarum* and its association with human disease. *J. Allergy Clin. Immunol.* 113, 200-08.

Institute of Medicine, 2004. Damp Indoor Spaces and Health. National Academies Press, Washington DC.

Islam, Z., Amuzie, C. J., Harkema, J. R., and Pestka, J. J., 2007. Neurotoxicity and inflammation in the nasal airways of mice exposed to the macrocyclic trichothecene Roridin A: kinetics and potentiation by bacterial lipopolysaccharide coexposure. *Toxicological Sciences* 98, 526-541.

Islam, Z., Harkema, J. R., Pestka, J. J., 2006. Satratoxin G from the Black Mold *Stachybotrys chartarum* Evokes Olfactory Sensory Neuron Loss and Inflammation in the Murine Nose and Brain. *Environmental Health Perspectives* 114, 1099-1107.

Jarvis, B. B., Sorenson, W. G., Hintikka, E. L., Nikulin, M., Zhou, Y., Jiang, J., Wang, S., Hinkley, S., Etzel, R. A., and Dearborn, D., 1998. Study of toxin production by isolates of *Stachybotrys chartarum* and *Memnoniella echinata* isolated during a study of pulmonary hemosiderosis in infants. *Appl. Environ. Microbiol.* 64, 3620-3625.

Johanning, E., Biagini, R., Hull, D., Morey, P., Jarvis, B., and Lansbergis, P., 1996. Health and immunology following exposure to toxigenic fungi (*Stachybotrys chartarum*) in a water-damaged office environment. *International Archives of Occupational and Environmental Health* 68, 207-218.

Kai, K., Satoh, H., Kajimura, T., Kato, M., Uchida, K., Yamaguchi, R., Tateyama, S., and Furuhashi, K., 2004. Olfactory epithelial lesions induced by various cancer chemotherapeutic agents in mice. *Toxicol Pathol* 32, 701-709.

Karunasena, E., Cooley, J. D., Douglas, D. R., and Straus, D. C., 2004. Protein translation inhibition by *Stachybotrys chartarum* conidia with and without the mycotoxin containing polysaccharide matrix. *Mycopathologia* 158, 87-97.

Kilburn, K. H., 2004. Role of molds and mycotoxins in being sick in buildings: neurobehavioral and pulmonary impairment. *Adv. Appl. Microbiol.* 55, 339-59.

Leino, M., Mäkelä, M., Reijula, K., Haahtela, T., Mussalo-Rauhamaa, H., Tuomi, T., Hintikka, E., and Alenius, H., 2003. Intranasal exposure to a damp building mould, *Stachybotrys chartarum*, induces lung inflammation in mice by Satratoxin-independent mechanisms. *Clinical and Experimental Allergy* 33, 1603-1610.

- Li, M. and Pestka, J. J., 2008. Comparative induction of 28S ribosomal RNA cleavage by ricin and the trichothecenes deoxynivalenol and T-2 toxin in the macrophage. *Toxicological Sciences* 105, 67-78.
- Mason, C. D., Rand, T. G., Oulton, M., MacDonald, J. M., and Scott, J. E., 1998. Effects of *Stachybotrys chartarum* (*atra*) conidia and isolated toxin on lung surfactant production and homeostasis. *Natural Toxins* 6, 27-33.
- Mitchell, R. N., and Cotran, R. S., 2003. Acute and Chronic Inflammation. In: Kumar, V., Cotran, R. S., and Robbins, S. L. (Eds.), *Robbins Basic Pathology*, 7th Edition. Saunders, Philadelphia, PA, pp. 33-59.
- Mitchell, R. N., and Kumar, V., 2003. Diseases of Immunity. In: Kumar, V., Cotran, R. S., and Robbins, S. L. (Eds.), *Robbins Basic Pathology*, 7th Edition. Saunders, Philadelphia, PA, pp. 33-59.
- Nielsen, K. F., Huttunen, K., Hyvärinen, A., Andersen, B., Jarvis, B. B., Hirvonen, M., 2002. Metabolite profiles of *Stachybotrys* isolates from water-damaged buildings and their induction of inflammatory mediators and cytotoxicity in macrophages. *Mycopathologia* 154, 201-205.
- Nikulin, M., Reijula, K., Jarvis, B. B., Veijalainen, P., and Hintikka, E. L., 1997. Effects of intranasal exposure to spores of *Stachybotrys atra* in mice. *Fundam. Appl. Toxicol.* 35, 182-188.
- Ochiai, E., Kamei, K., Hiroshima, K., Watanabe, A., Hashimoto, Y., Sato, A., and Ando, A., 2005. The Pathogenicity of *Stachybotrys chartarum*. *Japanese Journal of Medical Mycology* 46, 109-117.
- Pestka, J. J., Yike, I., Dearborn, D. G., Ward, M. D. W., and Harkema, J. R., 2008. *Stachybotrys chartarum*, trichothecene mycotoxins, and damp building-related illness: new insights into a public health enigma. *Toxicological Sciences* 104, 4-26.
- Rand, T. G., Mahoney, M., White, K., and Oulton, M., 2002. Microanatomical changes in alveolar type II cells in juvenile mice intratracheally exposed to *Stachybotrys chartarum* spores and toxin. *Toxicological Sciences* 65, 239-245.
- Rand, T. G., White, K., Logan, A., and Gregory, L., 2002. Histological, immunohistochemical and morphometric changes in lung tissue in juvenile mice experimentally exposed to *Stachybotrys chartarum* spores. *Mycopathologia* 156, 119-131.

- Rao, C. Y., Brain, J. D., and Burge, H. A., 2000. Reduction of pulmonary toxicity of *Stachybotrys chartarum* spores by methanol extraction of mycotoxins. *Applied and Environmental Microbiology* 66, 2817-2821.
- Ressler, K. J., Sullivan, S. L., and Buck, L. B., 1993. A zonal organization of odorant receptor gene expression in the olfactory epithelium. *Cell* 73, 597-609.
- Rosenblum Lichtenstein, J. H., Molina, R. M., Donaghey, T. C., Brain, J. D., 2006. Strain differences influence murine pulmonary responses to *Stachybotrys chartarum*. *Am. J. Respir. Cell. Mol. Biol.* 35, 415-423.
- Salvi, S. and Holgate S. T., 1999. Mechanisms of particulate matter toxicity. *Clinical and Experimental Allergy* 29, 1187-1194.
- Shifrin, V. I., and Anderson, P., 1999. Trichothecene mycotoxins trigger a ribotoxic stress response that activates c-Jun N-terminal kinase and p38 mitogen-activated protein kinase and induces apoptosis. *Journal of Biological Chemistry* 274, 13985-13992.
- Sorenson, W. G., Frazer, D. G., Jarvis, B. B., Simpson, J., and Robinson, V. A., 1987. Trichothecene mycotoxins in aerosolized conidia of *Stachybotrys atra*. *Applied and Environmental Microbiology* 53, 1370-1375.
- Sorenson, W. G., Gerberick, G. F., Lewis, D. M., and Castranova, V., 1986. Toxicity of mycotoxins for the rat pulmonary macrophage *in vitro*. *Environ Health Perspect* 66, 45-53.
- Suzuki, Y., and Farbman, A. I., 2000. Tumor necrosis factor- α -induced apoptosis in olfactory epithelium *in vitro*: possible roles of caspase 1 (ICE), caspase 2 (ICH-1), and caspase 3 (CPP32). *Exp Neurol* 165, 35-45.
- Tucker, K., Stolze, J. L., Kennedy, A. H., and Money, N. P., 2007. Biomechanics of conidial dispersion in the toxic mold *Stachybotrys chartarum*. *Fungal Genetics and Biology* 44, 641-647.
- Tuomi, T., Reijula, K., Johnsson, T., Hemminki, K., Hintikka, E. L., Lindroos, O., Kalso, S., Koukila-Kahkola, P., Mussalo-Rauhamaa, H., and Haahtela, T., 2000. Mycotoxins in crude building materials from water-damaged buildings. *Appl. Environ. Microbiol.* 66, 1899-1904.
- Tuomi, T., Saarinen, L., and Reijula, K., 1998. Detection of polar and macrocyclic trichothecene mycotoxins from indoor environments. *Analyst* 123, 1835-41.

- Ueno, Y., 1984. General toxicology. In: Ueno, Y. (Ed.), *Trichothecenes: Chemical, Biological, and Toxicological Aspects*. Elsevier, New York, pp. 135-145.
- Vesper, S. J., and Vesper, M. J., 2002. Stachylysin may be a cause of hemorrhaging in humans exposed to *Stachybotrys chartarum*. *Infection and Immunity* 70, 2065-2069.
- Wilkins, C. K., Larsen, S. T., Hammer, M., Poulsen, O. M., Wolkoff, P., and Nielsen, G. D., 1998. Respiratory effects in mice exposed to airborne emissions from *Stachybotrys chartarum* and implications for risk assessment. *Pharmacology and Toxicology* 83, 112-119.
- Yang, G., Jarvis, B. B., Chung, Y., and Pestka, J. J., 2000. Apoptosis induction by the Satratoxins and other trichothecene mycotoxins: relationship to ERK, p38 MAPK, and SAPK/JNK activation. *Toxicology and Applied Pharmacology* 164, 149-160.
- Yeh, H. C., Muggenburg, B. A., Harkema, J. R., 1997. In vivo deposition of inhaled ultrafine particles in the respiratory tract of rhesus monkeys. *Aerosol. Sci. Technol.* 27, 465-470.
- Yike, I., and Dearborn, D. G., 2004. Pulmonary effects of *Stachybotrys chartarum* in animal studies. *Adv. Appl. Microbiol.* 55, 241-273.
- Yike, I., Miller, M. J., Sorenson, W. G., Walenga, R., Tomashefski, Jr. J. F., and Dearborn, D. G., 2002. Infant animal model of pulmonary mycotoxicosis induced by *Stachybotrys chartarum*. *Mycopathologia* 154, 139-152.
- Yike, I., Rand, T. G., and Dearborn, D. G., 2005. Acute inflammatory responses to *Stachybotrys chartarum* in the lungs of infant rats: time course and possible mechanisms. *Toxicological Sciences* 84, 408-417.
- Yike, I., Rand, T. G., and Dearborn, D. G., 2007. The role of fungal proteinases in pathophysiology of *Stachybotrys chartarum*. *Mycopathologia* 164, 171-181.
- Zhou, H., Islam, Z., and Pestka, J. J., 2005. Induction of competing apoptotic and survival signaling pathways in the macrophage by the ribotoxic trichothecene deoxynivalenol. *Toxicological Sciences* 87, 113-122.

CHAPTER 6

Conclusions and Future Directions

Olfaction is facilitated by the positioning of the OSNs such that inhaled environmental odorants are readily able to bind to odorant receptors. However, constant exposure to the environment makes OSNs unique among neurons in that they are immediately susceptible to the deleterious effects of inhaled chemicals and toxins.

The results I presented in Chapter 3 indicate that repeated intranasal instillations of RA resulted in dose-dependent atrophy of OE, loss of OSNs, and neutrophilic rhinitis. Unlike previous work utilizing single intranasal instillations of macrocyclic trichothecenes, additional effects were seen in the respiratory and transitional epithelium, as well as in several glandular structures found throughout the nose. This implies that additional mechanisms of injury are at work when repeated exposures to macrocyclic trichothecenes occur and that the nasal passages are attempting to compensate by glandular release of copious amounts of mucus into the airways.

Repeated exposures to macrocyclic trichothecenes could have long-term consequences for human health. Atrophy of the outer neuronal layer of OB accompanied by loss of OMP staining and sporadic neutrophils was also discussed in Chapter 3. The effects I observed in the OB may be involved in the cognitive and neurobehavioral symptoms reported by some people. Further work is needed to determine if there is a threshold of exposure beyond which the OB cannot recover. Unlike the OSNs in this study, the OB recovered OMP staining and there was no evidence of remaining atrophy on histopathology at 3 weeks after the last exposure. This apparent recovery could be due to

regenerating OSNs, and thus studies are needed to test whether olfaction is intact in these animals. One question is whether the OSNs would recover if the OB did not, and vice versa. An investigation of whether macrocyclic trichothecenes are reaching the OB via the axons of OSNs and causing damage to this tissue could reveal whether the atrophy I observed in the OB is due solely to loss of OSNs and their axons, or if additional tissue damage may be taking place. OB damage is likely not dependent on the direct toxicity of macrocyclic trichothecenes reaching the OB. It could result solely from toxicity to the OSNs, which form the outer neuronal layer and a portion of the glomerular layer of the OB. More significant damage may occur if macrocyclic trichothecenes are indeed reaching deeper layers of the OB. Studies could utilize c-fos labeling or other methods to determine if the OB is receiving signals after repeated exposures to OE. It would also be interesting to determine if mice can detect odors at various times after repeated exposures – for example, when the OB has returned to normal on histopathology but the OSNs have not. Another question is whether recovery is entirely functional, or if OSNs can reconnect with the proper glomeruli in the OB.

In Chapter 3, I also discussed the persistence of lesions resulting from repeated exposures to RA. Neutrophilic rhinitis had resolved and the thickness of OE had returned to a state similar to that of saline control animals at 21 days after the last instillation of RA. However, the number of OSNs per mm basal lamina in mice exposed to RA remained significantly different from saline control mice. This indicates that the effects of repeated exposures to macrocyclic

trichothecenes on OSNs persist in spite of the fact that atrophy of OE was no longer detectable. The number of OSNs per mm basal lamina had increased at 21 days after the last instillation of RA compared to that observed at 24 hours following instillation. It is therefore possible that OSNs would at some point return to the levels seen in saline control animals. It would be beneficial to determine the effects of more chronic exposures to macrocyclic trichothecenes on all cell populations in the OE, particularly with respect to whether a threshold of injury or time of exposure exists beyond which the OSNs are incapable of regenerating. A study that allows mice a longer “recovery” period than the three weeks allotted in this study could help to determine whether mice would recover fully. It would also be interesting to test whether mice are capable of detecting odors, and to determine when and if their sense of smell returns after exposure to macrocyclic trichothecenes. Two types of basal cells exist in the OE, globose and horizontal basal cells. It is possible that recovery of OSNs is occurring by proliferation of horizontal basal cells, which have a slower rate of proliferation than the rapidly reproducing globose basal cells. This would indicate that globose basal cells may be affected by exposure to macrocyclic trichothecenes. This possibility makes it all the more important to investigate the effects of macrocyclic trichothecenes on all cell populations within the nose.

The mechanism(s) by which macrocyclic trichothecenes cause loss of OSNs is unknown at this time. Studies should investigate whether interaction between macrocyclic trichothecenes and olfactory receptors on OSNs is taking place, and whether this might be involved in loss of OSNs. Given that other

studies have demonstrated loss of OSNs through apoptosis, it would be interesting to determine if macrocyclic trichothecenes induce apoptosis by interacting with olfactory receptors. Molecular and *in vitro* studies to investigate cell signaling and gene expression would be particularly useful to determine this. The structure of macrocyclic trichothecenes could also be compared to the structures of known odorants that bind to olfactory receptors to look for similar moieties. Similarity to molecular structures found in known odorants may provide evidence for the possibility of macrocyclic trichothecene-olfactory receptor interactions. Further studies should also investigate the mechanisms by which macrocyclic trichothecenes cause damage to other cell populations within the nose, such as NTE and RE. It is possible that these cells are somehow less susceptible to the effects of macrocyclic trichothecenes and thus required repeated exposures for loss to occur. It is also possible that different mechanisms are resulting in damage to different cell populations within the nose.

I presented the results of a comparison of the susceptibility of weanling and adult mice to the nasal effects of SG in Chapter 4. Weanling and adult mice were similarly susceptible to SG-induced apoptosis of OSNs, atrophy of OE, and neutrophilic rhinitis. This suggests that exposure to *S. chartarum* is a concern in both children and adults, and that further work is needed to assess the risk that *S. chartarum* poses to children. While the susceptibility of weanling and adult mice exposed to SG was shown to be similar, studies should investigate the differences in the risk of exposure to SG. Given the properties of *S. chartarum* spores and the habits and physiology of children, it is possible they may be at

greater risk for exposure or possibly be exposed to higher doses than adults living in similar environments. Future studies should establish time-course and dose-response effects of macrocyclic trichothecenes in weanling mice. As stated in Chapter 4, saline control weanling mice had a higher number of neutrophils in the nasal mucosa than saline control adult mice, and weanling mice exposed to SG had a smaller percent increase in neutrophils in the nasal mucosa than adult mice exposed to SG. Studies investigating the inflammatory cellular infiltrates and proinflammatory cytokines in the noses and lungs of adult and weanling mice, including assessment of nasal lavage and BALF, might shed further light on the mechanisms behind the differences I observed in the neutrophilic rhinitis in weanling and adult mice. The persistence of lesions in weanling mice should be investigated to determine whether the duration of the effects of exposure to macrocyclic trichothecenes is the same as that in adult animals. As younger animals tend to have higher turnover of OSNs, it is possible that SG-induced lesions in weanling mice may be less persistent. Given my findings in this chapter, studies should also investigate the effects of macrocyclic trichothecene exposure on the OB of weanling mice. Another area of focus is whether neutrophilic rhinitis and encephalitis of the OB have long-term implications in young children.

The results of my study investigating the effects of *S. chartarum* spores, SG, and instillations of both in the noses of mice indicate that macrocyclic trichothecenes cause significant nasal pathology but that the spores do not contribute to loss of OSNs and atrophy of OE. The spores did, however,

enhance the inflammatory response in the nose when SG and spores were instilled together. This indicates that rhinitis, and therefore symptoms, might be worse when exposure to both macrocyclic trichothecenes and *S. chartarum* spores occurs. Collection of nasal lavage in a future study to assess proinflammatory cytokines would allow further investigation of the inflammatory-enhancing effect of the spores. Rt-PCR for proinflammatory and apoptotic gene expression might also shed further light on the mechanisms behind the increased inflammatory response in the presence of spores and SG. Studies assessing the effects of intranasal instillations of toxin-containing *S. chartarum* spores should be undertaken to determine if the presence of the spore impedes induction of OE lesions by macrocyclic trichothecenes. It is possible that toxin leaking out of spores would only cause localized lesions next to the spores, or that toxin would leach out of all parts of the spore rather than just the area closest to the OE. In this case, OE damage would likely be most pronounced in areas of the nose where spores lodge. Instillations of mycelial fragments, house dust, and other macrocyclic trichothecene-containing particulates could confirm whether inhalation of such exposure sources results in apoptosis of OSNs.

The spores of *S. chartarum* caused significant inflammatory cell infiltration and changes in proinflammatory cytokines in the lungs of mice, but SG did not contribute to these changes. This might be accounted for by rapid clearance of SG from the lung. Rt-PCR assessment of gene expression might provide further insight into the mechanisms behind these results and would likely be different in animals receiving spores alone or macrocyclic trichothecenes and spores.

Neutrophils, eosinophils, and lymphocytes were found in BALF in this study. Future studies should investigate the type of lymphocytes present in the BALF of spore-instilled mice to determine whether a shift in the Th1/Th2 balance has occurred that might have resulted in infiltration of eosinophils into the lungs. Flow cytometry could be performed on BALF to quantify cytokines typically associated with Th2 responses, such as IL-2, IL-4, and IL-5. Studies of more chronic exposures to the spores of *S. chartarum* could be used to determine if repeated exposure leads to sensitization and an allergic-type response.

The differences observed in the responses of the nose and lung are likely due characteristics inherent to each location. Alveolar macrophages which are normally present in the lung would rapidly respond to arrival of SG and spores in the lung by release of cytokines and chemokines to attract other leukocytes. The nose lacks a resident macrophage population and thus the inflammatory response is dependent on factors released upon tissue insult and injury. An interesting question is whether reactive oxygen species and a ribotoxic stress response are induced in the nose and lungs when macrocyclic trichothecenes are present, as has been suggested by a number of studies. To further investigate the effects of macrocyclic trichothecenes in the lungs, mice could be intranasally instilled with the spores of an atranone-producing strain of *S. chartarum*. Several authors have noted that the two chemotypes may be found growing in the same indoor environment, and thus the effects of co-exposure to both chemotypes should also be investigated in the nose and lungs. It has not been determined if atranones are capable of causing effects in the nose, and

investigations of the effects of intranasal instillations of these mycotoxins should therefore be carried out.

Given that toxicity due to macrocyclic trichothecenes is not dependent on the presence of *S. chartarum* spores, instillations of toxin-containing mycelial fragments should also be investigated. The potential for simultaneous exposure to multiple sources of these toxins, such as spores and house dust, should also be investigated to see if an additive effect is elicited.

These results raise potential implications for human health in that people who experience multiple or chronic exposures to these mycotoxins might have additional, or more severe, effects than those who are subjected to only a single or acute exposure. They also suggest that people who are exposed to macrocyclic trichothecenes multiple times may experience adverse effects for some time after exposure ceases. However, further studies are needed to better characterize the effects of exposure to macrocyclic trichothecenes in people.